Identification and Characterization of Spruce Genes Involved in Somatic Embryo Development

BY

DEREK ALBERT LAW

A Thesis
Submitted to the Faculty of Graduate Studies
in Partial Fulfillment of the Requirements
for the Degree of

MASTER OF SCIENCE

Department of Plant Science
University of Manitoba
Winnipeg, Manitoba

ACKNOWLEDGEMENTS

I would first like to thank my supervisor and friend, Dr. Claudio Stasolla for his guidance and support. Dr. Stasolla has been a constant presence throughout my graduate program, always available to answer questions, provide insights and share ideas. His character and humour have helped make these past two years fun and exciting.

This work would not have been completed without the help of the people working in Dr. Stasolla's lab. Thank you to Muhammad Tahir, for teaching me many of the molecular techniques described in this thesis and for introducing me to Pakistani food; Mark Belmonte, who taught me many of the tissue culturing techniques, answered all of the questions I was too embarrassed to ask Dr. Stasolla, and always had something interesting to talk about; Bert Luit, for maintaining and producing the tissue that I used, teaching me about photography, and introducing me to new music and movies. I am proud to call all of these people my friends. Their presence motivated me to come to the lab on days when I could have otherwise completed my work at home. Thanks also to past summer students Nikki Lwiwski and Heather Flood for all of their help.

Thank you to my committee members Dr. Fouad Daayf and Dr. Michele Piercey-Normore for their guidance and for taking the time to meet with me throughout the year to discuss the outcomes of my project. Special thanks to those in other labs who provided assistance and answered questions: Ralph Kowatsch, Doug Durnin, Dr. Genyi Li and Dr. Lakhdar Lamari, the Plant Science office staff, the greenhouse staff, all of my excellent professors and my fellow graduate students. This project would not have been possible without the funding provided by CELLFOR and the PGS M provided by NSERC.

Lastly, and most importantly, I'd like to thank my parents, Arnold and Orisia Law, my brother Gavin and his wife Sonia and especially my wife Meagan for their love and support.

TABLE OF CONTENTS

ACKNOWLEDGEMENTS ..... **ii**

LIST OF TABLES ..... **vi**

LIST OF FIGURES ..... **vii**

LIST OF ABBREVIATIONS ..... **ix**

ABSTRACT ..... **x**

1.0 INTRODUCTION **1**

2.0 LITERATURE REVIEW **3**

2.1 The Somatic Embryogenesis System in Spruce **3**
2.1.1 Induction and maintenance of embryogenic tissue 3
2.1.2 Maturation of somatic embryos 4
2.1.3 Embryo conversion 5
2.2 Morphological events occurring during embryogenesis **8**
2.2.1 Zygotic embryo morphology 8
2.2.2 Somatic embryo morphology 8
2.2.2.1 Early morphogenic stages: studies on Norway spruce (Picea abies) 9
2.2.2.2 Late embryogenic stages: studies on white spruce (Picea glauca) 12
2.3 Physiological events occurring during somatic embryogenesis **15**
2.3.1 Physiological events taking place during the early phases of somatic embryo development 15
2.3.1.1 The role of programmed cell death (PCD) during PEM development 15
2.3.1.2 The role of PCD during suspensor degradation 16
2.3.2 Physiological events taking place during the late phases of somatic embryo development 19
2.3.2.1 The role of ABA during somatic embryogenesis 19
2.3.2.2 The role of osmoticum during somatic embryogenesis 20
2.4 Molecular events occurring during somatic embryogenesis **21**
2.5 Genes involved in meristem development **22**
2.5.1 Genes involved in shoot apical meristem initiation and maintenance in flowering plants 22
2.5.2 Genes involved in shoot apical meristem initiation and maintenance in conifers 25
2.5.2.1 Homeobox genes 25
2.5.2.2 Argonaute-like genes 26
2.6 Research Objectives **27**

3.0 MATERIALS AND METHODS **29**

3.1 Plant material **29**
3.1.1 White spruce (Picea glauca) 29

3.1.2 Norway spruce (Picea abies) 29
3.2 Generation of full length PgAGO 30
3.2.1 cDNA library construction 30
3.2.1.1 First strand cDNA synthesis 30
3.2.1.2 cDNA amplification by Long Distance PCR 31
3.2.1.3 Sfi 1 digestion 31
3.2.1.4 cDNA size fractionation by CHROMA SPIN-400 32
3.2.1.5 Ligation of cDNA to λTriplEx2 vector and insertion into a λ phage 32
3.2.1.6 Obtaining the titer of the un-amplified library 32
3.2.2 PgAGO probe preparation and cDNA library screening 36
3.2.3 PgAGO Rapid Amplification of cDNA Ends (RACE) 36
3.2.3.1 RNA processing 36
3.2.3.2 Reverse transcription 37
3.2.3.3 Nested PCR for 5' RNA Ligase Mediated (RLM)-RACE 37
3.2.3.4 3' RLM-RACE 37
3.3 Molecular characterization of PgAGO 38
3.4 In-situ hybridization studies 38
3.4.1 Chemical fixation and tissue processing 38
3.4.2 Probe preparation and hybridization 39
3.5 Reverse Transcriptase (RT)-PCR studies 39
3.6 Spruce Transformation 40
3.6.1 Preparation of construct 40
3.6.2 Plasmid Preparation 40
3.6.3 Tissue Preparation 41
3.6.4 Tissue transformation 41
3.7 RNA Blot analysis 42
3.8 Morphological observations 42
3.9 Histological observations 42
3.10 Generation of the full-length sequence of HBK2, expression studies and transformation studies 43
3.10.1 HBK2 Probe Preparation and cDNA library screening 43
3.10.2 HBK2 Rapid Amplification of cDNA Ends (RACE) 43
3.10.3 Molecular characterization of HBK2 44
3.10.4 In-situ hybridization studies 44
3.10.5 RT-PCR studies 44
3.10.6 Spruce transformation with HBK2 44
3.10.7 Morphological observations 44
3.10.8 Histological observations 44

4.0 RESULTS 45

4.1 Molecular cloning of PgAGO 45
4.2 PgAGO Gene Expression Studies 55
4.3 RNA-mediated suppression of PgAGO during embryo development 59
4.4 Characterization of transformed PgAGO lines 59
4.5 Molecular cloning of HBK2 65
4.6 HBK2 Gene Expression Studies 73
4.7 Characterization of the transformed HBK2 line 73

5.0 DISCUSSION 78

5.1 Characterization of PgAGO 78
5.2 Characterization of HBK2 82

6.0 GENERAL DISCUSSION AND CONCLUSIONS 84

LITERATURE CITED 87

APPENDIX 1: 101

LIST OF TABLES

Table 4.1. List of proteins selected for the phenogram as shown in Figure 4.2 48

Table 4.2. Identity matrix showing similarity in amino acid sequence between *Pg*AGO and other AGO proteins belonging to the same monophyletic subclass (AGO4-ATH, AGO2-Rice, AGO3-Rice, AGO6-ATH and AGO9-Rice) and a member (ZLL-ATH) belonging to a different monophyletic subclass..... 50

Table 4.3. Identity matrix showing similarity in amino acid sequence between the PAZ domain of *Pg*AGO and the respective domain of other AGO proteins from other plant and animal species 53

Table 4.4. Identity matrix showing similarity in amino acid sequence between the PIWI domain of *Pg*AGO and the respective domain of other AGO proteins from both plant and animal species 54

Table 4.5. List of proteins selected for the phenogram shown in Figure 4.10..... 68

Table 4.6. Percentage similarity in amino acid sequence between HBK2 and other Homeobox-like proteins belonging to the same subclass (STM-like-Eca, KN2, KN1-1, H1 and STM-like-Phy) 70

Table 4.7. Percentage similarity in amino acid sequence between the Homeobox domain of HBK2 and the respective domain of other Homeobox-like proteins from other plant and animal species 72

LIST OF FIGURES

Figure 2.1. The stages involved in both somatic and zygotic embryogenesis in both white and Norway spruce 6

Figure 2.2. The stages of zygotic embryogenesis in conifers in relation to those described by Singh (1978)..... 10

Figure 2.3. The process of somatic embryo formation in *Picea abies* (Norway spruce) 11

Figure 2.4. The four stages of conifer somatic embryo development 13

Figure 2.5. Apical meristem morphology of cotyledonary white spruce embryos..... 14

Figure 2.6. Varying processes of programmed cell death in animals and plants..... 18

Figure 2.7. The architecture of the SAM in *Arabidopsis*..... 24

Figure 3.1. Steps involved in the construction of cDNA libraries..... 34

Figure 4.1. Hydropathy analysis showing hydrophobic and hydrophilic regions of the deduced protein encoded by the *Pg*AGO gene 47

Figure 4.2. Phenogram of the AGO superfamily showing the similarity between the new *Pg*AGO protein and AGO proteins identified in other plant and animal species..... 49

Figure 4.3. Alignment of the deduced *Pg*AGO sequence with other proteins belonging to the same monophyletic subclass (AGO4-ATH, AGO2-Rice, AGO3-Rice, AGO6-ATH and AGO9-Rice) and two members (ZLL-ATH and AGO1-ATH) belonging to a different monophyletic subclass 51

Figure 4.4. Expression pattern of *Pg*AGO during white spruce somatic embryogenesis 56

Figure 4.5. Expression profile of *Pg*AGO in the embryogenic line ((E)WS1) and a line unable to produce cotyledonary embryos ((NE)WS) from day 0 to 40 in the maturation period 58

Figure 4.6. Screening of three positive spruce cultures *Pg*AGO-A1, A2, and A3, transformed with antisense *PgAGO*..... 61

Figure 4.7. Structural studies of developing embryos produced from control (A-H) and the antisense line *Pg*AGO-A3 (I-N) 62

Figure 4.8. Germinating embryos produced by control (left panel) and *Pg*AGO-A3 cells (right panel) after about 2 months in culture 64

Figure 4.9. Hydropathy analysis showing hydrophobic and hydrophilic regions of the deduced protein encoded by the HBK2 gene..... 67

Figure 4.10. Phenogram of the Homeobox superfamily showing the similarity between the HBK2 protein and other Homeobox-like proteins identified in other plant and animal species 69

Figure 4.11. Alignment of HBK2 sequence with other proteins belonging to the same monophyletic subclass 71

Figure 4.12. Expression pattern of *HBK2* during white spruce somatic embryogenesis. 74

Figure 4.13. Expression profile of *HBK2* in the embryogenic line (E)WS1 and a line unable to produce cotyledonary embryos ((NE)WS) during the 40 days in the maturation period 76

Figure 4.14. Differences in embryo maturation in tissue cultures of an untransformed line (control) and a line transformed with *HBK2* in antisense orientation 77

LIST OF ABBREVIATIONS

ABA, abscisic acid
AGP, arabinogalactan protein
AGO, ARGONAUTE
BA, N^6-benzyladenine
CIP, calf-intestine phosphatase
CLV, CLAVATA
CZ, central zone
2,4-D, 2,4-dichlorophenoxyacetic acid
dsRNA, double-stranded RNA
EST, expressed sequence tag
HBK, homeobox of the KNOX class
KNOX, knotted-like homeobox
LEA, late embryogenic abundant
L1, layer 1
L2, layer 2
L3, layer 3
LV, Litvay
PAS, periodic acid-Schiff
PCD, programmed cell death
PCR, polymerase chain reaction
PDT, partial drying treatment
PEG, polyethylene glycol
PEM, proembryogenic mass
*Pg*AGO, *Picea glauca* ARGONAUTE
PZ, peripheral zone
RACE, rapid amplification of cDNA ends
RAM, root apical meristem
RISC, RNA induced silencing complex
RNAi, RNA interference
RZ, rib zone
SAM, shoot apical meristem
STM, SHOOTMERISTEMLESS
siRNA, short interfering RNA
TAP, tobacco acid phosphatase
TBO, toluidine blue O
WUS, WUSCHEL
ZLL, ZWILLE

ABSTRACT

Law, Derek Albert. M.Sc., The University of Manitoba, May, 2006. Identification and Characterization of Spruce Genes Involved in Somatic Embryo Development. Major Professor; Claudio Stasolla

Somatic embryogenesis can provide researchers with an important tool to study the physiological and molecular mechanisms involved in embryo development. In spruce, few lines are able to produce fully developed embryos due to the presence of malformed meristems. Genes from two families known as *KNOX* (knotted-like homeobox) and *ARGONAUTE* (*AGO*) have previously been found to be involved in meristem development and maintenance. This work documents the discovery of a new member of the AGO family of proteins designated as *Pg*AGO and the further study of a *KNOX* gene known as *HBK2*. The complete coding sequence of both *PgAGO* and *HBK2* was obtained through screening of cDNA libraries generated from white spruce (*Picea glauca*) somatic embryos. RNA in-situ hybridization studies showed that *PgAGO* mRNAs accumulate preferentially within cells of the shoot and root apical meristems in developing spruce embryos. In addition, the expression of *PgAGO* was low in white spruce lines unable to produce embryos in culture. Norway spruce (*Picea abies*) embryogenic tissue was transformed via microprojectile bombardment with an antisense construct of *PgAGO*. Down-regulation of *PgAGO* altered proper development of the apical meristems and reduced embryo regeneration. RNA in-situ hybridization studies showed that *HBK2* is specifically expressed in the sub-apical and cortical regions of developing embryos. Like *PgAGO*, *HBK2* expression was diminished in white spruce lines unable to produce embryos in culture. Transformation experiments with antisense constructs of *HBK2* completely arrested somatic embryo development. This study reveals the importance of a functional meristem during embryo development.

1.0 INTRODUCTION

White spruce, *Picea glauca* (Moench) Voss, can be found throughout North America where it is logged for use in the pulp and paper industries (Grossnickle, 2000). The forestry industry accounts for 2.3% of all employment within Canada and each year contributes 37 billion dollars to the Canadian economy. Ten percent of the world's forested area is located within Canada. Reforestation is required due to industry removal, fires, and death due to insects and diseases. In 2003, Canadian reforestation practices required the planting of 509 million seedlings on 378,746 hectares of land while about 17,651 hectares were seeded (Natural Resources Canada, 2006). The current methods of seedling propagation (cuttings and from seed) are reliable, but time consuming. An in-vitro propagation process known as somatic embryogenesis reduces the amount of time and space required to produce healthy seedlings.

Somatic embryogenesis is a process in which somatic cells are induced to generate genetically identical embryos through careful manipulations of their culture conditions. Somatic embryos undergo a maturation process similar to the one observed in seed embryos, and germinate to produce viable and vigorous plants. This process was first developed by Steward et al. (1958) using carrot. More than twenty years after this study, viable somatic embryos were produced in *Picea abies* (Chalupa, 1985) and now more than 40 species of gymnosperms have been successfully regenerated through somatic embryogenesis (Stasolla et al., 2002). A wide array of plants have produced somatic embryos in culture including wheat (*Triticum aestivum* L.) (Oziasakins and Vasil, 1982), cotton (*Gossypium klotzschianum andress*) (Finer et al., 1983), banana (*Musa ornata* Roxb.) (Cronauermitra and Krikorian, 1988) and rose (*Rosa spp.*) (Dewit, 1990).

Besides its value as a propagation tool, somatic embryogenesis is also used as a model system to investigate the physiological and molecular events that regulate embryogenesis (Stasolla and Yeung, 1999). Compared to zygotic or seed embryos, which are embedded in the maternal tissue and therefore difficult to dissect, somatic embryos are easily produced in a synchronous fashion, and no dissection is required for observation. In white spruce, the development of somatic embryos is strictly genotype-

dependent, as several cell lines are unable to produce embryos, or produce abnormal embryos that fail to undergo post-embryonic growth (Belmonte and Yeung, 2004). This is why, in the past few years much effort has been spent on improving the embryogenic process through manipulations of the culture media components, and through the optimization of the culture environment (Stasolla and Yeung, 2003). However, rational improvements of somatic embryogenesis can only be achieved through the understanding of the molecular mechanisms that regulate and control the development of the embryos.

Many genes are developmentally regulated during the different phases of spruce embryo development (Stasolla and Yeung, 2003). In particular, a study by Stasolla et al. (2003) has documented a set of genes which can be correlated with improved embryo quality. This information leads to the speculation that somatic embryogenesis can indeed be improved through the manipulation of gene expression. Several genes involved in the formation and maintenance of shoot apical meristems are among possible candidate genes that may regulate the embryogenic process. These genes are critical for the production of high quality somatic embryos, capable of generating vigorous plants (Stasolla et al., 2003). Using a pine cDNA microarray, Stasolla et al. (2003) found that many genes involved in meristem maintenance in white spruce were differentially regulated when a cell line was induced to form higher numbers of somatic embryos via the addition of polyethylene glycol (PEG) into the growing medium. *ZWILLE* (*ZLL*), a member of the *ARGONAUTE* (*AGO*) family, along with other *AGO* genes, and a member of the *KNOX* family were all up-regulated in media that promoted somatic embryo formation.

2.0 LITERATURE REVIEW

2.1 The Somatic Embryogenesis System in Spruce

Somatic embryogenesis is the process by which embryos are produced asexually from somatic cells. In spruce, somatic embryogenesis was described several years ago (Lu and Thorpe, 1987) and consists of three distinct steps: (a) induction and maintenance of embryogenic tissue, (b) maturation of somatic embryos, and (c) conversion of embryos into viable plants. Each of these steps requires the careful manipulation of the culture medium at specific times throughout embryo development. A schematic summary of the different steps involved during somatic embryogenesis in spruce is shown in Figure 2.1.

2.1.1 Induction and maintenance of embryogenic tissue

Induction of embryogenic tissue can be achieved using explants of a number of different juvenile tissue types such as cotyledons, female gametophytes or more commonly, immature seed embryos (Lelu et al., 1990, Becwar et al., 1988). Embryonic tissue arising from more mature tissue has only been observed in a select number of species (Westcott, 1992). Induction of embryogenic tissue is generally achieved by culturing explants on half-strength Litvay (1/2LV) media (Litvay et al., 1985) containing 1-3% sucrose and the growth hormones 2,4-dichlorophenoxyacetic acid (2,4-D) and N6-benzyladenine (BA) (Figure 2.1). Tautorus et al. (1991) showed that variations in the concentrations of the above mentioned factors along with other environmental and culturing factors also affect the induction process. Formation of the embryogenic tissue occurs after 3-4 weeks of culture in darkness. This tissue is composed of immature filamentous embryos consisting of an embryogenic head subtended by an elongated suspensor region. Filamentous embryos have a similar morphology to immature zygotic embryos (Stasolla et al., 2002).

Maintenance of the embryogenic tissue is achieved on a medium very similar to the induction medium, but with lower levels of BA (Lu and Thorpe 1987). Under these conditions, the embryogenic tissue doubles in size over the course of a week.

Proliferation of new embryogenic tissue during this stage is thought to occur via cleavage polyembryony wherein the tissue divides and each individual head is able to further proliferate and form new somatic embryos (Singh, 1978). Multiplication by cleavage polyembryony can occur by cleavage of early somatic tissue, by asymmetrical cell division, or by formation from the meristematic cells within the suspensor (von Arnold and Hakman, 1988). The embryogenic tissue is sub-cultured every seven days into fresh liquid media, or every 10-14 days if on solid media (Gupta and Durzan, 1987). The potential of the tissue to produce somatic embryos is reduced over time, and therefore, alternative methods of tissue storage are often required and can include cryopreservation or other low temperature storage (Kartha et al., 1988; Attree and Fowke, 1993).

2.1.2 Maturation of somatic embryos

Maturation of somatic embryos consists of two steps: development and desiccation (Figure 2.1). Development of somatic embryos is achieved by first reducing auxin and cytokinin levels within the medium. Embryogenic tissue is placed onto medium devoid of 2,4-D and BA for 7 days, and then transferred onto a medium enriched with abscisic acid (ABA) and higher levels of sucrose and other osmoticum agents (Lu and Thorpe, 1987). ABA is commonly used in a number of different conifers to induce embryo maturation; however, if embryogenic tissue has not properly developed, then ABA treatment will not have any effect (Stasolla et al., 2002; Filonova et al., 2000a). Levels of ABA required for embryo maturation vary from 40uM (high) to 12uM (low) depending on genera and genotype (Harry and Thorpe, 1991; Attree et al., 1990). Besides ABA, osmoticum agents, which act to restrict water uptake by the tissue, are also required for proper development. Both permeating and non-permeating osmoticum agents have been used as media components, each having different effects on the tissue. Permeating agents, which are able to penetrate the plasma membrane, include sucrose, mannitol, amino acids and inorganic salts, and may lead to toxic effects. Non-permeating agents, which are unable to penetrate the plasma membrane, such as polyethylene glycol (PEG) or dextran, have been shown to improve the embryogenic process (reviewed by Stasolla et al., 2002). The overall developmental process lasts between 40 to 50 days,

depending on the species (Figure 2.1). Developing somatic embryos are sub-cultured after 20 days onto fresh ABA-containing maturation media. At the end of the culture period, opaque embryos showing a ring of cotyledons can be observed.

Similar to their zygotic counterparts, fully developed cotyledonary embryos must undergo a desiccation period in order to complete the maturation process. In spruce, this is achieved through a partial drying treatment (PDT) (Figure 2.1) that reduces the moisture content by approximately 10% over a 10 day period (Roberts et al. 1990). Embryos are placed into the central wells of culture plates, with sterile water in the outer wells to limit the amount of moisture loss. After the PDT, the cotyledonary embryos become fully mature and will convert into viable plants once transferred to germination medium. In some instances, PEG has also been used to partially desiccate embryos (Attree et al., 1991). Full desiccation of embryos, resulting in higher moisture loss, has also proven to be successful (Hay and Charest, 1999).

2.1.3 Embryo conversion

Success in somatic embryogenesis is defined in terms of conversion, which is the ability of mature embryos to produce a functional root and shoot system once transferred onto germination medium. Embryo conversion occurs in the absence of growth regulators (Stasolla and Yeung, 1999). The conversion rate varies among cell lines and is strictly dependent on the degree of maturation reached by the embryos. Generally, embryos matured under sub-optimal conditions fail to convert and have reduced post-embryonic growth.

Figure 2.1. The stages involved in both somatic and zygotic embryogenesis in both white and Norway spruce. The stages of somatic embryogenesis (**A**). During the induction phase, Zygotic embryos are placed onto medium containing 2,4-D and BA, which promotes the formation of embryogenic tissue. After a period of three to four weeks, embryogenic tissue is transferred onto maintenance media containing 2,4-D and lowered levels of BA. During this maintenance phase, tissue is sub-cultured every seven days. This process allows the tissue to stay healthy while continually proliferating. In the case of white spruce, embryogenic tissue is directly sub-cultured onto maturation media containing ABA, which promotes tissue differentiation (development). For Norway spruce, this embryogenic tissue is instead placed onto a hormone-free medium before being placed onto media containing ABA. After forty to fifty days, depending on species, fully mature cotyledonary embryos form. Finally, embryos are desiccated over a period of ten days before being placed onto germination media where they are converted into plantlets. The stages of zygotic embryogenesis (**B**) as described by Singh (1978) as they roughly correspond to somatic embryogenesis (see Figure 2.2 for details).

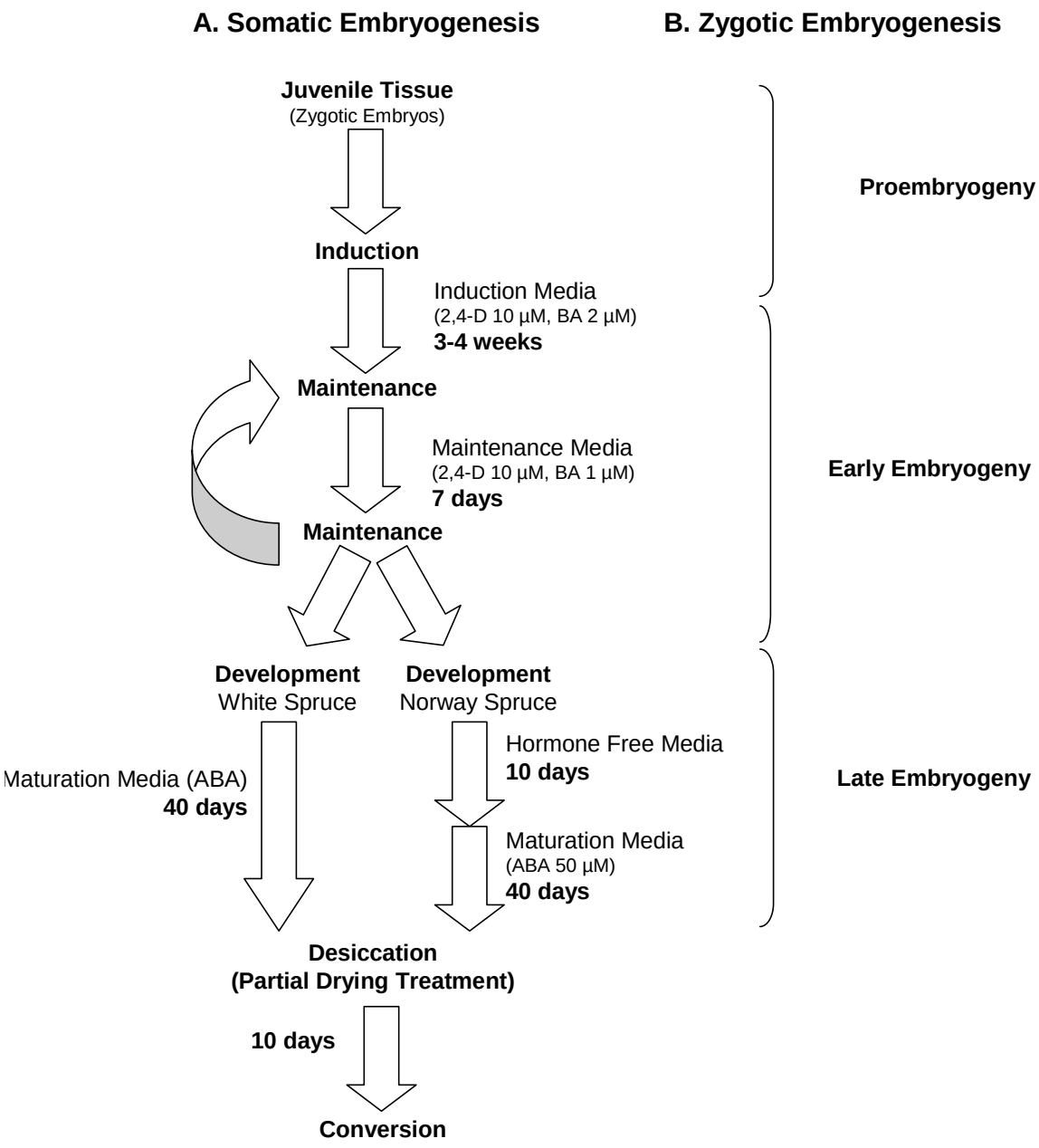
A. Somatic Embryogenesis
B. Zygotic Embryogenesis
Juvenile Tissue
(Zygotic Embryos)
Induction
Induction Media
(2,4-D 10 µM, BA 2 µM)
3-4 weeks
Maintenance
Maintenance Media
(2,4-D 10 µM, BA 1 µM)
7 days
Maintenance
Development
White Spruce
Development
Norway Spruce
Maturation Media (ABA)
40 days
Hormone Free Media
10 days
Maturation Media
(ABA 50 µM)
40 days
Desiccation
(Partial Drying Treatment)
10 days
Conversion
Proembryogeny
Early Embryogeny
Late Embryogeny

2.2 Morphological events occurring during embryogenesis

Somatic embryogenesis in spruce, along with many other coniferous species, is initiated with an asymmetric cell division resulting in two distinct cell types: an elongated, highly vacuolated suspensor-like cell and a circular, highly cytoplasmic embryogenic head (Filonova et al., 2000a). The suspensor acts as a support, transporting nutrients from the culture media to the embryogenic head, which will later give rise to the embryo proper (Nagmani et al., 1995).

2.2.1 Zygotic embryo morphology

Singh (1978) described the developmental pathway of zygotic embryos as consisting of three phases: proembryogeny, early embryogeny and late embryogeny (Figure 2.2). These stages roughly correspond to the steps involved in producing somatic embryos (Figure 2.1). During proembryogeny, the suspensor of the embryo has not yet elongated, roughly corresponding to the early stages of initiation during somatic embryogenesis. In the second phase, early embryogeny, the suspensor has elongated but meristem establishment has not yet occurred, as in late initiation and maintenance during somatic embryogenesis. In the third and final phase, late embryogeny, both the root and shoot apical meristems develop and the embryo continues to differentiate until maturity. Fully cotyledonary zygotic embryos closely resemble their somatic counterparts.

2.2.2 Somatic embryo morphology

Two species have been used as model systems to study the morphogenic events during somatic embryogenesis in spruce: *Picea abies* (Norway spruce) for the early embryogenic stages and *Picea glauca* (white spruce) for the late embryogenic stages.

2.2.2.1 Early morphogenic stages: studies on Norway spruce (*Picea abies*)

Norway spruce development consists of a series of steps in which proembryogenic masses (PEMs) form mature embryos (Figure 2.3). PEMs can be separated into 3 classes depending on their size and morphology. The first class, PEM I, contains a single suspensor-like cell attached to a small head of densely packed cytoplasmic cells. The second class, PEM II, is similar to PEM I, but contains more than one vacuolated cell. The third class, PEM III, contains a larger amount of less densely packed cytoplasmic cells with vacuolated cells radiating in all directions, thus denoting the loss of polarity (Figure 2.3) (Filonova et al. 2000a).

Time lapse tracking, carried out by immobilizing Norway spruce cells in agarose media and observing their further development, has proven to be a useful tool in distinguishing the morphological and physiological changes that occur during PEM development (Filonova et al., 2000a). Using this technique, the following developmental pathway was reported. In the presence of auxins and cytokinins, a PEM I, elongates its vacuolated cell and enlarges its embryogenic head by further division of the cytoplasmic cells after two days in culture. The PEM I develops into a PEM II, when additional vacuolated cells begin to form from the embryogenic head in a polarity-dependant manner. Over the next seven days, new vacuolated cells are formed and the embryogenic head continues to divide. Polarity at this stage is maintained. After day 10, polarity is lost as the cytoplasmic cells continue to proliferate until, eventually, PEMs III are formed. Portions of PEMs III can become separated from the mass, thereby becoming analogous to a PEM I with the ability to develop into a PEM II and III. Somatic embryos arise from the PEMs III after transfer onto media devoid of plant growth regulators (Figure 2.3).

Four days after transfer onto media containing ABA, the early somatic embryos lose their translucent appearance, the suspensors are sloughed off and elongation occurs. Finally, 18 to 20 days after the initial culturing on ABA media, cotyledons begin to form (Filonova et al., 2000a). Early somatic embryos first show histological differentiation through the initiation of a protoderm layer. Later, a root meristem, along with a visible pith and shoot apex, is established (Filonova et al., 2000a).

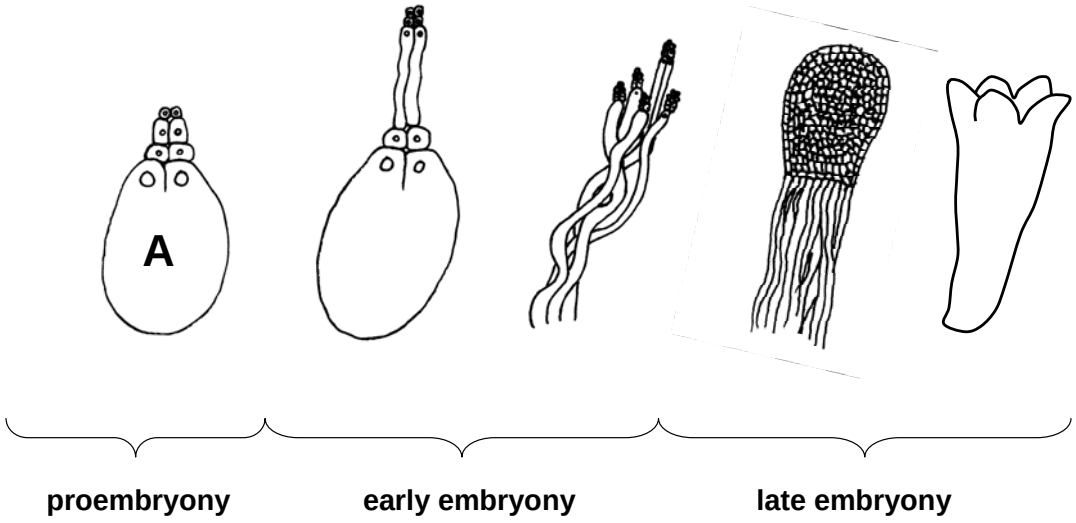

Figure 2.2. The stages of zygotic embryogenesis in conifers in relation to those described by Singh (1978). During proembryony, the archegonium continually divides until it reaches what is known as the 16 cell stage. The suspensor has not yet elongated. During early embryony the suspensor elongates, pushing the apical cells found at the tip of the suspensor into the gametophytic tissue. Secondary suspensor cells form and the apical cells split via a process known as cleavage polyembryony. As a result multiple embryos are able to form. In late embryony one embryo continues to develop while others are degraded, forming a shoot and root apical meristem, and then maturing further into a cotyledonary embryo. Adapted from Steeves and Sussex (1989) and von Arnold et al. (2002). A, archegonium.

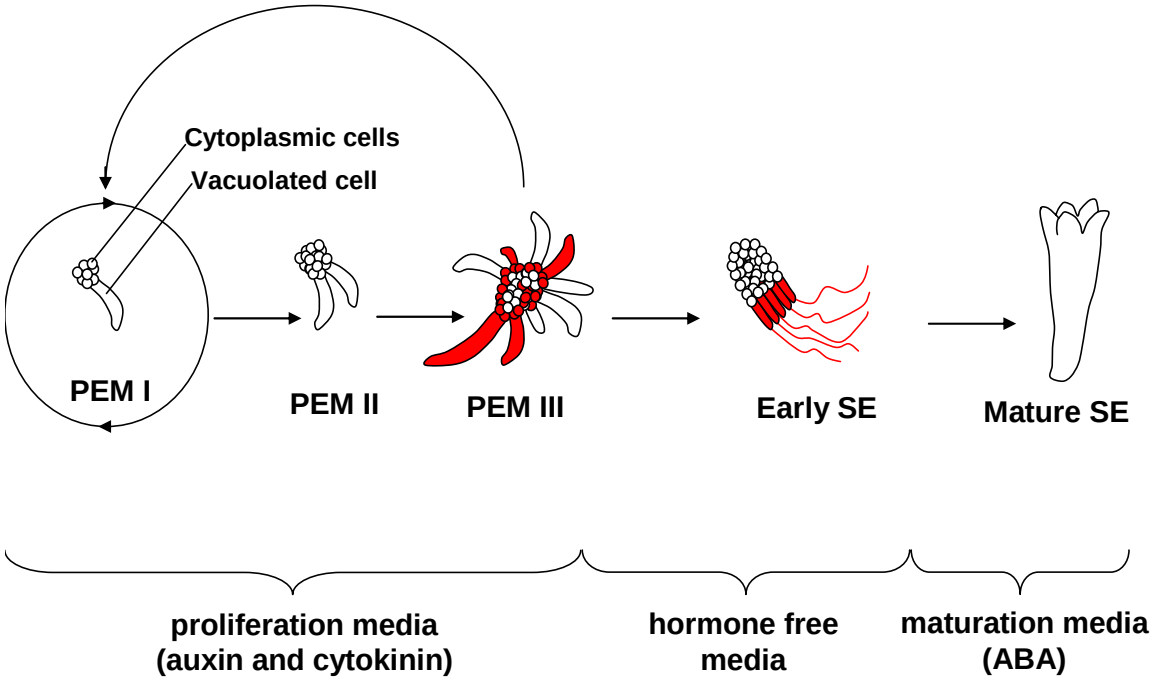

Figure 2.3. The process of somatic embryo formation in *Picea abies* (Norway spruce). In media containing the hormones auxin and cytokinin, PEMs proliferate. PEMs I are continually formed and develop into PEMs II and III. PEMs III can divide to produce more PEMs I. After transfer onto hormone-free media, early somatic embryos (SE) are formed from PEMs III. Once transferred onto media containing ABA, the SEs mature into viable cotyledonary embryos. Portions highlighted in red indicate areas where programmed cell death occurs. Adapted from Filonova et al. (2000a).

2.2.2.2 Late embryogenic stages: studies on white spruce (*Picea glauca*)

The later stages of embryo development in white spruce have been widely studied than early development. Here, embryo development can be divided into four stages that slightly overlap with those described for Norway spruce. These stages are delineated by precise morphological changes of the developing embryo (Figure 2.4). After 10 days on maturation medium, the early somatic embryos protruding from the embryogenic tissue are defined by an increase in the size of the embryogenic heads and suspensor-like tails (stage 1). After 20 days (stage 2), the embryos acquire a well-defined axis with the shoot (SAM) and root (RAM) apical meristems occupying the apical regions of the embryo proper. During this phase, a ring of cotyledons becomes visible at the apical pole. At 30 days (stage 3) the cotyledons expand and the embryonic axis elongates. Fully developed cotyledonary embryos (stage 4) are visible at the end of the 40 days. These embryos have expanded cotyledons, and a creamy-white color denoting the presence of abundant storage products, mainly starch and proteins (Stasolla and Yeung, 2003).

Studies have shown a distinct sequence of storage product deposition in white spruce somatic embryos: starch, followed by lipids and proteins (Joy et al., 1991). Starch is observed near the suspensor region of early somatic embryos and in the shoot pole and cortex of cotyledonary embryos (Joy et al., 1991; Kong et al., 1999). Proteins and lipids accumulate in a gradient beginning at the basal end during early embryogeny and ending at the apical end. Correspondingly, the RAM at the basal pole is established before the SAM suggesting a role of proteins and lipids in tissue patterning (Yeung et al., 1998).

The shoot apical meristem consists of an apical layer of densely cytoplasmic cells and a sub-apical layer of highly vacuolated cells rich in storage products (Figure 2.5) (Kong, 1994). Often, shoot apical meristems in somatic embryos are not as well organized as their zygotic counterparts; they are flat as opposed to rounded and have large intracellular spaces. These aberrations result in a lowered conversion frequency (Kong and Yeung, 1995). The structural events leading to the formation of the root apical meristem are unknown; however, organization of this structure is similar in both somatic and zygotic embryos, as both consist of isodiametric cells containing large nuclei (Kong, 1994) (Figure 2.5).

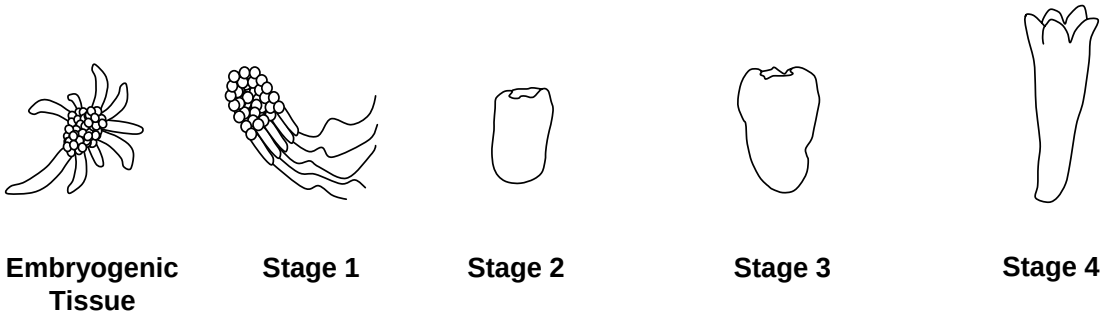

Figure 2.4. The four stages of conifer somatic embryo development. Embryogenic tissue is placed onto maturation media containing ABA. After ten days, stage 1 is reached. Somatic embryos begin to form, denoted by an increase in size of the embryo proper. After twenty days, stage 2 is reached. Cotyledons are initiated and root (RAM) and shoot (SAM) meristems begin to form. Stage 3 is observed after thirty days. Cotyledons begin to expand and the embryonic axis elongates. Finally after forty days, embryos reach stage 4. At this time, cotyledonary embryos become visible.

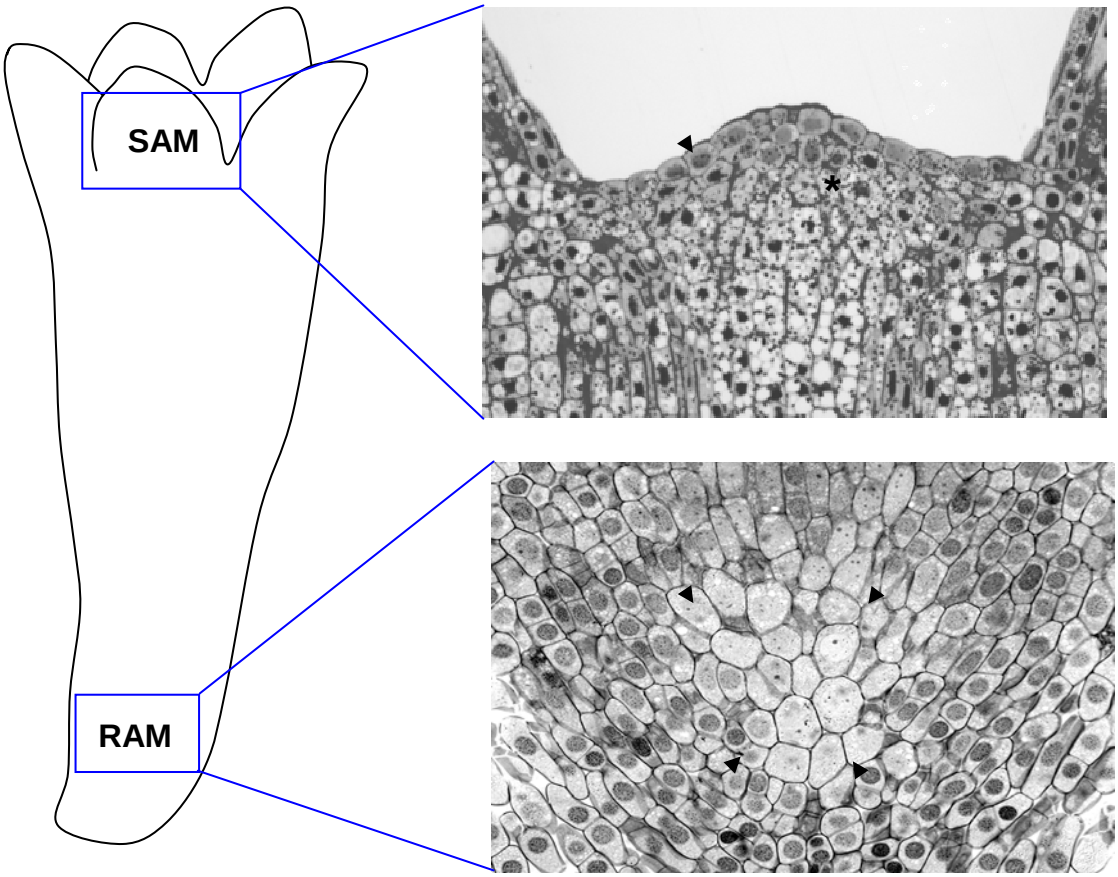

Figure 2.5. Apical meristem morphology of cotyledonary white spruce embryos. The shoot apical meristem consists of an apical layer of densely cytoplasmic cells (arrow) with a sub-apical layer of highly vacuolated cells (*) rich in storage products. The root apical meristem consists of isodiametric cells containing large nuclei (arrows).

2.3 Physiological events occurring during somatic embryogenesis

Much is known about morphological events occurring during somatic embryogenesis; however, with regard to physiological events, complications arise, as in many cases, contradictory data are reported for different genotypes (Stasolla et al., 2002). What is clear is that programmed cell death (PCD) plays an important role during the early stages of development, while ABA and osmoticum play a more important role during the later stages.

2.3.1 Physiological events taking place during the early phases of somatic embryo development

2.3.1.1 The role of programmed cell death (PCD) during PEM development

PCD is a process by which cells of a living organism are induced to undergo destruction via pre-programmed genetic cues (Ameisen, 2002). This process differs from other forms of cell death, for example necrosis, due to the fact that this is an event that is controlled by the plant, not due to external factors such as frost or herbicide damage. PCD can occur in one of two ways: apoptosis or autophagy (Summarized in Figure 2.6). By definition, apoptosis involves the process of a living cell engulfing a dying cell and degrading it in its lysosome, whereas during autophagy, degradation of a dying cell is carried out internally by a cell's own lysosome. The process by which programmed cell death occurs differs between plants and animals. Animals carry out either apoptosis or autophagy, whereas plants only carry out autophagy with some slightly similar characteristics to apoptosis (reviewed by van Doorn and Woltering 2005).

PCD occurs in many regions of the plant. External cues such as stress, toxins, or pathogens can result in either widespread or area specific cell death in a process known as hypersensitive response (Beers and McDowell, 2001). Developmental requirements such as tracheary element formation, trichome development, leaf senescence and root cap formation are all brought about by PCD (Pennell and Lamb, 1997). Perhaps most importantly is the proper development of embryos, where PCD plays a vital role in

embryo patterning. The morphological events caused by PCD during somatic embryogenesis have been extensively researched in Norway spruce (Filonova et al., 2000a; 2000b; Bozhkov et al., 2002; Filonova et al., 2002; Smertenko 2003).

The phenomenon of polyembryony, in the form of multiple PEMs within culture, is also observed during zygotic embryogenesis in pine. However, often only one embryo within a polyembryonic seed develops to maturity while the others are eliminated by PCD (Filonova et al., 2002). Filonova et al. (2000b) have described two PCD events that occur during somatic embryogenesis, which are required for proper embryo formation and can be correlated with similar events leading to the formation of polyembryonic seeds. The first event occurs when the concentration of the growth regulators auxin and cytokinin are reduced within the media. At this point, the number of somatic embryos increase while PEM numbers are reduced by PCD. Furthermore, it was also revealed that the majority of PCD occurs early in the vacuolated, suspensor-like cells of the PEM, followed later by PCD in the cytoplasmic, embryogenic heads. The second PCD event occurs as the somatic embryos mature. At this time, PCD is observed in the elongated suspensor cell, eventually leading to complete degradation of the suspensor, and allowing the embryo to continue normal development (Filonova et al., 2000b). Many PEMs die during development; therefore, the function of the large amount of PEMs produced has been questioned. In a study on carrot by McCabe et al. (1997), it was found that without a critical mass of embryogenic tissue (PEMs), PCD is induced. This implies that the main function of PEMs not destined to become mature embryos is to provide chemical cues to surrounding tissue and to maintain the embryogenic potential of the culture (Filonova et al., 2000b).

2.3.1.2 The role of PCD during suspensor degradation

The inability of a plant to degrade its suspensor has been observed in two *Arabidopsis* mutants, *twin* and *raspberry* (reviewed by Filonova et al., 2000b). In the case of *twin*, instead of dying, the suspensors proliferate, which results in the formation of multiple embryos. In *raspberry* mutants, the embryos are unable to continue maturation, and instead continue to form additional cytoplasmic and vacuolar cells.

Within spruce, the inability to degrade the suspensor has been observed in the non-embryogenic cell line 88.1 (Filonova et al., 2000a). In this case, suspensor degradation occurs late, an event that is thought to result in increased radial as opposed to axial growth, lack of protoderm, late shoot and root apical meristem formation, and degeneration of pith and cortex (once these tissues did finally form). These defects often resulted in the inability of mature embryos to germinate (Filonova et al., 2000a).

Figure 2.6. Varying processes of programmed cell death in animals and plants. Apoptosis in animals first involves chromatin condensation, followed by membrane envagination and DNA fragmentation (**A**). Cell contents are sequestered into apoptotic bodies that are then engulfed by other cells, where they are degraded in the lysosome. Autophagy in plants, as in animals, first involves chromatin condensation and DNA fragmentation (**B**). A double-membrane structure known as an autophagosome sequesters cytoplasmic contents for transportation to the vacuole. Cytplasmic contents are deposited into the vacuole where they are degraded. Tracheary element formation in plants involves similar processes as autophagy (**C**). The vacuole enlarges and ruptures releasing degrading enzymes into the cytoplasm. The cell wall thickens and becomes reticulated. Adapted from Lam (2004) and van Doorn and Woltering (2005).

2.3.2 Physiological events taking place during the late phases of somatic embryo development

2.3.2.1 The role of ABA during somatic embryogenesis

Much of what is known about the role of ABA during somatic embryo development has been extrapolated from the knowledge of what occurs within zygotic embryos. In zygotic embryos, ABA is supplied by the megagametophyte tissue (Kong et al., 1997). Levels of ABA vary during embryo development as well as in the different tissues of the seed: the megagametophyte and the embryo itself. Within the gametophyte, initial levels of ABA are relatively low before reaching a maximum midway through maturation of the embryo. ABA levels decline as the embryo continues to mature and, eventually, desiccate. Within the embryo, levels of ABA decline throughout maturation even while levels in the megagametophyte continue to increase (Kong et al., 1997). One explanation for high ABA levels during maturation is the need for increased storage product deposition and the inhibition of precocious germination (Bewley and Black, 1994). The requirement for ABA during embryogenesis has also been observed in culture, where it is needed to reduce proliferation of embryogenic tissue, a requirement for somatic embryo initiation and, like their zygotic counterparts, for promoting storage product accumulation (Dunstan et al., 1992). Studies suggest that the reduction in cell proliferation is due to the inhibitory effect of ABA on nucleotide salvage enzymes. Ashihara et al. (2001) observed a reduction in the activities of the salvage enzymes, adenosine kinase and adenine phosphoribosyltransferase during maturation in the presence of ABA. These enzymes are responsible for salvaging the purines, adenosine, adenine and inosine for nucleic acid synthesis. The reduction of this enzyme activity, in turn, causes a reduction of the cellular nucleotide pool, leading to decreased cell division (Ashihara et al., 2001).

Accumulation of storage proteins rich in arginine and glutamine occurs in response to ABA treatment, possibly due to preferential incorporation of inorganic, as opposed to organic, nitrogen. This causes an alteration in the amino acid profile and an increase in inorganic nitrogen assimilation enzyme activity (Joy et al., 1997). ABA

however is not solely responsible for the generation of mature embryos. When compared to their zygotic counterparts, white spruce somatic embryos matured on ABA still lack major polypeptides resulting in differences in protein body structure (Joy et al., 1991). Ascorbic acid metabolism, storage product accumulation, polyamine biosynthesis and ethylene accumulation are also affected by ABA (for review see Stasolla et al., 2002).

2.3.2.2 The role of osmoticum during somatic embryogenesis

As discussed above, the presence of osmoticum is required for embryo development and maturation. In angiosperm zygotic embryos, the negative osmolarity of the liquid endosperm is an important factor in slowing embryo development to accommodate proper embryo patterning (Yeung, 1995). The additive effects of ABA, along with osmoticum such as PEG, a non-permeating osmoticum agent, have been demonstrated. Attree et al. (1991) observed that including PEG in the medium increased embryo production and promoted storage product accumulation. The inclusion of both ABA and PEG in the maturation medium has also been shown to increase drying tolerance, as well as lipid and protein storage product deposition (Attree et al., 1992; 1995). As mentioned above, somatic embryos matured in the presence of ABA lack some major polypeptides. However, some of these polypeptides were produced when somatic embryos were matured in the presence of both PEG and ABA (Misra et al., 1993). This difference can be explained by the fact that synthesis of these polypeptides is initiated by ABA, but regulated by PEG (Misra et al., 1993). PEG has more recently been shown to cause alterations in the ascorbate-glutathione pool in a manner that mimics that of zygotic embryos. These alterations have been shown to be required for proper embryo development (Belmonte et al., 2005).

A PDT is used to mimic the water stress occurring during the final stages of maturation of zygotic embryos in preparation for germination. As observed by Kong and Yeung (1995), embryos matured with a PDT had lower endogenous ABA levels and were less responsive to further ABA treatment then embryos that did not experience a PDT. A study by Stasolla et al. (2001) showed that during the PDT, the activities of purine and

pyrimidine salvage enzymes, especially uridine kinase, increased in preparation for resumption of growth at germination.

2.4 Molecular events occurring during somatic embryogenesis

It is apparent that many morphological and physiological events accompany embryo development. Unfortunately, unlike angiosperms, the molecular mechanisms regulating embryogenesis in gymnosperms remain unknown. Studies on global gene expression patterns during embryogenesis reveal a reduction in transcript levels during the transition from PEM I to PEM III and an increase in transcript levels during the transition from PEM III to early somatic embryos. This pattern appears to be essential for normal embryo development as it is reversed in non-embryogenic lines (Stasolla et al, 2004). This transcription pattern, also observed in the animal system, has been interjected by Forlani et al. (1998), who suggested that the initial period of gene silencing might act to delay embryo differentiation until the appropriate developmental stage is reached.

The inclusion of specific growth regulators into the culture medium controls the rate of cell proliferation and differentiation during embryogenesis. Studies that focus on elucidating the molecular mechanisms regulating both processes are underway. The induction of embryogenic tissue in both angiosperms and gymnosperms requires the presence of auxin. Many auxin-responsive markers have been isolated, including DC3 and ECP31, both of which were discovered in carrot somatic embryos (De Vries et al., 1988; Kiyosue et al., 1992). In conifers, studies have shown that non-embryogenic lines lack the expression of certain peroxidases, chitinases and extracellular components thought to be essential for embryogenic tissue induction (Egertsdotter et al., 1993; Egertsdotter and von Arnold, 1995; Mo et al., 1996). A family of proteins known as arabinogalactans (AGPs), which are expressed in high levels in embryogenic lines, have been shown to increase the potential of a non-embryogenic line to become embryogenic when over-expressed in the tissue (Egertsdotter and von Arnold, 1995). Dong and Dunstan (1996) showed that upon exposure to ABA, expression levels of genes encoding storage proteins and late-embryogenesis abundant (LEA) proteins increased. Previous

studies have shown that the presence of storage proteins and LEAs can be considered as a good marker for embryo maturation in both angiosperms and gymnosperms. Accumulation of storage proteins and LEAs is important for embryo maturation as both are required during the desiccation process (Dong and Dunstan, 2000).

2.5 Genes involved in meristem development

2.5.1 Genes involved in shoot apical meristem initiation and maintenance in flowering plants

During embryogenesis, basic patterning information and morphological fates are established. The disruption of these processes may be detrimental to further development. The shoot apical meristem (SAM) determines where and when organ and tissue formation occurs.

In *Arabidopsis,* the architecture of the SAM can be described using two models: the germ layer model and the zonation pattern model (Figure 2.7) (Carles and Fletcher, 2003). The germ layer model describes the meristem as having three layers, each giving rise to different tissue types. Layer 1 (L1) gives rise to the epidermis, Layer 2 (L2) gives rise to the stem cells and Layer (L3) gives rise to the vascular tissue. In the zonation pattern model, three zones are described. The central zone (CZ) contains slow-dividing stem cells. The peripheral zone (PZ) and the rib zone (RZ) are found adjacent and below the CZ respectively. These two zones contain faster dividing cells that give rise to lateral organs (PZ) or shoot cells (RZ).

An important function of the SAM is its ability to continually produce undifferentiated cells (Lenhard and Laux, 1999). Over time and space, these cells differentiate and are incorporated into different organs depending on where they are located. A balance between cell differentiation and proliferation must be maintained in the meristem, where the number and location of meristematic cells do not change over time (Viet, 2004). Any disruption of this balance would cause the meristem to either over-produce undifferentiated cells or to completely lose function due to a lack of undifferentiated cells. In *Arabidopsis*, the expression of four genes, *WUSCHEL* (*WUS*),

CLAVATA (*CLV*), *SHOOTMERISTEMLESS* (*STM*), and *ZWILLE* (*ZLL*), helps to maintain meristem function (Fletcher and Meyerowitz, 2000).

WUS is a homeodomain transcription factor that is expressed in the L3 of the CZ (Laux et al., 1996). Experiments on loss of function mutants have elucidated its role as specifying stem cell fate by acting non-autonomously in L1 and L2 (Mayer et al., 1998). *CLAVATA* refers to a family of genes made up of *CLV1*, *CLV2* and *CLV3*, which are all part of the CLAVATA signal transduction pathway that acts to limit SAM over-proliferation (Clark et al., 1995; Kayes and Clark, 1998). *CLV1* is expressed in the L3 of the CZ while *CLV2* is expressed in a wider region. Both *CLV1* and *CLV2* act as receptors for *CLV3*, which is a ligand expressed in the L1 and L2 of the CZ (Brand et al., 2000). WUS expression induces the expression of *CLV3* and, in turn, *CLV3* signaling, through *CLV1* and *CLV2*, acts to inhibit *WUS* expression (Schoof et al., 2000). Through this feedback mechanism the size of the stem cell pool is kept constant.

Running parallel but independent of the WUS/CLV negative feedback loop is *STM*. *STM* is a Knotted-1 like homeobox (KNOX) transcription factor that acts to inhibit stem cells from differentiating into tissue and organ cells (Castellano and Sablowski, 2005). *STM* expression is regulated by *ZLL* (Groβ-Hardt and Laux, 2003).

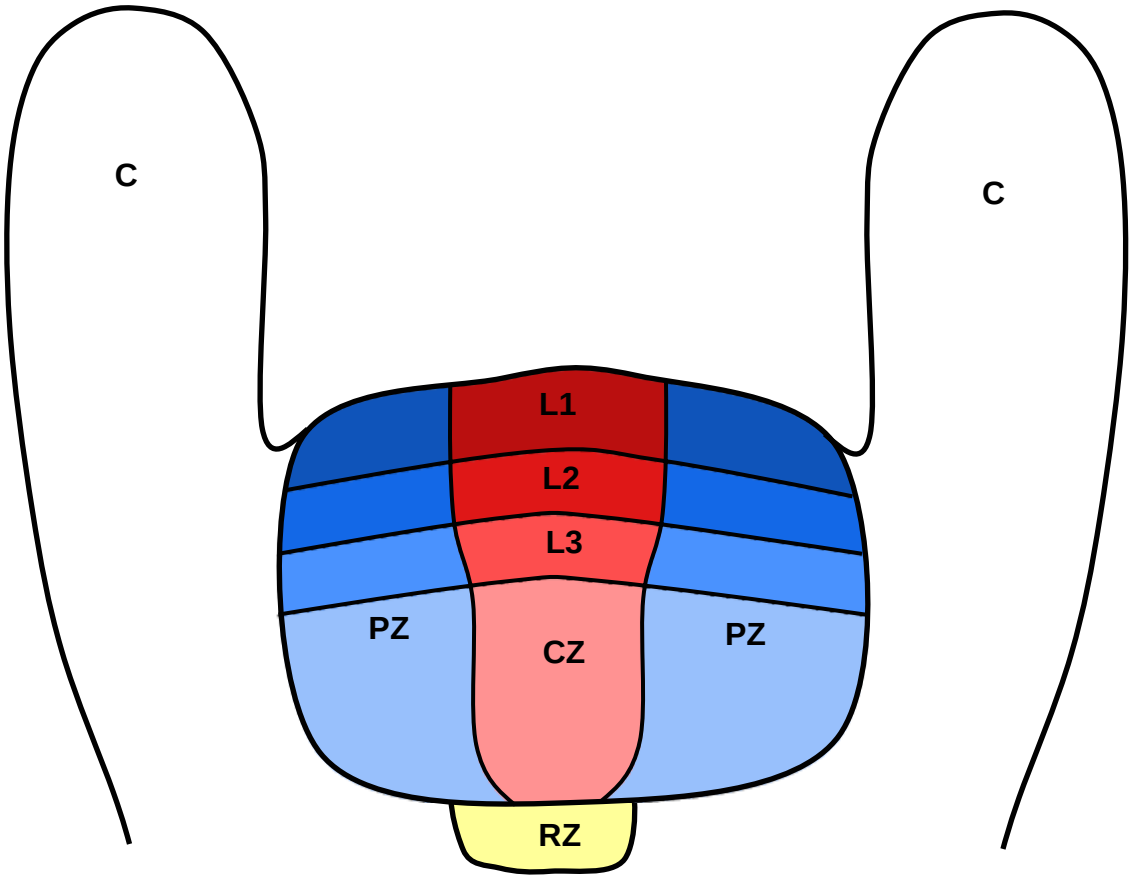

Figure 2.7. The architecture of the SAM in *Arabidopsis*. The germ layer model divides the meristem into three layers. Layer 1 (L1) gives rise to the epidermis, Layer 2 (L2) gives rise to the stem cells and Layer 3 (L3) gives rise to the vascular tissue. The zonation pattern model divides the meristem into three zones. The central zone (CZ) contains slow-dividing stem cells. The peripheral zone (PZ) and the rib zone (RZ) contain faster dividing cells that give rise to lateral organs in the PZ or shoot cells in the RZ. Adapted from Carles and Fletcher (2003). C, cotyledon.

2.5.2 Genes involved in shoot apical meristem initiation and maintenance in conifers

Compared to flowering plants, the molecular mechanisms that regulate conifer embryogenesis are poorly understood. In the past few years, much effort has been directed towards the identification of putative genes which may control embryo growth and SAM development. Microarray analysis using expressed sequenced tags (ESTs) have revealed a large degree of gene expression occurring during the different phases of embryo development and between embryos of different quality (Stasolla et al., 2003). These studies represent a framework for further investigations on the molecular network which governs embryo development in vitro.

2.5.2.1 Homeobox genes

Homeobox genes have been found to encode transcriptional factors in plants as well as all other eukaryotes (Kerstetter et al., 1994). These transcriptional factors are regulatory proteins which, through the activation of other genes, specify cell identity and regulate tissue patterning (Sundås-Larsson et al., 1998). Homeobox genes are identified by a common 180 bp sequence that encodes the Homeobox or Homeodomain region (Buchanan et al., 2000), which is the DNA binding domain responsible for the activation and transcription of target genes. Homeobox genes have been discovered in many different organisms, including plants and animals (Holland and Garcia-Fernàndez, 1996; Reiser et al., 2000; Ruddle et al., 1994). Two homeobox genes, *Knotted-1* (*Kn1*) in maize and *STM* in *Arabidopsis*, belonging to the *knotted-like homeobox* (*KNOX*) class of homeobox genes, are specifically expressed in meristems (Sundås-Larsson et al., 1998). Through gain and loss of function experiments, it has been shown that these two genes play an important role in meristem development (Long, 1996; Hay, 2003). The *KNOX* gene family includes members which are homologous in several species including maize, rice, barley, *Arabidopsis*, soybean, tobacco, tomato and white spruce (Reiser et al., 2000). These genes can be divided into two classes depending on the localization of their transcripts. Class I genes are only expressed in the meristem, while Class II genes are found expressed in all organs (Hjortswang et al., 2002).

A Class I gene, *HBK1* (homeobox of the KNOX class), was the first KNOX gene to be discovered in a conifer (Sundås-Larsson et al., 1998). Two other genes of the same family have since been discovered in spruce, *HBK2* and *HBK3* (Hjortswang et al., 2002). HBK3 was found to have 86% protein sequence identity to HBK1, while HBK1 and HBK3 were found to show about 50% identity to HBK2 (Hjortswang et al., 2002). Interestingly, compared to *HBK1* and *HBK3*, which are expressed in all cell lines, *HBK2* is only expressed in embryogenic lines. This information suggests that *HBK2* may be required for proper embryo development in conifers (Hjortswang et al., 2002).

2.5.2.2 Argonaute-like genes

As indicated previously, *ZLL* plays an important role in meristem regulation in angiosperms. An extensive study on the role of *ZLL* in *Arabidopsis* has been completed by Moussian et al. (1998). Here, it was shown that the spatial expression of *STM* is altered during embryonic development in *ZLL* mutant plants. In-situ hybridization studies showed that *ZLL* was expressed in the embryo apex as well as in provascular cells. Through map-based cloning techniques, the gene was completely sequenced and found to be 2964 bp long, encoding a protein that is similar to ARGONAUTE1 (AGO1), a protein required for leaf development in *Arabidopsis* and thought to have a redundant function to *ZLL* (Moussian et al., 1998).

ARGONAUTE (AGO) proteins are defined as having two conserved domains, a C-terminal 300-amino acid PIWI domain and an N-terminal PAZ domain (Cerutti et al., 2000). Structural studies of AGO proteins had focused on the PAZ domain (Yan et al., 2003); however, the ability to produce large amounts of full length AGO from eukaryotes proved difficult, and thus the complete structure of AGO remained unknown (Tanaka Hall, 2005). Song et al. (2004) were the first to describe the structure of an AGO protein. Instead, using a protein derived from a prokaryote, *Pyrococcus furiosus* (PfAgo), they found the structure of AGO to be composed of 4 domains: the N-terminal, PIWI, and Middle domains which constitute the crescent shaped base, and the PAZ domain, which lies above the base connected by a region attached to the N-terminal domain. Since this discovery, other full-length AGO protein structures have also been described in

Archaeoglobus fulgidus (AfPiwi) (Parker et al., 2004) and *Aquifex aeolicus* (AaAgo) (Yuan et al., 2005), furthering our understanding of AGO protein structure and function.

AGO proteins are required for gene silencing through RNA interference (RNAi) (Cerutti et al., 2000). RNAi involves mRNA degradation from sequence specific gene silencing by double-stranded RNA (dsRNA). In this process dsRNA is converted into 25 nt segments known as short interfering RNAs (siRNAs), which are used as a template by an RNA-induced silencing complex (RISC) to target and degrade complementary mRNA (Reviewed by Carmell et al., 2002). Song et al. (2004) have proposed that the function of the PAZ domain is to bind siRNA, which in turn binds target mRNAs through the active site of the PIWI domain. This interaction results in mRNA degradation and gene silencing of the target gene.

Evidence from studies on *Drosophila* and *C. elegans* have revealed the importance of AGO proteins in determining stem cell identity and cell fate. In a study by Cox et al. (1998), it was shown that the *Drosophila* AGO protein PIWI was responsible for maintaining a pool of undifferentiated stem cells. The AGO1 protein in *C. elegans* is responsible for stem cell maturation (Kataoka et al., 2001). The requirement of AGO proteins in stem cell regulation was also described in plants. Studies on *Arabidopsis* ZLL mutants have been described by Moussian et al. (1998). Wild-type seedlings have a characteristic rosette of leaves produced by the SAM, while mutant seedlings either have absence of growth where the SAM should be, the initiation of an undifferentiated structure, or a leaf. These symptoms further substantiate evidence of the role of AGO proteins in meristem regulation.

2.6 Research Objectives

Based on the above information, the objectives of the proposed research program are:

1. To identify the homolog of *ZLL* in spruce and to study its function during spruce somatic embryo development.
2. To study the role of *HBK2* during spruce somatic embryo development.

These objectives will be achieved through three steps. First, the full length genes will be obtained through screening of cDNA libraries and through 5' RACE (Rapid Amplification of cDNA Ends). The study conducted by Hjortswang et al. (2002) only provides a partial sequence (about 1200 bp) of *HBK2* with an incomplete 5' region. A 370 bp expressed sequence tag (EST) clone containing a partial sequence of *ZLL* is available from loblolly pine (*Pinus taeda*). This will be achieved with two alternative techniques: screening of three cDNA libraries constructed from RNA of embryos at different stages of development, and extension of the untranslated regions through RACE. The results from these different techniques can be compared to confirm that the missing part of the clone has indeed been obtained.

Secondly, RNA in-situ hybridization will be used to determine the localization of *HBK2* and *ZLL* transcripts during embryo development.

Finally, the function of these genes during embryo development will be investigated through RNA antisense transformation studies. Down-regulation of *HBK2* and *ZLL* will be followed by morphological studies aimed at investigating both embryo number and quality.

3.0 MATERIALS AND METHODS

3.1 Plant material

3.1.1 White spruce (*Picea glauca*)

White spruce, *Picea glauca* (Moench) Voss, embryogenic tissue was generated from immature zygotic embryos (Lu and Thorpe, 1987). Briefly, immature seeds were sterilized in 20 % commercial Javex bleach for 20 min., and then rinsed 3 times in sterile distilled water. Dissected embryos were placed on induction medium (Appendix 1). The initiated stock cultures were kept in the dark at 26° C for 4-6 weeks. Embryogenic tissue was transferred to a solid maintenance medium (Appendix 1) and sub-cultured every 7 days to fresh medium. Established cultures were also maintained in liquid maintenance media (Appendix 1). Maturation of somatic embryos was initiated by spreading 100 mg (fresh weight) of embryogenic tissue directly onto solid maturation medium (Appendix 1) (Belmonte and Yeung, 2004). Mature somatic embryos, characterized by the presence of fully elongated cotyledons, were harvested after 40 days (Belmonte and Yeung, 2004). Partial drying of embryos was achieved following the methods of Roberts et al. (1990). Mature embryos were placed onto sterile 42.5 mm Whatman 1 filter papers within a 60mm x 15mm petri plate. This small plate was placed uncovered into the centre of a 100 mm x 15 mm petri plate. Sterile distilled water was poured into the 100 mm plate 3/4 full to maintain relative humidity, then covered, sealed with parafilm, and left in the dark for 10 days. Embryos were then placed upright in hormone-free germination media (Appendix 1) for 8 weeks at 25^{o}C under light with a 16 h photoperiod.

3.1.2 Norway spruce (*Picea abies*)

Norway spruce, *Picea abies* (L.) Karst., embryogenic tissue was generated from immature zygotic embryos as described by Filonova et al. (2002). Initiation and maintenance of embryos was achieved using similar methods to those described in section 3.1.1 with the exception that proliferation media (Appendix 1) was used to

maintain the cultures. Embryos were matured by placing 100 mg of tissue onto DKM prematuration media (Appendix 1), devoid of growth regulators, for 10 days. The tissue was then transferred onto DKM maturation media (Appendix 1) until mature embryos formed.

3.2 Generation of full length *PgAGO*

The first step of this research program was to obtain full length cDNA of *PgAGO*. The sequence available for *PgAGO* was a 513 bp EST clone from *Pinus taeda* similar to *Arabidopsis thaliana* sequence coding for a ZLL-like protein. The complete sequence was obtained using a combination of two techniques: screening of cDNA libraries constructed from RNA of embryos at different stages of development, and extension of the 5' or 3' regions of partial sequences through RACE.

3.2.1 cDNA library construction

Two cDNA libraries were obtained from immature (day 20) and mature (day 40) white spruce somatic embryos. Total RNA was extracted using the RNeasy Plant Mini Kit (Qiagen, Santa Clarita, CA, USA) following the manufacturer's instructions. The extracted RNA was used for cDNA library production with the SMART™ cDNA Library Construction Kit (CLONTECH, USA). The steps of cDNA library construction are summarized below and in Figure 3.1.

3.2.1.1 First strand cDNA synthesis

A reaction mixture was produced using approximately 1 µg of purified RNA from either immature or mature embryos. Also included in this reaction were the SMART IV oligonucleotide, CDS III/3' primer, and PowerScript™ reverse transcriptase. The PowerScript™ reverse transcriptase enzyme transcribed from the 3' end of the RNA with the aid of the CDS III/3' primer. This primer annealed to the polyA tail found at the 3' end of the RNA. The chemistry of the reverse transcriptase is such that, as transcription reaches the 5' end of the RNA, the enzyme adds additional cytosines. This tail of

cytosines allows the SMART IV oligonucleotide, with its terminal sequence of oligo guanines, to anneal to it. The reverse transcriptase enzyme continues to synthesize the first strand of DNA now using the annealed SMART IV oligonucleotide as a template. The result is a single strand of DNA that contains the complete RNA sequence as well as *Sfi* digestion sites at either end that were encoded within the CDS III/3' primer and the SMART IV oligonucleotide sequences. This first strand of DNA remains annealed to the mRNA acting like double stranded DNA ready for polymerase chain reaction (PCR).

3.2.1.2 cDNA amplification by Long Distance PCR

A PCR reaction was produced using the 5' PCR primer provided with the SMART^{TM} cDNA Library Construction Kit, containing a complementary sequence to the SMART IV oligonucleotide, along with the CDS III/3' primer. The ability to amplify larger sequences was achieved by using the 50X Advantage 2 polymerase mix included in the kit as well as a longer extension time (6 min) within the PCR cycle. The double stranded DNA produced contained the complete RNA sequence along with *Sfi* restriction sites at either end, allowing for insertion into vectors without the loss of coding regions of the gene. Following this step the cDNA was purified using the QIAquick PCR purification kit (Qiagen, Santa Clarita, CA, USA) following the manufacturer's instructions.

3.2.1.3 *Sfi* 1 digestion

The *Sfi* 1 restriction enzyme cleaved each end of the cDNA to produce "sticky" ends that would be used for insertion into an *Sfi* 1 digested vector. The restriction enzyme sites on each end were different and thus were not able to ligate to each other before being exposed to the vector.

3.2.1.4 cDNA size fractionation by CHROMA SPIN-400

After the cDNA was digested with the *Sfi* 1 enzyme, the product contained both digested ends and cDNAs of different lengths. To increase the probability of correct hybridization during screening, it was recommended to reduce the amount of DNA used. This was accomplished through size fractionation. The cDNA was passed through the CHROMA SPIN-400 column that first elutes the larger strands of cDNA followed by smaller strands. Each drop from the column was collected in a separate vial. After collection, each fraction was visualized by electrophoresis. Fractions containing the most cDNA in the appropriate size range were pooled. This fractionation also acted as a purification step removing any digested ends. The cDNA was then recovered from the solution by a precipitation reaction.

3.2.1.5 Ligation of cDNA to λTriplEx2 vector and insertion into a λ phage

The cDNAs were inserted into a digested λTriplEx2 vector provided with the kit, then packaged into a phage using Gigapack III Gold Packaging Extract (Stratagene, La Jolla, CA, USA).

3.2.1.6 Obtaining the titer of the un-amplified library

Petri plates containing LB media were inoculated with a bacterium and phage mixture. After a few hours, the plate became covered with bacteria, commonly described as a "lawn" of bacteria. Eventually, clear patches formed on the lawn. These clear patches indicated areas where phage infected bacterial cells were lysed. These areas were covered with dead bacteria as well as phages containing many copies of inserted cDNA. The clear patches are commonly referred to as "plaques".

An estimate of the number of plaques on each plate was obtained. This number was applied to a formula provided in the SMART^{TM} cDNA Library Construction Kit User Manual and the amount of phage per mL, or Titer, was calculated.

$$\text{Titer (pfu/mL)} = \frac{\text{number of plaques x dilution factor x 103 μL/mL}}{\text{μL of diluted phage plated}}$$

3.2.1.7 Library amplification

The number of plaques per plate was increased and many plates were produced. SM buffer (Amresco, Solon, Ohio) was then used to remove the cDNA from the plates. The cDNA was then pooled and a stock of amplified cDNA library was produced at a concentration of about 10^{10} pfu/mL.

Figure 3.1. Steps involved in the construction of cDNA libraries. All reactions were carried out following the instructions and using the chemicals provided in the SMART™ cDNA Library Construction Kit. In step one, the first strand of cDNA was synthesized from Poly A+ RNA. The CDSIII Primer, containing an *Sfi* 1 restriction enzyme digest site, annealed to the poly A 3' end of the RNA. cDNA was transcribed by the Powerscript™ reverse transcriptase enzyme. Once the enzyme reached the 5' end of the RNA, terminal cytosines were added to the cDNA, allowing the SMART IV oligonucleotide, also containing an *Sfi* 1 restriction enzyme site, to anneal. Reverse transcription continued, and a single strand of full length cDNA was produced. In the second step, a long distance PCR reaction was prepared, resulting in double stranded cDNA. In the third step, the ends of the cDNA were digested with the *Sfi* 1 restriction enzyme producing sticky ends. In the fourth step, the digested cDNAs were fractionated by size through the CHROMA SPIN-400 column producing a pool of cDNAs of the appropriate size. In the fifth step, cDNAs were ligated into the λTriplEx2 vector which is then packaged into a phage using Gigapack III Gold Packaging Extract. Libraries were amplified in step six.

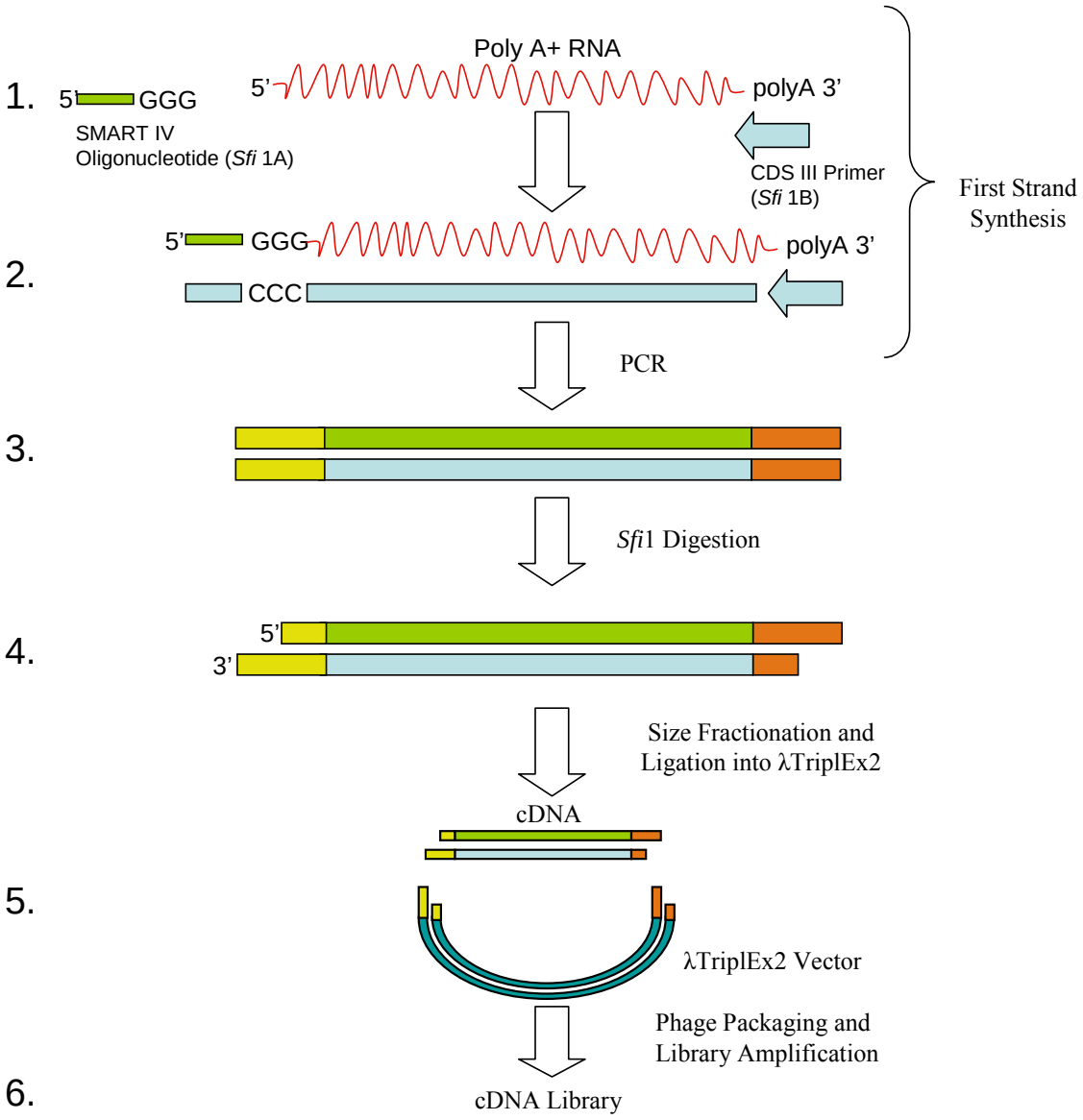
1.
5'
GGG
SMART IV
Oligonucleotide (Sfi 1A)
Poly A+ RNA
5'
polyA 3'
CDS III Primer
(Sfi 1B)
First Strand
Synthesis
2.
5'
GGG
polyA 3'
CCC
PCR
3.
Sfi1 Digestion
4.
5'
3'
Size Fractionation and
Ligation into λTriplEx2
cDNA
5.
λTriplEx2 Vector
Phage Packaging and
Library Amplification
6.
cDNA Library

3.2.2 *PgAGO* probe preparation and cDNA library screening

A *Pinus taeda* EST clone NXSI_035_A04 (Gene Bank # BF518099) similar to *Arabidopsis thaliana* sequence (At5g21150) coding for ZLL/PNH-like protein was obtained from the Forest Biotechnology Group, North Carolina State University, USA. Using appropriate primers (5'-GAATCGCAATTTGACCAGGT and 5'-CATTTAGCT-GCGAGCCAGATGCAA) designed from the BF518099 sequence, a P^{32}-labeled ~400 bp DNA fragment was generated using the EST clone as a template (Sambrook and Russel, 2003). The labeled DNA fragment was then used as a probe to screen the two spruce cDNA libraries. A large number (~10^{4-6}) of cDNA clones from the cDNA libraries were transferred to nylon membranes and hybridized with the labeled probe in 50% formamide, 6X SSC, 5X Denhardt's solution, 0.5% SDS, and 0.1 mg/mL salmon sperm DNA at 42°C for 14-16 h. The filters were subjected to a first wash (2X SSC, 0.1% SDS) at room temperature followed by a second wash (0.2X SSC, 0.1% SDS) at 65°C (Sambrook and Russel, 2003). Positive clones embedded in λTripleEx2 vector were retrieved by in-vivo excision following the methods described by BD Biosciences, and sequenced at Macrogen facility (www.macrogen.com).

3.2.3 *PgAGO* Rapid Amplification of cDNA Ends (RACE)

In cases where library clones were sequenced and found to be incomplete, the missing ends were amplified from RNA using RACE. This was accomplished using the FirstChoice® RLM-Race Kit from Ambion, following the instructions listed by the manufacturer and briefly summarized below.

3.2.3.1 RNA processing

The RNA obtained from developing spruce somatic embryos was first treated with Calf Intestine Phosphatase (CIP) and Tobacco Acid Pyrophosphatase (TAP). CIP removed 5' phosphates from incomplete RNA and DNA and rendered them incapable of being processed further. The full length mRNAs were not affected by CIP and were

treated with TAP to remove the cap structure found at the 5' end. A ligation reaction was carried out in order to attach the 5' RACE Adapter to the mRNA.

3.2.3.2 Reverse transcription

Using random decamers, a reverse transcriptase reaction was set up to synthesize a single strand of DNA. This single strand contained the complete mRNA sequence with the inclusion of the 5' RACE Adapter.

3.2.3.3 Nested PCR for 5' RNA Ligase Mediated (RLM)-RACE

A PCR reaction was set up to amplify a segment of the 5' end. A primer included with the kit (5'-CGCGGATCCGAACACTGCGTTTGCTGGCTTTGATG) acted as the forward primer and annealed to a segment of the 5' adapter. Another primer designed specifically for *PgAGO* (5'-AGGATGGCAAATCTGGGAATCT) acted as the reverse primer. The final product was the 5' end of the *PgAGO* sequence, along with a partial sequence of the adapter. The product from this reaction was used again for a nested PCR reaction to confirm the amplification product.

This PCR product was visualized on agarose gel to see if a single band was obtained, then ligated and sub-cloned into *E. coli* using the pGEM®-T Easy Vector System II (Promega), and then sequenced (www.macrogen.com).

New clones generated by RACE that, after further analysis, still did not contain a complete sequence, were used as probes to re-screen the libraries. This method of extension was continued until a full length clone was obtained.

3.2.3.4 3' RLM-RACE

3' RLM-RACE was used in cases where the 3' end of the cDNA was truncated. In these cases, no RNA processing of the 5' end was needed. The methods used were similar to those described in sections 3.2.3.2 and 3.2.3.3 with the exception of the use of a 3' RACE adaptor during reverse transcription, and the use of a gene specific forward primer and a reverse primer provided by the kit for the nested PCR.

3.3 Molecular characterization of *PgAGO*

Protein sequences that were similar to *Pg*AGO were found using blastp available from the NCBI-BLAST home page (http://www.ncbi.nih.gov/BLAST/). Sequences were chosen based on both high similarity along the entire protein length as well as similarity within the PIWI and PAZ domains. Sequence alignment was carried out using the ClustalX (v1.83) program. The alignment was visualized using BOXSHADE (v3.21) available online at http://www.ch.embnet.org/software/BOX_form/html. The phenogram was produced using the MegAlign program, a component of DNASTAR. Inc. Software. The phenogram produced was based on the Clustal method with the PAM250 residue table.

Description of the hydropathy of the protein defines whether the putative protein is hydrophobic, hydrophilic, or a combination of both, allowing for proper localization in the chloroplast, mitochondrion, or spanning a membrane. These descriptions were obtained using the ProtScale program (www.expasy.org/tools/protscale.html), available through the ExPASy Proteomics server, and the TargetP program, available through the Center for Biological Sequence Analysis website (www.cbs.dtu.dk/services/TargetP/).

3.4 In-situ hybridization studies

3.4.1 Chemical fixation and tissue processing

Chemical fixation and tissue processing were performed as described by Belmonte et al. (2005). Briefly, developing embryos were fixed in 4% (w/v) freshly prepared paraformaldehyde in PBS pH. 7.4, vacuum-infiltrated for 15 min, and incubated on a rotator for 3 hours at room temperature. The samples were dehydrated in an ethanol series (30%, 50%, 70%, 95%, 100%, 100%) for 45 min at 4°C and left overnight in 100% ethanol. The samples were treated with increasing concentrations of xylene at room temperature and incubated overnight at 42°C in xylene and a few pellets of paraffin. The tissue was then incubated at 60°C and the xylene was slowly replaced with molten paraffin. After 8 changes with paraffin, blocks were made and the paraffin-embedded

embryos were sectioned at a thickness of 7 μm, using disposable blades in a Leica (RM 2145) microtome. Prior to hybridization, paraffin was removed with two changes of xylene for 15 min, and the sections were re-hydrated.

3.4.2 Probe preparation and hybridization

A truncated *PgAGO* gene of 1200bp was amplified with primers containing T7 and T3 sites (5'-TAATACGACTCACTATAGGGGCGTTTCTCTGGCTTTGAGG and 5'-AATTAACCCTCACTAAAGGTTTGGCAATTTCTCGACGAT). The PCR product was used for in vitro transcription using digoxigenin-11-UTP, as described in the DIG RNA labeling kit (Roche Molecular Biochemicals). Sense and antisense probes were hydrolyzed for 40 min at 60°C in the presence of 60 mM Na_2CO_3 and 40 mM $NaHCO_3$, and stored at -80°C prior to hybridization.

Tissue treatments and pre-hybridization washes were conducted exactly as described in Cantón et al. (1999). Sections were hybridized with equal concentrations (25 μg/mL) of sense or antisense probes in 1x Denhardt's, 1 mg/mL tRNA, 10% dextran sulfate, 50% formamide, and 1x salts (Regan et al., 1999). Probes were denatured at 65°C for 5 min and hybridization was carried out at 50°C for 16 hours. Post-hybridization washes and an antibody treatment were performed as described by Regan et al. (1999). Detection of DIG-labeled probes was carried out using a Wester Blue solution (Promega) containing 1 mM Levamisol. Depending on the developmental stages of the embryos, color development occurred between 3-12h.

3.5 Reverse Transcriptase (RT)-PCR studies

During the maturation period, total RNA was extracted using the RNeasy Plant mini kit (Qiagen) from the tissue of one embryogenic line (E)WS1 and one non-embryogenic line (NE)WS (Stasolla and Yeung, 2001) at days 0, 10, 20, 30, and 40. cDNAs were synthesized using 2 μg total RNA, 500 ng oligo-dT_{17}-adapter primer (5′-GACTCGAGTCGACATCGA-$(T)_{17}$V-3′) and 15 U M-MuLV reverse transcriptase in a 20 μL reaction. Gene-specific primers (5'-CACGTGAGCTTCAGCAATGT and 5'-TTTCGCAATTTCTCGACGAT) were

used to detect the expression of *PgAGO*. Amplification by PCR was as follows: 94 °C for 30 s, 50 °C for 30 s, 72 °C for 2 min, 29 cycles. Additional reactions using spruce actin (Gene Bank # AF172094) primers (5'-TTGGCATCTCTCAGCACATTC and 5'-TAGGTT-TCTGGTCACGTCTAC) confirmed that equal amounts of cDNA were used.

3.6 Spruce Transformation

3.6.1 Preparation of construct

The plasmid used for transformation was *pUTV45* (Clapham et al., 2000). Originally, this plasmid contained a GUS reporter gene downstream from a maize ubiquitin promoter. This GUS reporter was cleaved from the plasmid with *SacI* and *BamHI* restriction enzymes. The same segment of *PgAGO* used for the in-situ hybridization experiments described in section 3.4 was amplified using primers altered to contain the appropriate restriction enzyme sites (5'-GAATGAGCTCCGCAATTTGACC-AGG and 5'-TTGCGGATCCATCTGGCTCGCAGCTAAATG). This segment was then inserted into the plasmid in antisense orientation, and then used to transform *E. coli* using the pGEM®-T Easy Vector System II (Promega).

3.6.2 Plasmid Preparation

Norway spruce tissue was transformed via micro-projectile bombardment. Specific procedures were carried out according to the methods of Clapham et al. (2000) as modified by Ciavatta et al. (2002). Briefly, *PgAGO* antisense constructs were co-bombarded with equimolar amounts of pUbi-BAR, a plasmid containing a gene conferring resistance to the herbicide BASTA driven by a maize ubiquitin promoter. For a total of 80 transformation events, 2 vials containing 10 mg of gold particles were coated with a 1:2 ratio of resistance vector to gene vector (due to the smaller size of the gene vector). A mixture of sodium acetate and cold ethanol was added to the DNA and gold particle mixture, and left at -20^{o}C to allow the DNA to precipitate. After at least 1 hour of precipitation, the vials containing the DNA were quickly centrifuged and the

supernatant was discarded. The gold particles coated with DNA were re-suspended in 1.1 mL of 100% ethanol.

3.6.3 Tissue Preparation

Liquid Norway spruce cultures were allowed to sediment in four sterile 50 mL tubes to produce a total of 15 to 20 mL of sedimented cells per tube. These cells were resuspended with recovery media (Appendix 1) to a volume of 45 mL, and then gently mixed. A dual layer of sterile 125 mm Whatman 1 filter paper was placed into ten 150 mm x 15 mm Petri plates, and then saturated with liquid recovery media. Using a sterile vacuum filter, 2 mL of suspended culture was placed onto sterile 42.5 mm Whatman 1 filter paper and excess liquid was removed. This filter paper, coated with cells, was placed into the 150 mm Petri plates containing filter paper saturated with liquid recovery media. This process was repeated until each 150 mm plate contained 8 42.5 mm pieces of filter paper coated with cells.

3.6.4 Tissue transformation

Each 42.5 mm piece of filter paper, covered in cells, was bombarded with 20 μL of coated gold particles, and then placed onto 100mm x 15 mm plates containing solid recovery media to a total of 3 pieces of filter paper per plate. Tissue was kept on recovery media for 10 days at 26^{o}C in the dark, and then it was transferred onto selection media containing the herbicide BASTA (Appendix 1) for 30 days at 26^{o}C in the dark. Tissue was transferred onto fresh selection media after 30 days in culture.

After 60 days, tissue was observed to detect the presence of transformed cells. Any living tissue was transferred onto maintenance media to proliferate. Once enough tissue was available, genomic DNA was extracted and the presence of the antisense *PgAGO* gene was detected by PCR. Here, a forward primer annealing to the maize ubiquitin promoter (5'-GCTTTTTGTTCGCTTGGTTGTG) was used along with a reverse primer specific to *PgAGO* (5'-CACGTGAGCTTCAGCAATGT). The PCR

program was as follows: 94°C for 30 s, 50°C for 30 s, 72°C for 2 min, 29 cycles. Spruce actin was used as a control as described above.

3.7 RNA Blot analysis

Total RNA from positive clones was isolated using the RNeasy Plant mini kit (Qiagen) as described above. RNA blot analysis was carried out according to the methods of Sambrook and Russell (2001), wherein 15 μg of RNA was fractionated on a 1.0% (v/v) formaldehyde agarose gel, and then transferred to a nylon membrane. DIG-labeled sense and antisense *PgAGO* ribo-probes used in the RNA in-situ experiments described in section 3.4 were separately hybridized onto duplicate blots. Probe hybridization and colour development was carried out as described in the DIG Application Manual (Roche). As a control, spruce actin ribo-probes were hybridized to verify equal loading of RNA.

3.8 Morphological observations

Transformed tissue was used to produce embryos using the procedures described in section 3.1.2. Digital photos of the cultures were taken at 10 day intervals for 40 days using a Leica DC500 camera with Leica IM50 imaging software (V 1.2). Individual mature embryos were closely examined to detect the appearance of morphological abnormalities. Mature embryos were partially desiccated and placed onto germination media. Morphological observation and conversion frequencies were recorded.

3.9 Histological observations

Maturing embryogenic tissue was fixed for thin sectioning according to the methods of Yeung (1999). Tissue was collected in glass vials at 10 day intervals for 40 days in a solution of 2.5% glutaraldehyde and 1.6% paraformaldehyde in a 0.05 M Phosphate buffer, pH 6.9, and then placed in a vacuum chamber for 15 minutes for infiltration. Mature embryos were fixed in the same manner, but placed in the vacuum

chamber for 25 min. Germinating tissue was cut perpendicular to the primary axis, and then placed in the vacuum chamber twice at 15 minutes. Tissue was placed on a rotary shaker overnight. Tissue was dehydrated by replacing fixative with a solution of methyl cellosolve, and again placed on a rotary shaker overnight followed by two overnight changes of 100% ethanol to dehydrate. Ethanol was replaced with ever increasing concentrations of Historesin (Leica Canada, Toronto) in a series of overnight changes. Serial sectioning (3 μm) was carried out using a Leica (RM 2145) microtome. Sections were stained with a periodic acid-Schiff (PAS) reaction for observations of total carbohydrates, and counterstained with toluidine blue O (TBO) for general histological observation (Yeung, 1984).

3.10 Generation of the full-length sequence of *HBK2*, expression studies and transformation studies

3.10.1 *HBK2* Probe Preparation and cDNA library screening

A truncated sequence of *HBK2* was amplified using primers published by Hjortswang et al. (2002) from white spruce cDNA (5′-TCGAAAATCAGCTGGGTG, and 5′- GCCAATGCTATCTTCTGAC). Using these primers, a ~300 bp probe unique to *HBK2* was prepared and used to screen a cDNA library as described above.

3.10.2 *HBK2* Rapid Amplification of cDNA Ends (RACE)

The methods used for this procedure were as described in section 3.2.3. In December of 2004, a paper was published in which the complete sequence of *HBK2* was described (Guillet-Claude et al., 2004). This put a halt to efforts of trying to find the complete *HBK2* sequence through the above mentioned methods. The *HBK2* sequence published was used to produce primers (5'- ATGCTCAAAAGGTGGACTAAATTC and 5'-ACCATGTCAAGGTGCA-AACA), and the full-length *HBK2* was extracted from spruce tissue by PCR methods.

3.10.3 Molecular characterization of *HBK2*

The methods used for this procedure were as described in section 3.3 with the exception of the following. The phenogram was visualized using TreeView (v1.6.6).

3.10.4 In-situ hybridization studies

The methods used for this procedure were as described in section 3.4. Primers used were the original published primers described in section 3.10.1 with T7 and T3 sites inserted (5'- TAATACGACTCACTATAGGGTCGAAAATCAGCTGGGTG and 5' - AATTAACCCTCACTAAAGGGCCAATGCTATCTTCTGAC).

3.10.5 RT-PCR studies

The methods used for this procedure were as described in section 3.5. Primers used were the same as those described in section 3.10.1.

3.10.6 Spruce transformation with *HBK2*

The methods used for this procedure were as described in section 3.6. Antisense plasmids were produced using the full length sequence of the gene with the appropriate restriction enzyme sites inserted into the primers (5'- CAAAAGGAGCTCTAAATTCC-AGTTGAAATATA and 5'- GGCCCATTTTAGGGATCCAGCTATAC).

3.10.7 Morphological observations

The methods used for this procedure were as described in section 3.8.

3.10.8 Histological observations

The methods used for this procedure were as described in section 3.9

4.0 RESULTS

4.1 Molecular cloning of *PgAGO*

Stasolla et al. (2003) analyzed a pine EST collection generated by the Forest Biotechnology group at North Carolina State University (http://web.ahc.umn.edu/biodata/nsfpine/contig_dir6). A 400 bp pine EST (NXSI_035_A04) was identified as being expressed during spruce somatic embryogenesis. Further analysis revealed the EST to be a homolog of the *Arabidopsis ZLL* gene, a member of the AGO family (Moussian et al., 1998). This EST was used as a probe to screen two cDNA libraries, generated from immature and mature spruce somatic embryos. The resulting positive clones had identical sequences, but appeared to be truncated at both the 3' and 5' ends. Using the RACE technique, the complete 3' end was obtained, and through successive 5' RACE and library re-screening, the complete 5' end was obtained.

The sequenced clone was found to be 3452 bp long with an open reading frame of 2880 bp encoding 960 amino acid residues. The clone, which shared a 92% sequence similarity with the corresponding probe sequence, was designated *PgAGO* (*Picea glauca* ARGONAUTE). Analysis of the *Pg*AGO protein revealed an isoelectric point of 9.17, a mass of 107 kDa and a lack of any prominent hydrophobic or hydrophilic domains within its length (Figure 4.1). The amino acid sequence of *Pg*AGO was aligned with all known members of the AGO family, including those from *Arabidopsis thaliana* (serial number 2, 4, 6, 9, 11, 13, 15, 17, 19 and 49 in Table 4.1), rice (serial number 3, 5, 8, 10, 12, 14, 16, 18, 20, 45, 46, 47 and 48 in Table 4.1) and several animal species (Table 4.1).

A phenogram was produced to group AGO proteins of similar sequences into separate classes (Figure 4.2). *Pg*AGO belonged to the same monophyletic subclass of AGO4, AGO6, AGO8 and AGO9 of *Arabidopsis* and AGO2, AGO3 and AGO9 of rice. The protein sequence showing the highest similarity to *Pg*AGO was AGO9 from rice with 50% sequence similarity (Table 4.2). All other members of the subclass maintained at least a 39% sequence similarity to *Pg*AGO. Similarity between *Pg*AGO and the *Arabidopsis* ZLL, a member of a different grouping, is still relevant at 28% sequence similarity. An alignment of all of the proteins within the same subclass as *Pg*AGO, along

with ZLL from *Arabidopsis*, reveals similarities scattered along their entire sequence length (Figure 4.3). All ARGONAUTE proteins are defined by the presence of two domains known as PIWI and PAZ (Cerutti et al., 2000). In *Pg*AGO the N-terminal PAZ domain encompasses 117 amino acids (from residue 310 to 425, Figure 4.3) and shares a low degree of identity with similar domains in other species (less than 25%) (Table 4.3). The C-terminal PIWI domain is composed of 84 amino acids (from residue 825 to 909, Figure 4.3) and is highly conserved among species. The PIWI domain in *Pg*AGO is 58% similar to that of AGO1, a well characterized AGO protein in rice (Nishimura et al., 2002), 57% similar to ZLL from *Arabidopsis* and 57% similar to a protein as divergent as elF2C from rabbit (Table 4.4). Overall, a high degree of conservation, within the PIWI domain, is observed across both the plant and animal kingdoms (Table 4.4).

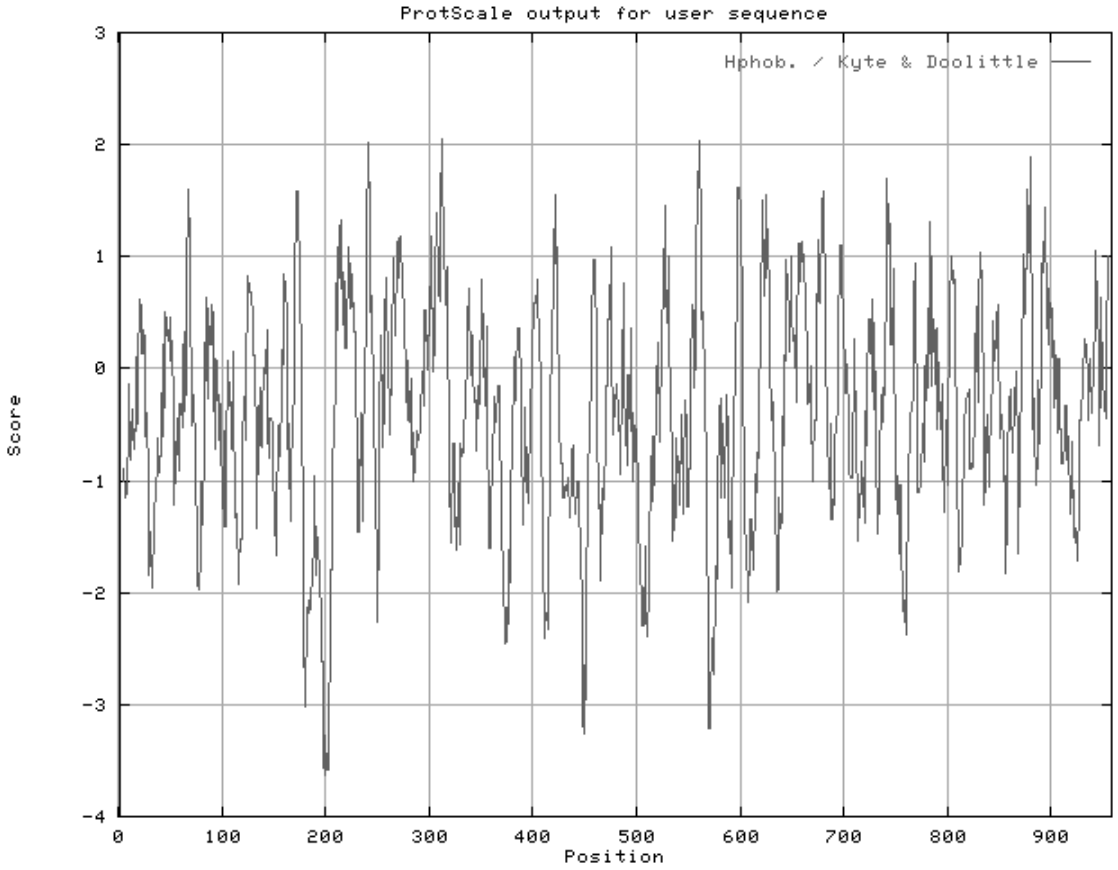

Figure 4.1. Hydropathy analysis showing hydrophobic and hydrophilic regions of the deduced protein encoded by the *Pg*AGO gene. Positive values indicate hydrophobic regions, while negative values indicate hydrophilic regions along the amino acid sequence of the protein. The Kyte and Doolittle (1982) method was used for the analysis.

Table 4.1. List of proteins selected for the phenogram as shown in Figure 4.2.

Serial No.	Name	ACC. No.	Description	Reference
1	PgAGO-Spruce	DQ068741	PgAGO homolog in spruce	This paper
2	AGO1-ATH	AAC18440	Argonaute protein [Arabidopsis thaliana]	Bohmert et al. (1998)
3	AGO1-Rice	BAB96814	AGO1 homologous protein [Oryza sativa (japonica cultivar-group)]	Nishimura et al. (2002)
4	AGO2-ATH	AAF24585	T19E23.7 [Arabidopsis thaliana]	Direct Submission
5	AGO2-Rice	NP_912975	unnamed protein product [Oryza sativa (japonica cultivar-group)]	Direct Submission
6	AGO3-ATH	AAF24586	T19E23.8 [Arabidopsis thaliana]	Direct Submission
7	AGO3-BOSt	AAR12162	argonaute 3 [Bos taurus]	Direct Submission
8	AGO3-Rice	BAD81109	zwille protein -like [Oryza sativa (japonica cultivar-group)]	Sasaki et al., 2002
9	AGO4-ATH	A84668	Argonaute (AGO1)-like protein [imported] - Arabidopsis thaliana	Lin et al. (1999)
10	AGO4-Rice	XP_473529	OSJNBa0005N02.3 [Oryza sativa (japonica cultivar-group)]	Direct Submission
11	AGO5-ATH	AAD21514	Argonaute (AGO1)-like protein [Arabidopsis thaliana]	Direct Submission
12	AGO5-Rice	NP_909924	putative argonaute protein [Oryza sativa (japonicacultivar-group)]	Direct Submission
13	AGO6-ATH	AAB91987	Argonaute (AGO1)-like protein [Arabidopsis thaliana]	Direct Submission
14	AGO6-Rice	BAD27856	putative argonaute protein [Oryza sativa (japonica cultivar-group)]	Direct Submission
15	AGO7-ATH	AAG60096	pinhead-like protein [Arabidopsis thaliana]	Direct Submission
16	AGO7-Rice	XP_469924	putative argonaute protein [Oryza sativa (japonica cultivar-group)]	Direct Submission
17	AGO8-ATH	AAO73892	PAZ (Piwi Argonaut and Zwille) family [Arabidopsis thaliana]	Direct Submission
18	AGO8-Rice	XP_468898	putative piwi domain containing protein [Oryza sativa (japonica cultivar-group)]	Direct Submission
19	AGO9-ATH	CAD66636	ARGONAUTE9 protein [Arabidopsis thaliana]	Direct Submission
20	AGO9-Rice	XP_477327	putative ARGONAUTE9 protein [Oryza sativa (japonica cultivar-group)]	Direct Submission
21	ALG-1	NP_510322	argonaute (plant)-Like Gene (110.9 kD) (alg-1) [Caenorhabditis elegans]	Kamath et al. (2003)
22	ALG-2	NP_493837	argonaute (plant)-Like Gene (99.5 kD) (alg-2) [Caenorhabditis elegans]	Morel et al. (2002)
23	Aubergine/Sting	AAD38655	sting [Drosophila melanogaster]	Direct Submission
24	dAgo1	NP_523734	CG6671-PB, isoform B [Drosophila melanogaster]	Findley et al. (2003)
25	Drosophila-1	NP_725341	CG6671-PA, isoform A [Drosophila melanogaster]	Findley et al. (2003)
26	eIF-2C	JC6569	translation initiation factor eIF-2C - rabbit	Zou et al. (1998)
27	ETIF-2c	XP_524664	PREDICTED: similar to eukaryotic translation initiation factor 2C, 3 isoform a; argonaute 3 [Pan troglodytes]	Direct Submission
28	ETIF-2c-1	XP_417775	PREDICTED: similar to eukaryotic translation initiation factor 2C, 3 isoform a; argonaute 3 [Gallus gallus]	Direct Submission
29	hAgo1	XP_029053	eukaryotic translation initiation factor 2C, 1 [Homo sapiens]	Direct Submission
30	hAgo3	XP_029051	hypothetical protein FLJ12765 [Homo sapiens]	Direct Submission
31	hAgo4	BAB13393	KIAA1567 protein [Homo sapiens]	Nagase et al. (2000)
32	Hili	AAH25995	Piwi-like 2 [Homo sapiens]	Strausberg et al. (2002)
33	Hiwi2	AAH31060	Piwi-like 4 [Homo sapiens]	Strausberg et al. (2002)
34	mAgo1	AAN75579	argonaute 1 protein [Mus musculus]	Carmell et al. (2002)
35	mAgo2	AAN75580	argonaute 2 protein [Mus musculus]	Carmell et al. (2002)
36	mAgo4	AAN75581	argonaute 4 protein [Mus musculus]	Carmell et al. (2002)
37	mAgo5	AAN75582	argonaute 5 protein [Mus musculus]	Carmell et al. (2002)
38	Mili	NP_067283	piwi like homolog 2 [Mus musculus]	Kuramochi-Miyagawa et al. (2001)
39	Miwi	NP_067286	piwi like homolog 1 [Mus musculus]	Deng and Lin (2002)
40	Piwi	NP_476875	CG6122-PA [Drosophila melanogaster]	Sarot et al. (2004)
41	Prg-1	CAA98113	Hypothetical protein D2030.6 [Caenorhabditis elegans]	*C. elegans* Sequencing Consortium, 1998
42	Prg-2	AAB37734	Hypothetical protein C01G5.2 [Caenorhabditis elegans]	*C. elegans* Sequencing Consortium, 1998
43	Qde2	AAF43641	QDE2 [Neurospora crassa]	Catalanotto et al. (2000)
44	Rde-1	AAF06159	RNA interference promoting factor RDE-1 [Caenorhabditis elegans]	Tabara et al. (1999)
45	SAM1-Rice	AAP68386	putative leaf development and shoot apical meristem regulating protein [Oryza sativa (japonica cultivar-group)]	Direct Submission
46	SAM2-Rice	XP_476934	putative leaf development protein Argonaute [Oryza sativa (japonica cultivar-group)]	Direct Submission
47	SAM3-Rice	BAD30662	putative leaf development protein Argonaute [Oryza sativa (japonica cultivar-group)]	Direct Submission
48	ZLL/PNH-Rice	BAB96813	ZLL/PNH homologous protein [Oryza sativa (japonica cultivar-group)]	Nishimura et al. (2002)
49	ZLL-ATH	CAA11429	Zwille protein [Arabidopsis thaliana]	Moussian et al. (1998)

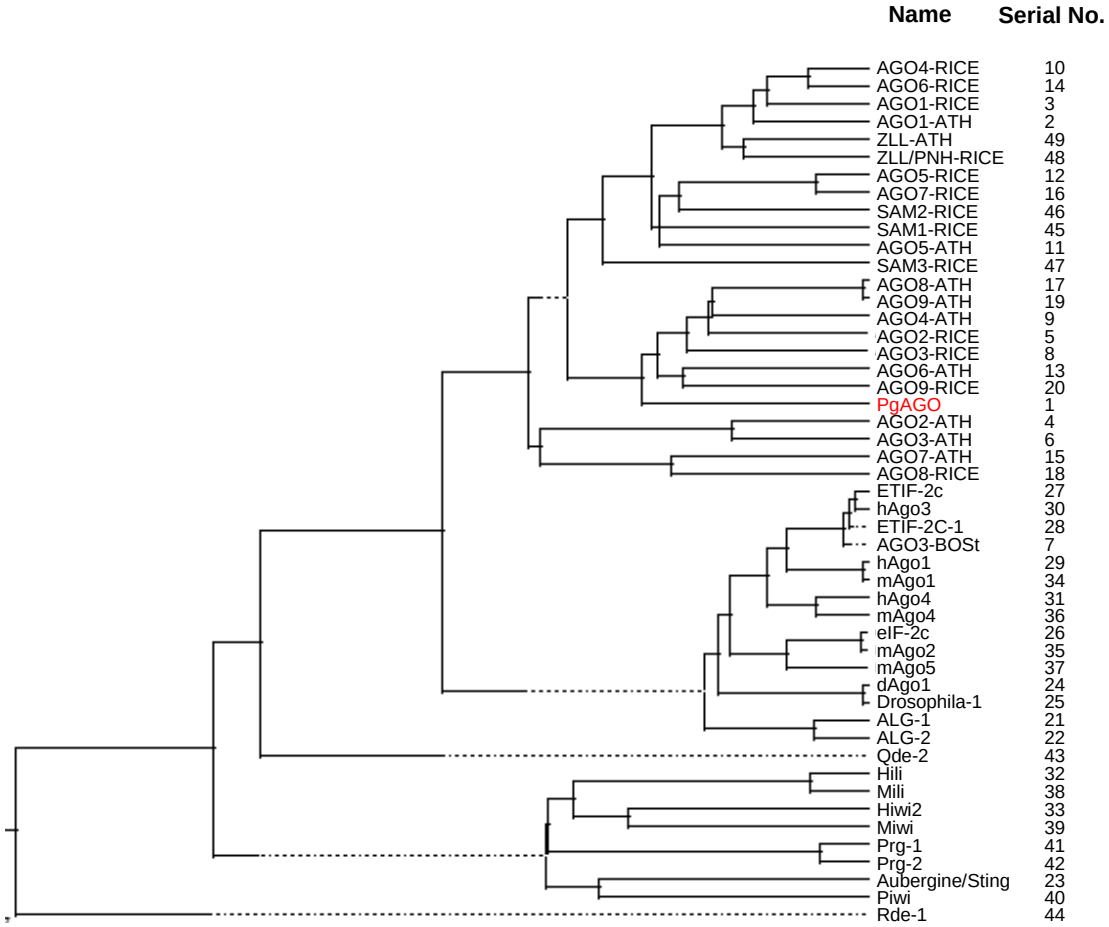

Figure 4.2. Phenogram of the AGO superfamily showing the similarity between the new *Pg*AGO protein and AGO proteins identified in other plant and animal species. See Table 4.1 for accession numbers and descriptions of the selected proteins.

Table 4.2. Identity matrix showing similarity in amino acid sequence between *Pg*AGO and other AGO proteins belonging to the same monophyletic subclass (AGO4-ATH, AGO2-Rice, AGO3-Rice, AGO6-ATH and AGO9-Rice) and a member (ZLL-ATH) belonging to a different monophyletic subclass (See Figure 4.2 for similarity relationships among the AGO proteins). ATH, *Arabidopsis thaliana*.

	PgAGO	AGO2-Rice	AGO3-Rice	AGO4-ATH	AGO6-ATH	AGO9-Rice	ZLL-ATH
ZLL-ATH	**28**	**29**	**26**	**26**	**28**	**27**	**100**
AGO9-Rice	**50**	**58**	**49**	**56**	**55**	**100**	
AGO6-ATH	**44**	**50**	**45**	**49**	**100**		
AGO4-ATH	**48**	**65**	**55**	**100**			
AGO3-Rice	**40**	**59**	**100**				
AGO2-Rice	**50**	**100**					
PgAGO	**100**						

Figure 4.3. Alignment of the deduced *Pg*AGO sequence with other proteins belonging to the same monophyletic subclass (AGO4-ATH, AGO2-Rice, AGO3-Rice, AGO6-ATH and AGO9-Rice) and two members (ZLL-ATH and AGO1-ATH) belonging to a different monophyletic subclass (see Figure 4.2). Sequence identities are indicated by filled boxes, and conservative changes are shaded. PAZ and PIWI domains are enclosed in boxes. See Table 4.1 for accession numbers and descriptions of the selected proteins.

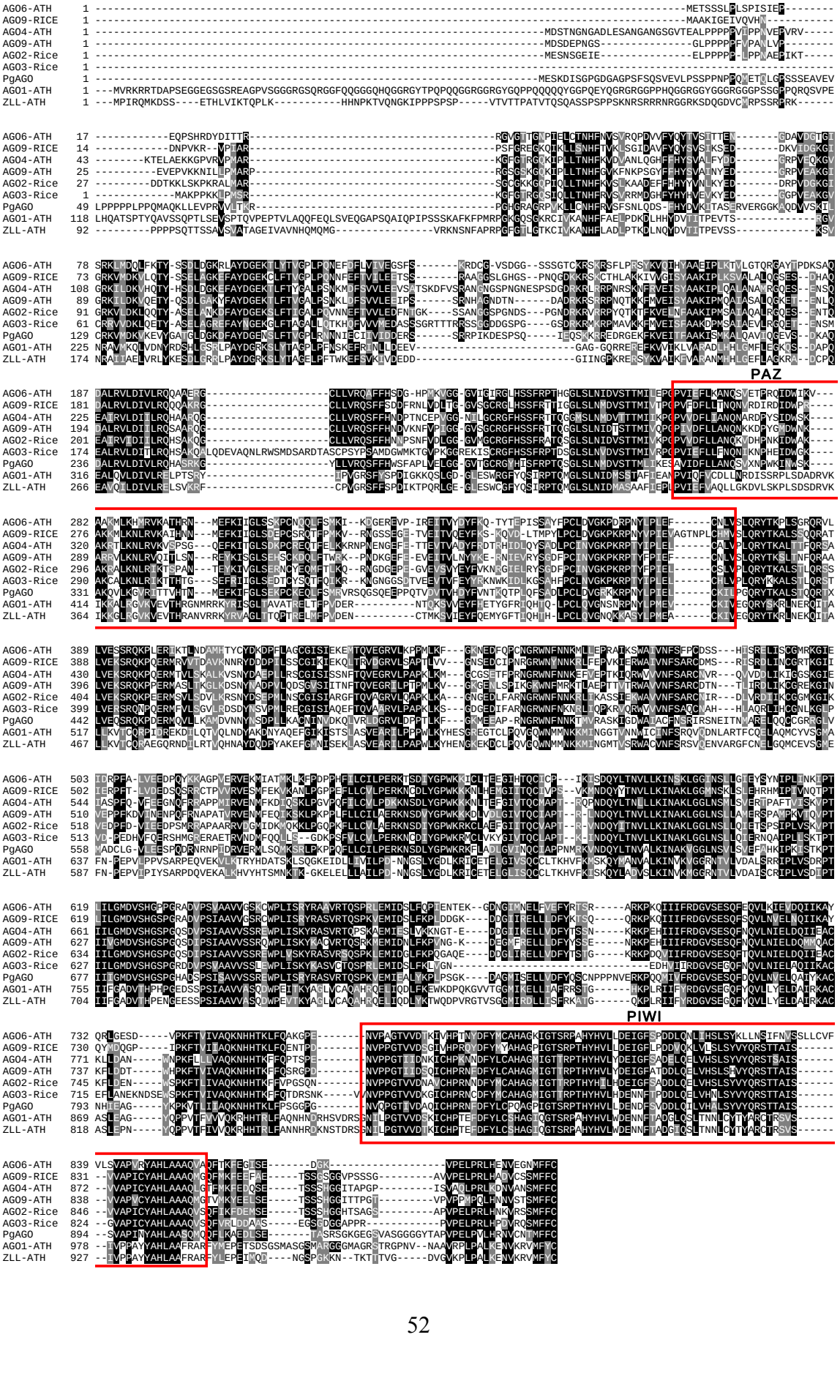
PAZ
PIWI

Table 4.3. Identity matrix showing similarity in amino acid sequence between the PAZ domain of *Pg*AGO and the respective domain of other AGO proteins from other plant and animal species. ATH, *Arabidopsis thaliana*. A, *Pg*AGO-Spruce; B, ZLL/PNH-Rice; C, ZLL-ATH; D, AGO1-Rice; E, AGO1-ATH; F, AGO1-*Drosophila*; G, elF2C-Rabbit; H, PIWI-*Drosophila*; I, GDE1-*N. crassa*; J, RDE-*C. elegans*; K, Aubergine/Sting-*Drosophila*.

	A	B	C	D	E	F	G	H	I	J	K
K	**12**	**16**	**13**	**13**	**13**	**11**	**12**	**40**	**15**	**15**	**100**
J	**12**	**14**	**14**	**11**	**12**	**13**	**12**	**13**	**20**	**100**	
I	**14**	**20**	**19**	**12**	**14**	**30**	**19**	**15**	**100**		
H	**11**	**17**	**14**	**15**	**18**	**14**	**13**	**100**			
G	**21**	**38**	**37**	**33**	**37**	**83**	**100**				
F	**22**	**38**	**38**	**32**	**38**	**100**					
E	**25**	**70**	**71**	**78**	**100**						
D	**19**	**69**	**69**	**100**							
C	**21**	**80**	**100**								
B	**23**	**100**									
A	**100**										

Table 4.4. Identity matrix showing similarity in amino acid sequence between the PIWI domain of *Pg*AGO and the respective domain of other AGO proteins from both plant and animal species. ATH, *Arabidopsis thaliana*. A, *Pg*AGO-Spruce; B, ZLL/PNH-Rice; C, ZLL-ATH; D, AGO1-Rice; E, AGO1-ATH; F, AGO1-*Drosophila*; G, elF2C-Rabbit; H, PIWI-*Drosophila*; I, GDE1-*N. crassa*; J, RDE-*C. elegans*; K, Aubergine/Sting-*Drosophila*.

	A	B	C	D	E	F	G	H	I	J	K
K	**37**	**36**	**35**	**35**	**36**	**37**	**36**	**73**	**19**	**31**	**100**
J	**36**	**42**	**41**	**40**	**41**	**45**	**42**	**30**	**27**	**100**	
I	**29**	**41**	**42**	**41**	**43**	**38**	**41**	**17**	**100**		
H	**34**	**35**	**33**	**31**	**33**	**40**	**35**	**100**			
G	**57**	**100**	**93**	**92**	**94**	**73**	**100**				
F	**51**	**73**	**74**	**73**	**76**	**100**					
E	**58**	**94**	**98**	**95**	**100**						
D	**58**	**91**	**93**	**100**							
C	**57**	**93**	**100**								
B	**57**	**100**									
A	**100**										

4.2 *PgAGO* Gene Expression Studies

The spatial expression of *PgAG*O during somatic embryogenesis was investigated using RNA in-situ hybridization with DIG-labeled antisense probes. Accumulation of *PgAGO* transcripts in early filamentous embryos (Figure 4.4 A) was restricted to the central region of the embryogenic head (Figure 4.4 B), with specific hybridization of the antisense probe occurring at the future site of the root apical meristem (RAM) (Figure 4.4 C). No signal was detected in sections probed with sense RNA (Figure 4.4 D).

The shoot apical meristem (SAM) of early cotyledonary embryos (Figure 4.4 E) showed specific hybridization of *PgAGO* antisense RNA in both the apical and sub-apical layers (Figure 4.4F), a pattern that was maintained in mature cotyledonary embryos except for a loss of expression in the sub-apical layers (Figure 4.4 G). Hybridization within the root apical meristem (Figure 4.4 H) was limited to the large central cells in both early and mature cotyledonary embryos (Figure 4.4 I, J). No sense probe hybridization was observed in shoot or root apical meristems of mature cotyledonary embryos (Figure 4.4 K, L).

RT-PCR studies confirmed the presence of *PgAGO* throughout the maturation period. *PgAGO* was amplified from cDNA extracted from both an embryogenic line, (E)WS1, and a line in which early filamentous embryos failed to develop further, (NE)WS. Within the embryogenic line, amplification of *PgAGO* was observed in low amounts during the initial stages of maturation (Figure 4.5). Between 10 and 40 days on maturation medium, the expression of *PgAGO* increased, reaching a maximum around day 30 before declining during the last days in culture. An opposite pattern was seen in line (NE)WS, wherein initial amplification of the gene was quite high, but was reduced dramatically after only a few days in maturation medium (Figure 4.5).

Figure 4.4. Expression pattern of *Pg*AGO during white spruce somatic embryogenesis. Immature embryos have a globular shape and are composed of highly cytoplasmic cells (**A**). In immature embryos, expression of *PgAGO* was mainly localized in the central region (**B**) and demarked the future site of the root apical meristem (arrows) (**C**). No signal was detected in immature embryos hybridized with sense ribo-probes (**D**). In cotyledonary embryos (**E**), a well developed shoot apical meristem (arrow) is visible. In both early and mature cotyledonary embryos, transcript accumulation becomes localized in the shoot apical meristem (arrow), which is surrounded by emerging cotyledons (C) (**F** and **G**). The root apical meristem (arrows) is located above the root cap (RC) (**H**). Transcript accumulation within the developing root is limited to the root apical meristem in both early and mature cotyledonary embryos (**I** and **J**). No signal was visible with sense hybridization (**K** and **L**).

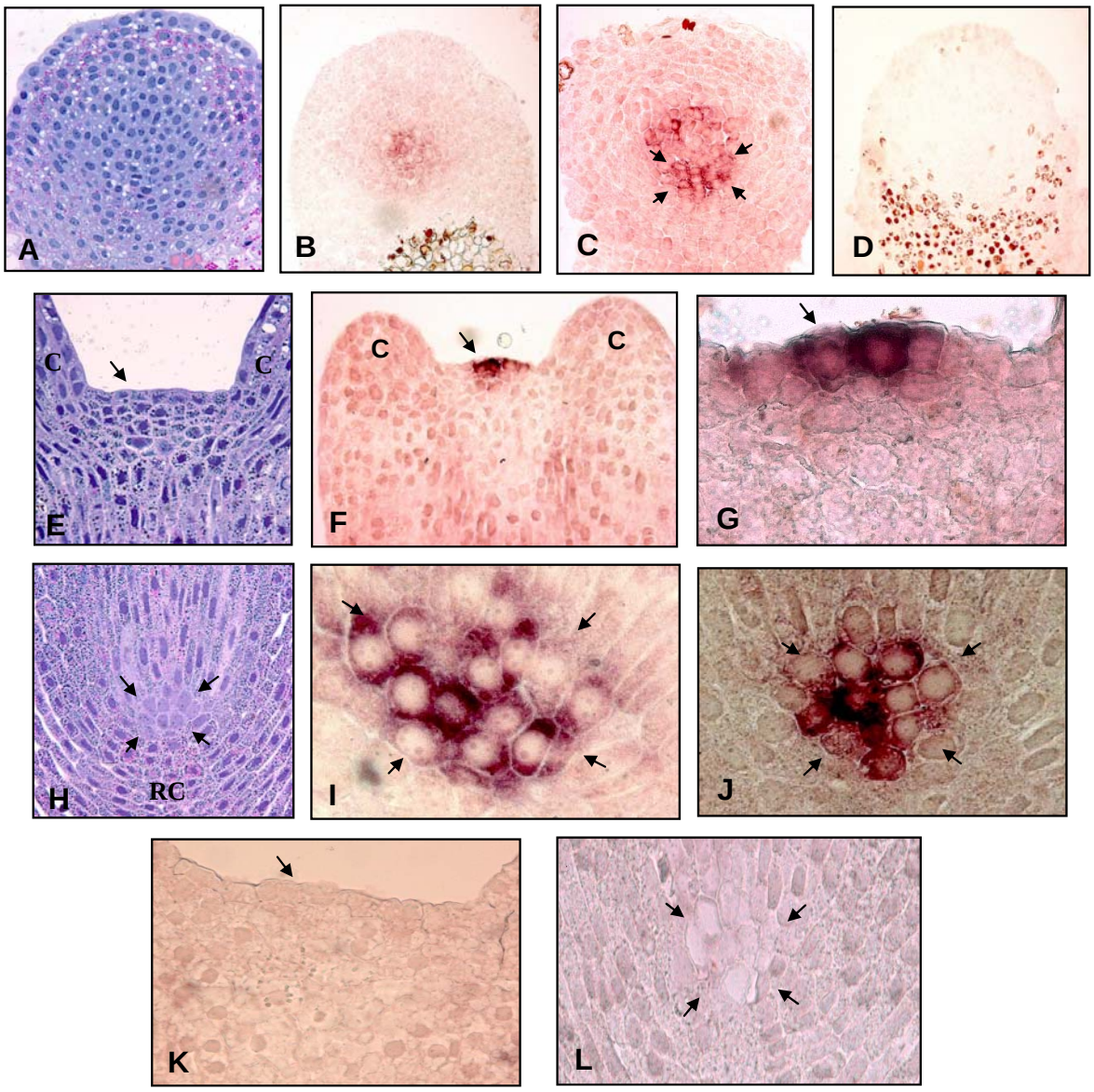
A
B
C
D
C
C
E
C
C
F
G
H
RC
I
J
K
L

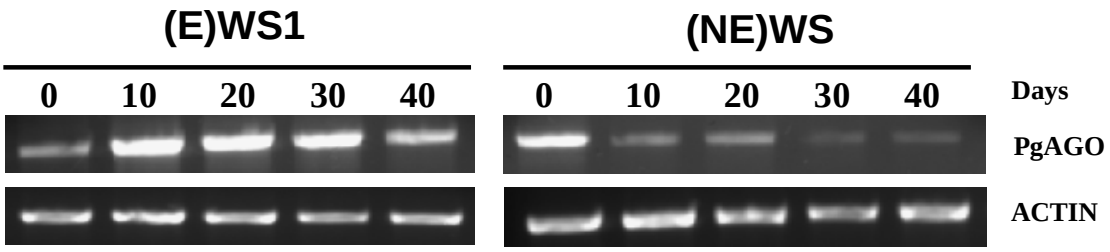

Figure 4.5. Expression profile of *Pg*AGO in the embryogenic line ((E)WS1) and a line unable to produce cotyledonary embryos ((NE)WS) from day 0 to 40 in the maturation period. Initially in the embryogenic line expression levels of *PgAGO* are low. At 10 days expression levels reach their peak before gradually lowering throughout the rest of the maturation period. In non-embryogenic lines the opposite expression pattern is observed. Initially expression levels are high. Expression levels decrease dramatically at day 10 and continue to decrease throughout the maturation period. Expression levels of spruce actin acts as a control to show equal loading of samples. See materials and methods for details on primers and conditions used.

4.3 RNA-mediated suppression of *PgAGO* during embryo development

PgAGO expression was silenced in Norway spruce cells, where the transformation procedure has been optimized (Clapham et al., 2000). Following bombardment with plasmids containing *PgAGO* in the antisense orientation, three positive sublines, named *P*gAGO-A1, A2 and A3, were identified. Genomic DNA from each of these lines was screened for the presence of antisense *PgAGO* by amplifying a PCR product (1363 bp) spanning a portion of the vector and the *PgAGO* sequence (Figure 4.6 A). No fragment was obtained from genomic DNA isolated from control cells.

Northern-blot hybridization analysis using a DIG-labeled sense RNA probe verified the PCR results (Figure 4.6 B). The use of a sense probe reveals the expression of *PgAGO* in antisense orientation in the transformed line. The use of an antisense probe showed the effective silencing of *PgAGO* in transformed lines as expression levels appeared to be greatly reduced compared to the untransformed line (Figure 4.6 B).

4.4 Characterization of transformed *Pg*AGO lines

Embryo growth in untransformed lines follows a precise developmental pathway, described in detail by Filonova et al. (2000a). Briefly, in proliferation medium, proembryogenic masses I (PEMs I) consist of an embryogenic head subtended by an elongated suspensor-like tail (Figure 4.7 A). PEMs I form into PEMs II when they develop additional vacuolated cells (Figure 4.7 B). PEMs II become PEMs III after further development and restructuring (Figure 4.7 C) and when transferred onto media containing ABA differentiate into immature somatic embryos (Figure 4.7 D). Immature somatic embryos further differentiate into globular shaped embryos (Figure 4.7 E) before ultimately developing into cotyledonary embryos (Figure 4.7 F), characterized by well developed root and shoot apical meristems (Figure 4.7 G and H respectively).

In all three transformed lines (*Pg*AGO-A1, A2 and A3), embryo production was reduced. *Pg*AGO-A1 and A2 lines were unable to produce mature cotyledonary embryos in culture, whereas *Pg*AGO-A3 produced only a few malformed, mature cotyledonary

embryos. Abnormalities in all phases of somatic embryogenesis were observed in transformed lines. PEMs III showed signs of early cellular degeneration and accumulation of phenolic compounds (Figure 4.7 I), and went on to form immature somatic embryos (Figure 4.7 J), which in turn developed into cotyledonary embryos displaying a wide range of abnormalities. Mature cotyledonary embryos from transformed lines showed signs of stunted growth, lateral as opposed to vertical expansion and in extreme cases a lack of cotyledons (Figure 4.7 K, L).

Structural analysis revealed that in transformed mature embryos, with lowered *PgAGO* expression, the apical meristems were poorly organized. Within the root the large central cells (Figure 4.7 G) that normally constitute the root apical meristem were in many cases absent (Figure 4.7 M). Within the shoot, the apical layer of cytoplasmic cells, referred to as the "apical initials" (Yeung et al., 1998), and the sub-apical layer of vacuolated cells (Figure 4.7 H) were poorly organized in many embryos with reduced *PgAGO* expression. In these cases, the apical initials were undefined and the sub-apical layer was marked by large intercellular spaces (Figure 4.7 N).

Meristem reactivation in germinating embryos from transformed lines was precluded, as post-embryonic root and shoot growth was never observed in all embryos analyzed (Figure 4.8).

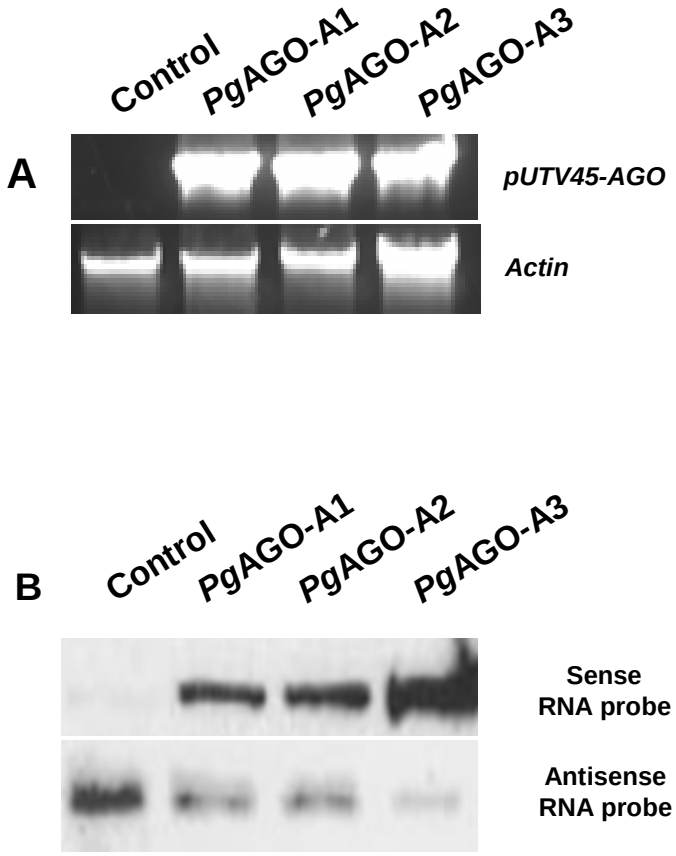

Figure 4.6. Screening of three positive spruce cultures *Pg*AGO-A1, A2, and A3, transformed with antisense *PgAGO*. The presence of the *pUTV45-AGO* construct in the cultures was verified using *ubi/PgAGO* primers from genomic DNA (**A**) (see Material and methods for details). Expected amplified products of 1363bp were observed in the three antisense lines, but not in the control line (top panel). Amplification of actin was used as a control to confirm that the DNA was intact (bottom panel). RNA gel-blot analysis (**B**) showing the presence of antisense *PgAGO* transcripts (top panel) and a reduction of sense *PgAGO* transcripts (bottom panel) in the lines *Pg*AGO-A1, A2, and A3. Equal loading was ensured by staining with ethidium bromide before blotting and by re-probing the same RNAs with spruce actin (data not shown).

Figure 4.7. Structural studies of developing embryos produced from control (**A**-**H**) and the antisense line *Pg*AGO-A3 (**I**-**N**). Proembryogenic mass I (PEM I) (**A**) characterized by a group of cytoplasmic cells and a single vacuolated cell (*). Upon further development, new vacuolated cells (*) originate from PEM I which becomes a PEM II (**B**). An increased number of cytoplasmic cells and formation of many vacuolated cells (*) radiating in all directions delineates the production of PEM III (**C**). Immature somatic embryos with defined embryo proper and suspensor regions differentiate from PEM III (**D**). In the presence of ABA, immature somatic embryos develop into large globular embryos (**E**). At the end of the developmental period, mature cotyledonary embryos are produced (**F**). They are characterized by a well defined embryonic axis and expanded cotyledons. In cotyledonary embryos, the root apical meristem is composed of large, rounded cells (arrowheads) at the base of the procambial region (P) (**G**). The shoot apical meristem of cotyledonary embryos is dome-shaped and characterized by the presence of an apical layer composed of highly cytoplasmic cells (arrow) (**H**). Cells of PEM III generated from the *Pg*AGO-A3 line accumulate phenolic compounds, which stain dark with toluidine blue O (arrows) (**I**). The few immature somatic embryos differentiating from these PEMs III are also characterized by cells accumulating phenolic compounds (arrow) (**J**). Abnormalities among embryos produced by the *Pg*AGO-A3 line include lateral as opposed to axial expansion (**K**) and lack of cotyledons (**L**). The root apical meristem of embryos produced by the *Pg*AGO-A3 line lacks the large central cells (arrowheads, compare with control meristem in Figure 4.7 G) at the base of the procambium (P) (**M**). Abnormalities in the shoot meristems of embryos generated by the *Pg*AGO-A3 line include the absence of defined apical cells (arrow) and the presence of intercellular spaces in the sub-apical region of the meristem (*) (**N**). Similar structural abnormalities were also observed for the embryos produced by the line *Pg*AGO-A2. Line *Pg*AGO-A1 did not produce any embryos (see the Results section).

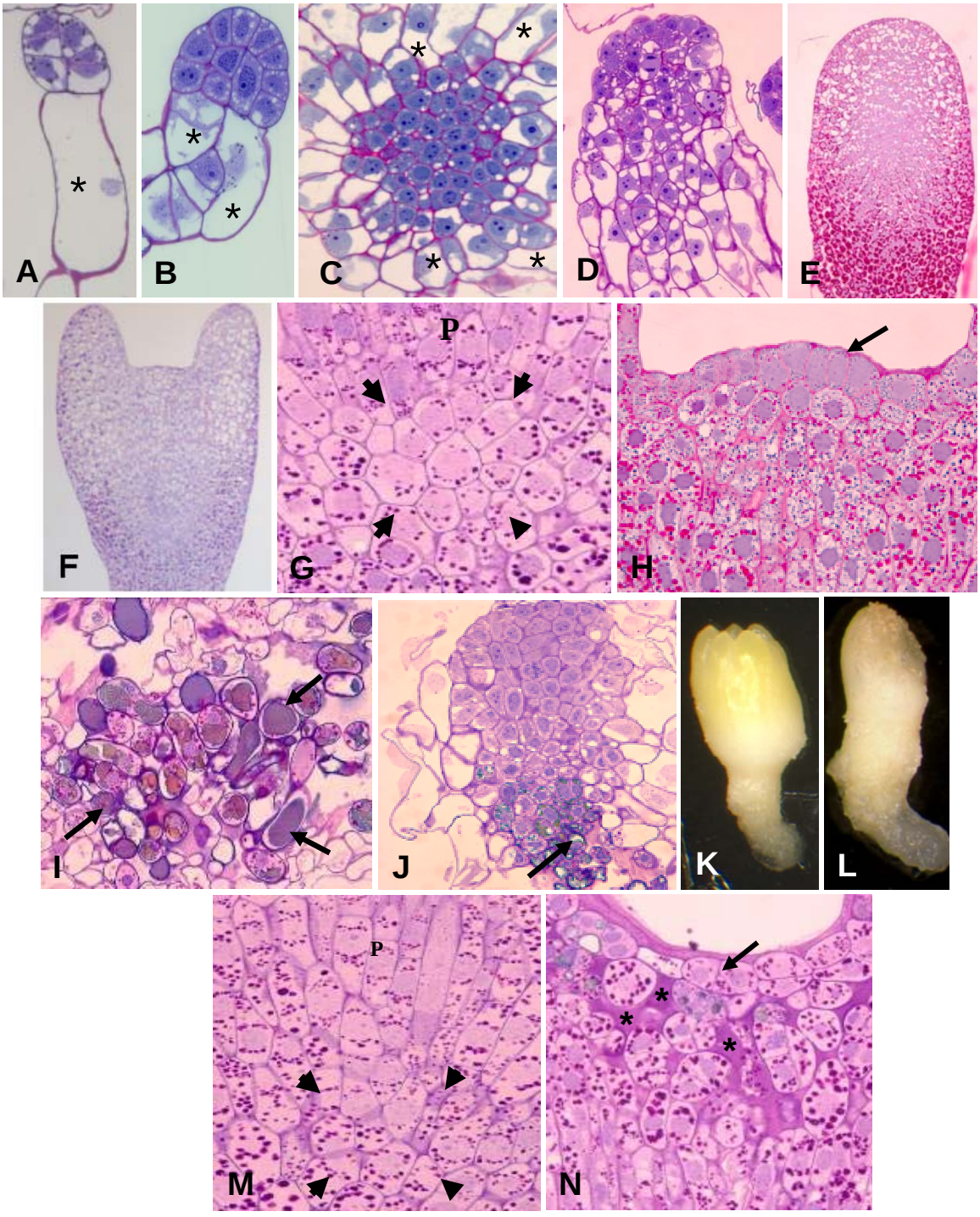
A
B
C
D
E
F
G
H
I
J
K
L
M
N
P
P

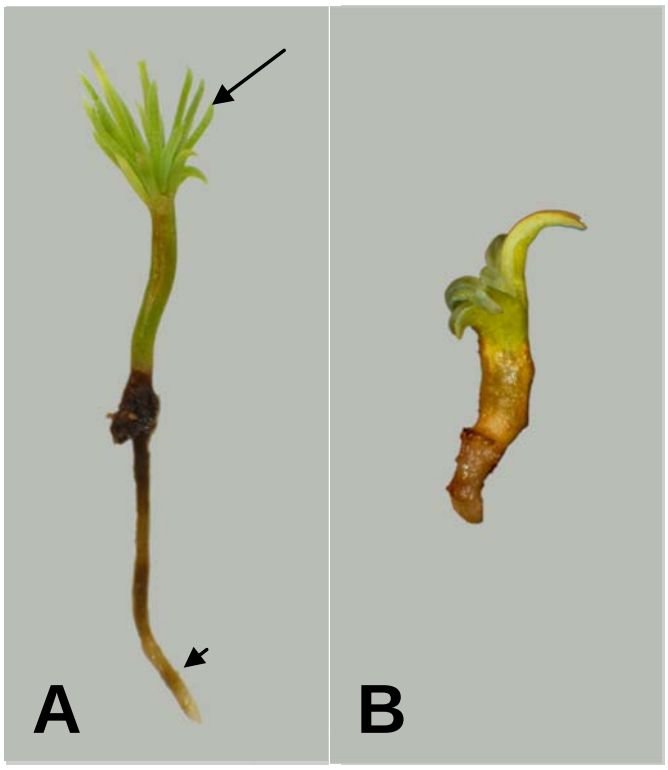

Figure 4.8. Germinating embryos produced by control (left panel) and *Pg*AGO-A3 cells (right panel) after about 2 months in culture. In control embryos, meristem reactivation generates new leaf primordia (arrow) and an elongated root (arrowhead) (**A**). Apical meristems fail to reactivate in *Pg*AGO-A3 embryos, resulting in growth cessation (**B**).

4.5 Molecular cloning of *HBK2*

Hjortswang et al. (2002) discovered that of the three homeobox genes (*HBK1*,*2* and *3*) found in Norway spruce, only one, referred to as *HBK2*, was absent in tissue not able to produce mature cotyledonary embryos. *HBK2* then became a candidate gene to study embryo development. Using gene specific primers published by Hjortswang et al. (2002), a ~300bp probe was obtained and used to screen the same cDNA libraries used to find *Pg*AGO. At the same time RACE was used to try to extend the 5' missing end of the sequence. Using this method, an extra 13 bp was added to the sequence. This new addition contained a start codon; however, analysis was not conclusive as to whether this was, in fact, the complete sequence. The RACE procedure was repeated two more times with similar results.

In December of 2004, a paper was published in which the complete sequence of *HBK2* was described (Guillet-Claude et al., 2004). This put a halt to efforts of trying to find the complete *HBK2* sequence through the above mentioned methods. The full length *HBK2* sequence was obtained from spruce tissue by PCR methods. The clone contained an open reading frame of 1254 bp encoding 418 amino acid residues. The predicted HBK2 protein from spruce has an isoelectric point of 5.79 and a mass of 46 kDa. The hydropathy profile of HBK2 shows an absence of any prominent hydrophobic or hydrophilic domains (Figure 4.9). Hydrophilic peaks are observed around residues 40 and 155 along with a very sharp peak within the homeodomain at around residue 380. The amino acid sequence of HBK2 was compared for similarity to the sequences of other known Homeobox-like proteins including those from *Arabidopsis thaliana* (serial number 1, 2, 3, 4, 5, 6, 7, 8 and 9 in Table 4.5), rice (serial number 24, 25, 26, 27, 28, 29 and 30 in Table 4.5) and animal species (Table 4.5).

A phenogram was produced to group Homeobox-like proteins of similar sequences into separate classes (Figure 4.10). HBK2 was grouped into a subclass with KN1-1 from sunflower, KN2 from a poplar hybrid, STM-like-Eca from poppy, H1 from tobacco and STM-like-Phy from a petunia hybrid. The protein sequence showing the highest similarity to HBK2 was STM-like-Eca from poppy with 50% sequence similarity (Table 4.6). All other members of the subclass maintained at least a 34% sequence

similarity to HBK2. An alignment of all of the proteins within the same subclass as HBK2, revealed similarities scattered along their entire sequence length, most notably in the C-terminal region in the area of the Homeobox (Figure 4.11), which characterizes all of the homeobox-like proteins (Moussian et al., 1998). In HBK2, the Homeobox domain encompasses 59 amino acids (from residue 331 to 383, Figure 4.11) and shares a high degree of similarity with Homeobox domains in other species (at least 43%) (Table 4.7). The Homeobox domain in HBK2 is 89% similar to that of KN1 in *Arabidopsis*, 85% similar to that in OSH1 in rice and 48% similar to domains found in proteins as divergent as mKN3 from mouse and hKN2 from human (Table 4.7). Overall, a high degree of conservation, within the Homeobox domain, is observed across both the plant and animal kingdoms (Table 4.7).

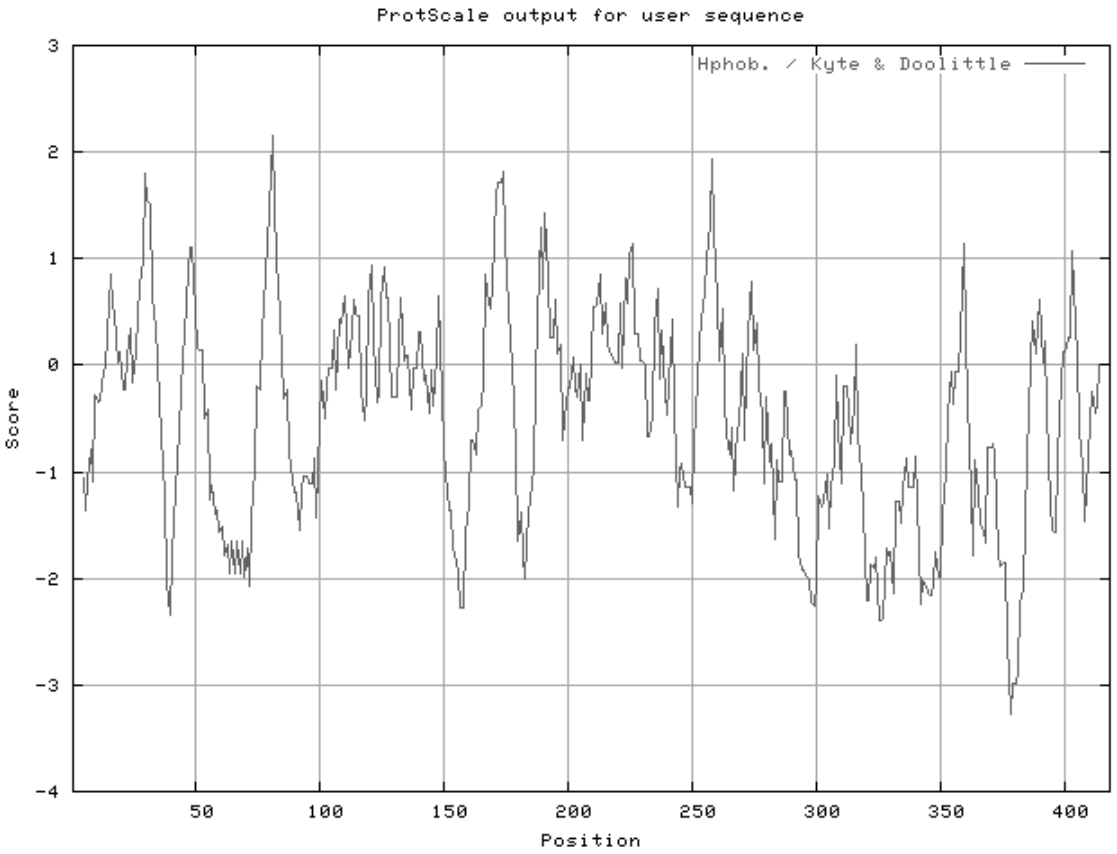

Figure 4.9. Hydropathy analysis showing hydrophobic and hydrophilic regions of the deduced protein encoded by the HBK2 gene. Positive values indicate hydrophobic regions, while negative values indicate hydrophilic regions along the amino acid sequence of the protein. The Kyte and Doolittle (1982) method was used for the analysis.

Table 4.5. List of proteins selected for the phenogram shown in Figure 4.10.

Serial No.	Name	ACC. No	Description	Reference
1	KN8-ATH	NP_195024	ATH1 (ARABIDOPSIS THALIANA HOMEOBOX GENE 1); transcription factor [Arabidopsis thaliana].	Direct Submission
2	KN9-ATH	CAA57122	ATK1 [Arabidopsis thaliana].	Dockx et al. (1995)
3	KN1-ATH	AAM03026	homeodomain protein KNAT1/BP [Arabidopsis thaliana].	Venglat et al. (2002)
4	KN2-ATH	NP_177208	KNAT2 (KNOTTED-LIKE FROM ARABIDOPSIS THALIANA 2); transcription factor [Arabidopsis thaliana].	Direct Submission
5	KN3-ATH	AAM63298	KNAT3 homeodomain protein [Arabidopsis thaliana].	Haas et al. (2002)
6	KN4-ATH	CAA63131	KNAT4 homeobox protein [Arabidopsis thaliana].	Serikawa et al (1996)
7	KN5-ATH	NP_194932	KNAT5 (ARABIDOPSIS THALIANA HOMEOBOX 1 GENE); transcription factor [Arabidopsis thaliana].	Direct Submission
8	KN6-ATH	NP_850951	KNAT6; DNA binding / transcription factor [Arabidopsis thaliana].	Direct Submission
9	KN7-ATH	NP_564805	KNAT7; DNA binding / transcription factor [Arabidopsis thaliana].	Direct Submission
10	HTHRX	AAC47759	homothorax [Drosophila melanogaster].	Rieckhof et al. (1997)
11	STM-like-Eca	AAY34562	shoot meristemless-like protein [Eschscholzia californica subsp.californica].	Groot et al. (2005)
12	KN1-1	AAM28231	knotted-1-like protein 1 [Helianthus annuus].	Tioni et al. (2003)
13	hKN1	AAK16581	SIX2 [Homo sapiens].	Direct Submission
14	hKN2	AAB19195	Meis1-related protein 2 [Homo sapiens].	Steelman et al. (1997)
15	hKN3	Q99687	Homeobox protein Meis3 (Meis1-related protein 2).	Strausberg et al. (2002)
16	hKN4	AAH00735	PKNOX1 protein [Homo sapiens].	Strausberg et al. (2002)
17	hKN5	AAH45626	PKNOX2 protein [Homo sapiens].	Strausberg et al. (2002)
18	mKN3	AAH03762	Mrg2 protein [Mus musculus].	Strausberg et al. (2002)
19	mKN1	CAA56585	six1 [Mus musculus].	Oliver et al. (1995)
20	mKN2	CAA56584	six2 [Mus musculus].	Oliver et al. (1995)
21	H1	AAO11694	Knotted-1-like homeobox protein H1 [Nicotiana tabacum].	Direct Submission
22	STM-like-Phy	AAM47027	shootmeristemless-like [Petunia x hybrida].	Stuurman (2002)
23	KN2	AAV49801	homeobox transcription factor KN2 [Populus balsamifera subsp.trichocarpa x Populus deltoides].	Guillet-Claude et al. (2004)
24	OSH1-Rice	P46609	Homeobox protein OSH1	Matsuoka (1993)
25	OSH3-Rice	BAB68310	transcription factor OSH3 [Oryza sativa (indica cultivar-group)].	Direct Submission
26	OSH43-Rice	BAA79225	knotted1-type homeobox protein OSH43 [Oryza sativa].	Sentoku (1999)
27	OSH45-Rice	BAA08552	OSH45 [Oryza sativa (japonica cultivar-group)].	Tamaoki et al. (1995)
28	OSH6-Rice	BAA79224	knotted1-type homeobox protein OSH6 [Oryza sativa].	Sentoku (1999)
29	OSH7-Rice	AAC32818	KNOX class homeodomain protein [Oryza sativa].	Postma-Haarsma et al. (1999)
30	OSH8-Rice	BAA77819	homeobox gene [Oryza sativa (japonica cultivar-group)].	Ito et al. (1999)
31	KN7-ZMA	AAP76320	homeobox transcription factor GNARLY1 [Zea mays].	Inada et al. (2003)
32	KN6-ZMA	AAP31409	knotted1-like homeodomain protein liguleless4a [Zea mays].	Direct Submission
33	KN4-ZMA	AAD13611	knotted class 1 homeodomain protein liguleless3 [Zea mays].	Muehlbauer et al. (1999)
34	HBK2-Pg	AY680385 and AY680396	Picea glauca homeobox transcription factor KN3 (Kn3) gene	Guillet-Claude et al. (2004)

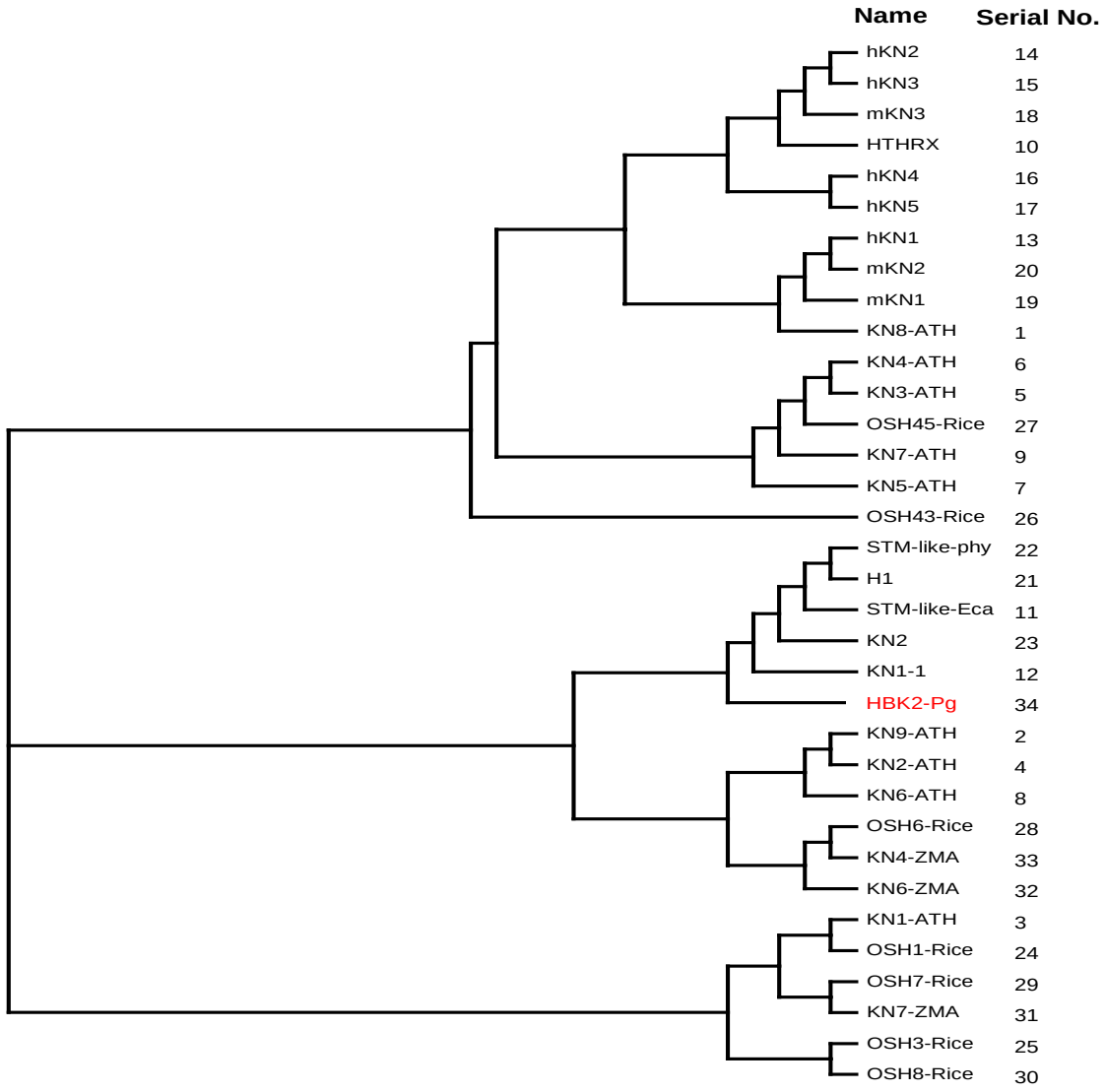

Figure 4.10. Phenogram of the Homeobox superfamily showing the similarity between the HBK2 protein and other Homeobox-like proteins identified in other plant and animal species. See Table 4.5 for accession numbers and descriptions of the selected proteins.

Table 4.6. Percentage similarity in amino acid sequence between HBK2 and other Homeobox-like proteins belonging to the same subclass (STM-like-Eca, KN2, KN1-1, H1 and STM-like-Phy)**.** See Figure 4.10 for similarity relationships among Homeobox-like proteins.

	HBK2-Pg	STM-like-Eca	KN2	Kn1-1	H1	STM-like-phy
STM-like-Phy	**38**	**81**	**70**	**71**	**85**	**100**
H1	**37**	**79**	**69**	**70**	**100**	
KN1-1	**34**	**76**	**68**	**100**		
KN2	**37**	**77**	**100**			
STM-like-Eca	**50**	**100**				
HBK2-Pg	**100**					

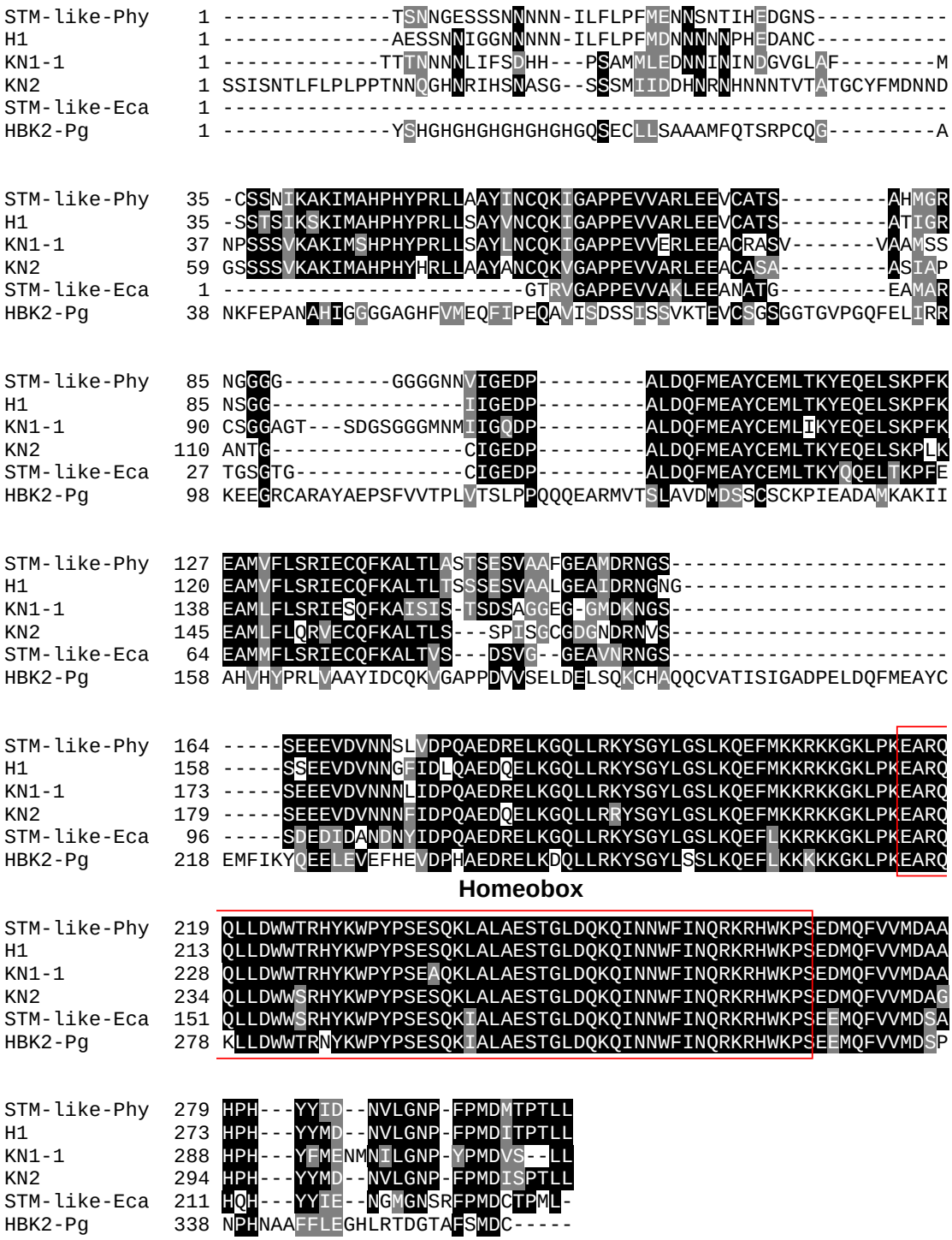

Figure 4.11. Alignment of HBK2 sequence with other proteins belonging to the same monophyletic subclass (STM-like-Eca, KN2, KN1-1, H1 and STM-like-Phy) (Figure 4.10). Sequence identities are indicated by filled boxes, and conservative changes are shaded. The Homeobox domain is enclosed in a box. See Table 4.5 for accession numbers and descriptions of the selected proteins.

Table 4.7. Percentage similarity in amino acid sequence between the Homeobox domain of HBK2 and the respective domain of other Homeobox-like proteins from other plant and animal species. ATH, *Arabidopsis thaliana*. A, HBK2-Pg; B, OSH1-Rice; C, KN1-ATH; D, hKN2; E, mKN3; F, HTHRX; G, KN8-ATH; H, OSH45-Rice.

	A	B	C	D	E	F	G	H
H	**55**	**61**	**57**	**46**	**46**	**46**	**37**	**100**
G	**43**	**43**	**43**	**45**	**45**	**46**	**100**	
F	**50**	**52**	**50**	**95**	**95**	**100**		
E	**48**	**50**	**48**	**100**	**100**			
D	**48**	**50**	**48**	**100**				
C	**89**	**91**	**100**					
B	**85**	**100**						
A	**100**							

4.6 *HBK2* Gene Expression Studies

Localization of *HBK2* transcripts in developing embryos was performed as described in section 4.2. In globular embryos, accumulation of *HBK2* transcripts was restricted to the central region of the embryo (Figure 4.12 A). In mature cotyledonary embryos, *HBK2* transcripts accumulated in the cortical and sub apical regions of the embryos (Figure 4.12 B). Control experiments with sense ribo-probes in both globular and cotyledonary embryos showed no signal, thereby confirming the specificity of the antisense probe (Figure 4.12 C, D).

Like *Pg*AGO, the expression level of *HBK2* was analyzed throughout embryo development by RT-PCR methods. *HBK2* was successfully amplified from cDNA derived from both embryogenic ((E)WS1) and non-embryogenic ((NE)WS) tissue (Figure 4.13). Expression levels of HBK2 remained constant throughout development in both lines. However, in the non-embryogenic line, (NE)WS, *HBK2* expression was much lower than in the embryogenic line, (E)WS1 (Figure 4.13).

4.7 Characterization of the transformed *HBK2* line

Antisense expression of *HBK2* was carried out in Norway spruce cells as described in section 4.4. Following bombardment, one positive subline HBK2-A1 was identified. This subline was screened for the presence of antisense *HBK2* and a PCR product of the correct size was obtained. Observations of developing tissue revealed that embryo production was arrested in the antisense transformed line, with cells not being able to differentiate past what appeared to be a maturing stage 2 embryo (Figure 4.14).

Figure 4.12. Expression pattern of *HBK2* during white spruce somatic embryogenesis. See Figure 4.4 for details of embryo structure. In immature embryos, expression of *HBK2* was localized in the central region of the embryo (arrowheads) (**A**). In mature cotyledonary embryos, expression of *HBK2* was observed in the cortical and sub-apical regions of the embryos (arrows) (**B**). No signal was detected in embryos hybridized with sense ribo-probes (**C** and **D**).


A


B


C

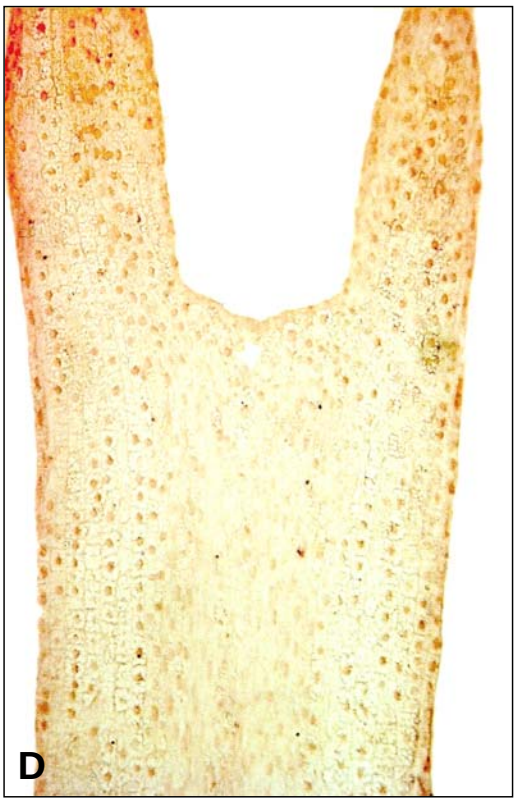
D

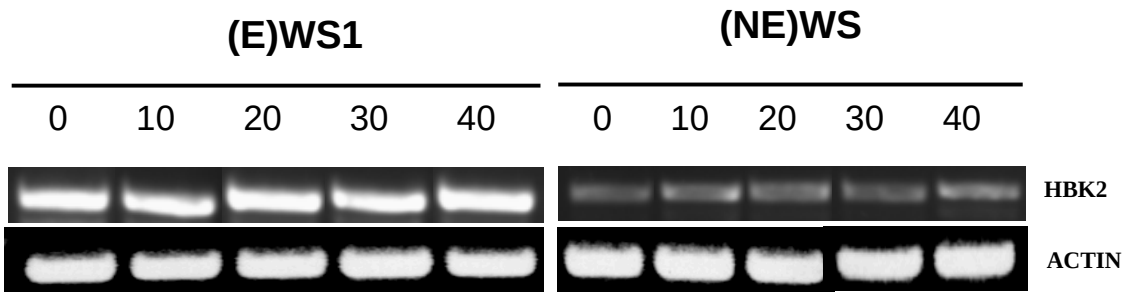

Figure 4.13. Expression profile of *HBK2* in the embryogenic line (E)WS1 and a line unable to produce cotyledonary embryos ((NE)WS) during the 40 days in the maturation period. See materials and methods for details on primers and conditions used.

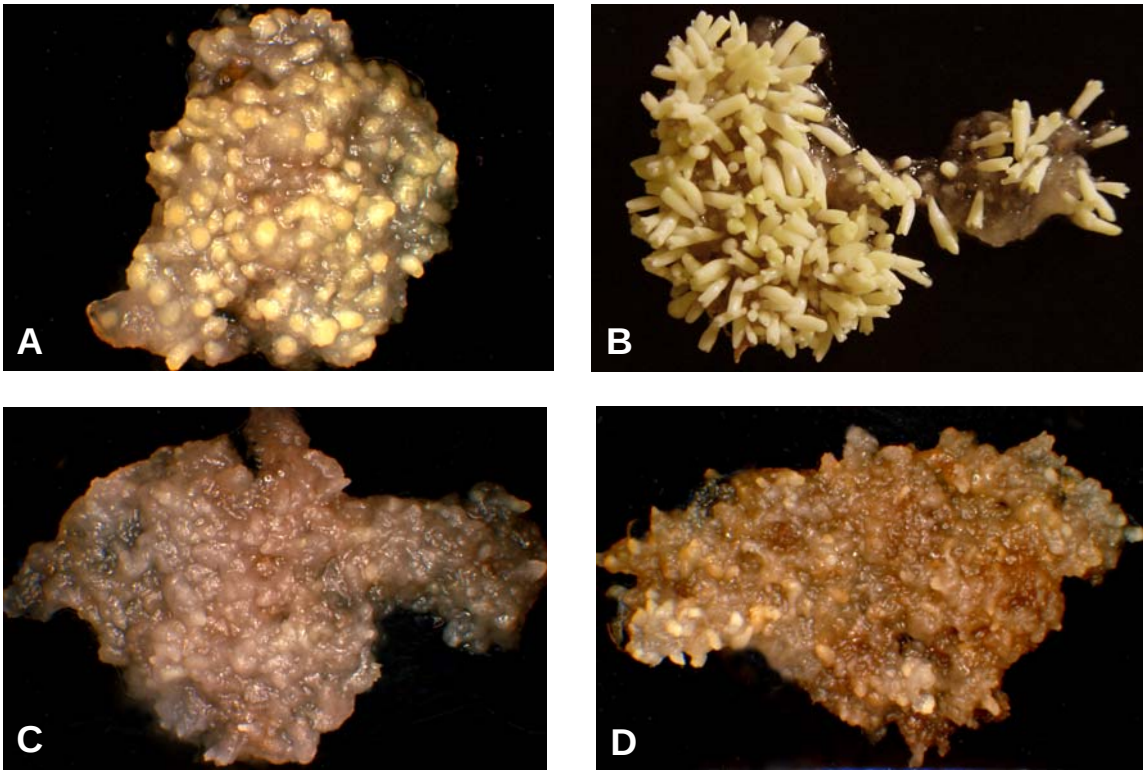

Figure 4.14. Differences in embryo maturation in tissue cultures of an untransformed line (control) and a line transformed with *HBK2* in antisense orientation. In the control line, at day 10 the embryogenic heads are clearly visible and storage products have started to accumulate (**A**). At day 50, in the control line, fully developed somatic embryos are visible with elongated bodies and expanded cotyledons (**B**). At day 10 in the HBK2-A1 line, no embryo development is observed (**C**). No mature embryos are visible in the transformed line at day 50 (**D**).

5.0 DISCUSSION

5.1 Characterization of *PgAGO*

For the first time, a member of the AGO family has been isolated in conifers. The gene, designated *PgAGO* was obtained by screening cDNA libraries generated from somatic embryos of white spruce. Relevant characteristics of other members of the AGO family from various species hold true for the predicted protein encoded by *PgAGO*, including a molecular weight of around 100 kDa (Cox et al., 1998; Kataoka et al., 2001; Carmell et al., 2002), a basic isoelectric point (Cox et al., 1998) and the absence of large hydrophobic domains (Figure 4.1). This suggests that *Pg*AGO is not a transmembrane protein. Like all AGO proteins, *Pg*AGO also contains the PIWI and PAZ domains.

AGO proteins have been implicated in numerous RNA degradation processes (see Carmell et al., 2002 for review) due to their affinity for RNA, as observed in in-vitro experiments (Kataoka et al., 2001), and their ability to form complexes, such as the RNA-induced silencing complex (RISC), which target RNA in-vivo (Deng and Lin, 2002). The PIWI and PAZ domain are thought to be the major factors required for proper RISC function. The less-conserved PAZ domain (Figure 4.3, Table 4.3) binds siRNA, which in turn binds target mRNA while the highly conserved PIWI domain (Figure 4.3, Table 4.4) functions to cleave the target mRNA, making it non-functional (Yan et al., 2003; Song et al., 2004). Specific examples of degradation processes, known as post-transcriptional gene silencing in plants, RNA interference in animals, and quelling in fungi, have been observed for the proteins AGO1 in *Arabidopsis* (Fagard et al., 2000), rde-1 in *Caenorhabditis elegans* (Tabara et al., 1999) and QDE-2 in *Neurospora* (Fagard et al., 2000). Given the previous examples, along with the fact that the degree of similarity between *Pg*AGO and other AGO proteins is high (Figures 4.2 and 4.3), it is likely that a similar function is retained in conifers, which have been on a separate evolutionary path from angiosperms for the past 300 million years (Bowe et al., 2000). Fagard et al. (2000) have shown that in the *Arabidopsis* AGO1 protein, a single Leu to Phe substitution at residue 571 results in a reduction in post-transcriptional gene silencing and co-suppression mechanisms. This Leu residue is also present in *Pg*AGO and is

conserved among other proteins analyzed in this study (Figure 4.2). The conservation of this residue along with its apparent importance indicates that *Pg*AGO might also be involved in some aspect of RNAi.

Although the actual target of many AGO proteins involved in RNAi remains unknown, recent work has revealed that it is possible that they affect genes involved in meristem regulation. Several members of the AGO family are involved in specifying stem cell fate and maintaining the balance between proliferation and differentiation within meristems (Carmell et al., 2002). The maintenance of this balance is under the control of both extrinsic signaling and cell-autonomous processes, and it is crucial for the survival of the organism (reviewed by Fletcher and Meyerowitz, 2000). A mutation in the *Drosophila* PIWI gene causes a reduction in germ-line stem cell division and cell death (Cox et al., 1998). Over-expressing the human HIWI gene caused a decrease in stem cell division, possibly due to a large increase in cell death (Sharma et al., 2001). Mutation studies of the *Arabidopsis ZLL* and *AGO1* genes, which appear to have overlapping functions (Lynn et al., 1999), have revealed their role in maintaining the stem cells of the shoot apical meristem in an undifferentiated state by relaying positional information and specifying proper expression of other meristem specific genes like *STM* (Bohmert et al., 1998; Moussian et al., 1998). The above examples show just how crucial AGO genes are for proper meristem regulation through various independent mechanisms. The similarity between spruce *Pg*AGO and *Arabidopsis* ZLL (27.9% amino acid identity and 57% similarity within the PIWI domain), as shown in Tables 4.2 and 4.4, indicates the likelihood of similar regulation mechanisms between these two genes. More importantly, it suggests that the mechanisms regulating plant development in angiosperms and gymnosperms are closer than one might suspect. The data supplied by the work from this thesis demonstrates that, as for ZLL in *Arabidopsis*, spruce *Pg*AGO is required for proper embryo development and possibly for the specification of stem cell identity in meristematic cells. Expression levels of *PgAGO* are higher in spruce lines able to generate embryos in culture compared to non-embryogenic lines (Figure 4.5). This higher level of expression indicates that *PgAGO* is required for the execution of the embryogenic pathway, possibly by maintaining PEMs III in a meristematic state where they can continue to divide and increase in number until they are competent to develop

into embryos upon exposure to environmental signals. Cellular degradation of PEMs III, which is observed in all antisense lines (Figure 4.7 I), leads to reduced embryo yield and production of abnormal embryos (Figure 4.7 K-L).

One of the early events during embryogenesis is demarked by the differentiation of the apical meristems, which delineate the apical-basal axis of the embryos. Data show that meristem development in spruce embryos is likely regulated in some way by *Pg*AGO. Expression of *PgAGO* is restricted to the meristematic cells of both the root and the shoot throughout development (Figure 4.4). In transformed embryos, where levels of *PgAGO* transcripts are reduced, abnormal meristems form. The large group of cells, which occupy the central region of the root meristem in control embryos (Figure 4.7 G), are missing in embryos produced from antisense lines (Figure 4.7 M). Yeung et al. (1998) described these cells as being analogous to the "quiescent center" of angiosperm roots and defined their roles during embryo development. The large central cells, found in spruce, appear early during embryogenesis in the central region of globular embryos (Figure 4.4 H) and, like the cells found in the quiescent center, remain mitotically inactive during embryogenesis. According to Yeung et al. (1998), it is likely that these cells provide positional cues required for proper embryo development, and that these cues are missing or miss-specified in embryos with suppressed *PgAGO* expression. This possibly causes the morphological abnormalities seen in Figure 4.7 K-L. Another role exercised by these central cells is to produce new root cells at the onset of germination through mitotic reactivation (Yeung et al., 1998). The lack of post-embryonic growth (Figure 4.8) is likely caused by the absence of the central cells in embryos with lowered levels of *PgAGO* transcripts. The requirement of *Pg*AGO for root meristem development is novel, since all other AGO genes involved in development do not seem to affect the root apex. Recent studies have shown that the involvement of AGO genes in root growth is plausible. The *Pinus taeda* EST clone, NXSI_035_A04, used in this study to screen the spruce libraries, and which shares 91.7% nucleotide sequence similarity with *PgAGO*, is up-regulated during the initial stages of root development in *Pinus contorta* (Brinker et al., 2004). The *ago1* mutant plants of *Arabidopsis* fail to generate adventitious roots in response to auxin (Sorin et al., 2005).

The role of *PgAGO* expression in the SAM (Figure 4.4) may be similar to that in the root meristem. Here, it would be required for proper specification of the apical initials. Embryos from antisense lines produce poorly organized SAMs in which the apical initials fail to acquire their cytological characteristics, and the sub-apical cells become disrupted by the presence of intercellular spaces (Figure 4.7 N). Stasolla et al. (2001) described these same abnormalities as being caused by the failure of meristem cells to acquire stem fate, thereby producing non-functional shoots. Yeung et al. (1998) found that the role of apical initials is to provide new cells to the converting shoot meristem through anticlinal, and sometimes periclinal, divisions. The results of this work show that expression of *PgAGO* is required for proper apical initial differentiation. A reduction in the expression levels of *PgAGO* results in the formation of non-functional meristems, and ultimately the failure to convert at germination (Figure 4.8).

The precise function of *PgAGO* during embryogenesis remains unknown. The involvement of AGO proteins in both RNAi and meristem regulation suggests that *Pg*AGO, like ZLL in *Arabidopsis*, may regulate meristematic activity through gene silencing.

The involvement of programmed cell death (PCD) in spruce embryo development has been well-documented (Filonova et al., 2000a; 2000b; Bozhkov et al., 2002; Filonova et al., 2002; Smertenko, 2003). Perhaps *Pg*AGO, either directly or indirectly, may be involved in PCD within embryos. The work of McCabe et al. (1997) in carrot suggests that a critical mass of embryogenic tissue is needed for embryo development in culture. Without this critical mass, the embryogenic tissue undergoes premature PCD, thus precluding embryo formation. This notion may be applicable in conifers and may explain possible roles of *PgAGO*. If the lowered expression levels of *PgAGO* in transformed tissues did, in fact, reduce the ability of PEMs III to proliferate, this would certainly reduce levels of PEMs, and, therefore, induce PCD before the PEMs are able to differentiate into somatic embryos.

As a more direct effect, it could be possible that *Pg*AGO possibly acts to silence a gene or genes involved in suspensor maintenance, normally resulting in the degeneration of the suspensor in a manner similar to PCD. The morphological observations on tissue with lowered expression levels of *PgAGO* are similar to those observed by Filonova et al.

(2000a) on a spruce line unable to degenerate suspensors. That line, like the transformed line in this study, showed radial, as opposed to axial, growth and late shoot and root apical meristem formation resulting in the inability of mature embryos to germinate (Filonova et al., 2000a).

5.2 Characterization of *HBK2*

HBK2, one of twelve documented *KNOX* genes found in gymnosperms, was isolated from white spruce tissue by PCR methods using sequence information published by Guillet-Claude et al. (2004). The sequence obtained shares all relevant features of other Knotted-like homeobox proteins, including a molecular weight of around 40 kDa, a pI of around 6 and the absence of any localized hydrophobic regions (Figure 4.9), indicating that HBK2 is not likely a transmembrane protein (Vollbrecht et al., 1991; Long et al., 1996). Like all homeobox proteins, HBK2 contains the conserved homeobox domain thought to be involved in binding specific promoter sequences of target genes, the ELK domain, which aids in protein-protein interactions, and the KNOX domain, which is thought to be involved in initiating transcription of target genes (Hjortswang et al., 2002 and references therein). The presence of these domains indicates that HBK2 is likely a transcription factor, although its role during embryogenesis remains unknown.

KNOX genes are typically divided into two classes: class 1 if they are expressed specifically in the meristem, and class 2 if they are expressed in all organs (Kerstetter et al., 1994). *HBK2* has previously been described as a class 1 *KNOX* gene because it is not found to be expressed in the needles of Norway spruce (Hjortswang et al., 2002). In-situ hybridization studies show that *HBK2* is specifically expressed in the cortical and sub-apical regions of the developing embryo (Figure 4.12), an expression pattern that has thus far not been observed in other class 1 *KNOX* genes. Most class 1 *KNOX* genes have been associated with cell fate specification in the shoot apical meristem (Chan et al., 1998). *SHOOTMERISTEMLESS* (*STM*), a class 1 *KNOX* gene from *Arabidopsis*, is involved in SAM development during embryogenesis (Long et al., 1996). HBK2 and STM proteins have an overall similarity of about 38%, and a specific similarity of 90% in the homeobox domain (data not shown). These similarities not only suggest a similar

function, but also, as with *Pg*AGO, the existence of similar mechanisms of regulating plant development in angiosperms and gymnosperms. Differential expression levels between embryogenic and non-embryogenic spruce cell lines further substantiate this argument. In cell lines unable to produce cotyledonary somatic embryos, *HBK2* expression is very low throughout the maturation period; however, in cell lines able to produce mature embryos, expression levels are quite high throughout development (Figure 4.13). Embryogenic lines in which *HBK2* expression was reduced were found to behave as non-embryogenic lines throughout the maturation period, as embryo formation was inhibited (Figure 4.14). Further investigations into the histological and morphological aspects of these transformed lines were abandoned due to time constraints and the priority of the *Pg*AGO discovery. The results observed thus far indicate that HBK2 is indeed required for the process of somatic embryogenesis. Like STM, it most likely is involved in controlling the transcription of a downstream gene in the meristem maintenance pathway.

6.0 GENERAL DISCUSSION AND CONCLUSIONS

Development during embryogenesis plays a crucial role in determining plant health during postembryonic growth. Somatic embryogenesis is an important tool required for the further understanding of the physiological and molecular mechanisms involved during this delicate time. Spruce somatic embryos provide researchers with the ideal model system to study these important factors, as many embryos can be obtained from different cell lines. Unfortunately, at this time, few spruce cell lines are able to complete the embryo maturation process. This is likely due to the development of a poor root or shoot apical meristem, a critical factor in producing healthy somatic embryos. The goal of this project was to isolate genes involved in shoot apical meristem regulation and maintenance, and determine their role during somatic embryogenesis.

The first part of this work involved isolating genes from spruce tissue that were known to be involved in meristem maintenance. Previous studies by other research groups provided two candidate genes known as *ZLL* and *HBK2*. *ZLL*, a gene isolated in *Arabidopsis*, is known to be involved in the regulation *STM*, which maintains the stem cell pool in an undifferentiated state. *HBK2*, like *STM*, is a *KNOX* class gene that is specifically expressed in Norway spruce cell lines able to produce fully mature somatic embryos. Full length sequences of both genes were isolated from white spruce tissue through screening of cDNA libraries, RACE and PCR-based methods. These genes were characterized and found to share all the relevant features of similar genes within their respective gene families, including molecular weight, iso-electric point, cellular location and relevant domains. The *ZLL* homologue was renamed *PgAGO* due its similarity to other *AGO*-like genes. Previous studies have shown that the genes in the AGO family are involved in both meristem development and RNAi. *HBK2*, like other *KNOX* genes, is likely a transcription factor.

The second objective was to determine the temporal and spatial localization patterns of these genes in developing embryos. In-situ hybridization studies found that *PgAGO* transcripts accumulated specifically in the shoot and root apical meristems from an early age onward. This expression pattern is novel, as no other *AGO*-like genes have been documented to be expressed in the root apical meristem. RT-PCR studies showed

that *PgAGO* is expressed throughout the embryo maturation period in cell lines able to produce mature somatic embryos. In non-embryogenic lines, *PgAGO* is only expressed during the initial stages of development, and not during the later stages. These findings confirmed that *PgAGO* is somehow involved in meristem development, and is necessary for the production of mature somatic embryos.

Transformation experiments revealed that down-regulation of *PgAGO* in Norway spruce significantly reduced embryo production. Furthermore, all embryos that were produced proved to be unable to become fully mature, and many showed severe structural abnormalities. These embryos showed morphological aberrations that are typically associated with loss of meristem function, including lateral as opposed to adaxial expansion of tissues, deformed cotyledons and, in extreme cases, absence of cotyledons. When placed onto germination promoting media, no root or shoot elongation was observed. The meristems of these embryos were studied further to determine their cellular makeup. Shoot apical meristems were found to contain intercellular spaces and cells which lacked meristematic identity. Stem cells in the root apical meristem were often non-existent.

In-situ hybridization studies involving *HBK2* revealed the presence of transcripts in the sub apical and cortical regions of developing embryos. The expression of *HBK2* during the maturation period, like *PgAGO*, was only observed in lines able to produce mature somatic embryos. It is therefore suggested that *HBK2* may be involved in meristem development, and is required to produce mature somatic embryos. Antisense transformation experiments involving *HBK2* provided little insight into what is specifically affected, as no embryos were produced.

The silencing of both genes (but more so with *PgAGO*) revealed conclusively their requirement for proper meristem development resulting in the ability to produce mature cotyledonary embryos.

The availability of *PgAGO* and *HBK2* sequences will allow for future library screening and isolation of more AGO and Homeobox family members in conifer tissue. Other future experiments involving microarray hybridization and analysis would result in the discovery of new genes that are differentially expressed between embryogenic, non-embryogenic and transformed lines, and perhaps allow for the discovery of downstream

genes that are affected by *PgAGO* and *HBK2*. These downstream genes would, in the case of *PgAGO*, reveal an RNA silencing pathway. More importantly, the discovery of these new genes will aid in the understanding of the genetics of meristem maintenance and development. With this new understanding, further transformation experiments could be devised to insert these genes into non-embryogenic lines in the sense orientation. This up-regulation could promote the development of mature somatic embryos. The result would allow for the study of physiology and genetics in a wide variety of conifer species that are currently not able to produce embryos in a culture medium.

This research has resulted in the isolation of the first known *ARGONAUTE*-like gene in conifer tissue as well as the further description of *HBK2*, two genes that are required for proper somatic embryo development. The protocols developed in this work will provide a solid framework for further work involving the understanding of the mechanisms involved in meristem regulation and maintenance during somatic embryogenesis in spruce.

LITERATURE CITED

Ameisen, J.C. 2002. On the origin, evolution, and nature of programmed cell death: a timeline of four billion years. Cell Death Differ. 9:367-393.

Ashihara, H., Stasolla, C., Loukanina, N. and Thorpe, T.A. 2001. Purine metabolism during white spruce somatic embryo development: salvage of adenine, adenosine, and inosine. Plant Sci. 160:647-657.

Attree, S.M., Budinir, S. and Fowke, L.C. 1990. Somatic embryogenesis and plantlet regeneration from cultured shoots and cotyledons of seedlings from stored seeds of black and white spruce (*Picea mariana* and *Picea glauca*). Can. J. Bot. 68:30-34.

Attree, S.M., Moore, D., Sawhney, V.K. and Fowke, L.C. 1991. Enhanced maturation and desiccation tolerance of white spruce (*Picea glauca* [Moench] Voss) somatic embryos: effects of a non-plasmolyzing water stress and abscisic acid. Ann. Bot. 68:519-525.

Attree, S.M., Pomeroy, M.K. and Fowke, L.C. 1992. Manipulation of conditions for the culture of somatic embryos of white spruce for improved triacylglycerol biosynthesis and desiccation tolerance. Planta 187:395-404.

Attree, S.M. and Fowke, L.C. 1993. Embryogeny of gymnosperms: advance in synthetic seed technology of conifers. Plant Cell Tiss. Organ Cult. 35:1-35.

Becwar, W.R., Wann, S.R., Johnson, M.A., Verhagen, S.A., Feirer, R.P. and Nagmani, R. 1988. Development and characterization of in vitro embryogenic systems in conifers. p. 1-18. In: Somatic cell genetics of woody plants. Ahuja, M.R., ed. Kluwer Academic Publishers, Dordrecht, The Netherlands.

Beers, E.P. and McDowell, J.P. 2001. Regulation and execution of programmed cell death in response to pathogens, stress and developmental cues. Curr. Opin. Plant Biol. 4:561-567.

Belmonte, M. and Yeung E.C. 2004. The effect of reduced and oxidized glutathione on white spruce somatic embryogenesis. In Vitro Cell. Dev.-Pl. 40:61–66.

Belmonte, M.F., Donald, G., Reid, D.M., Yeung, E.C. and Stasolla, C. 2005. Alterations of the glutathione redox state improve apical meristem structure and somatic embryo quality in white spruce (*Picea glauca*). J.Exp. Bot. 56:2355-2364.

Bewley, J. and Black, M. 1994. Seeds, Physiology of Development and Germination. Plenum Press, New York.

Bohmert, K., Camus, I., Bellini, C., Bouchez, D., Caboche, M., Benning, C. 1998. *AGO1* defines a novel locus of *Arabidopsis* controlling leaf development. EMBO J. 17:170-180.

Bowe, L.M., Coat, G. and dePamphilis, C.W. 2000. Phylogeny of seed plants based on all three genomic compartments: Extant gymnosperms are monophyletic and Gnetales' closest relatives are conifers. P. Natl. Acad. Sci. USA 97: 4092-4097.

Bozhkov, P.V., Filonova, L.H. and von Arnold, S. 2002. A key developmental switch during Norway spruce somatic embryogenesis is induced by withdrawal of growth regulators and is associated with cell death and extracellular acidification. Biotechnol. Eng. 77:658-667.

Brand, U., Fletcher, J.C., Hobe, M., Meyerowitz, E.M. and Simon, R. 2000. Dependence of stem cell fate in Arabidopsis on a feedback loop regulated by *CLV3* activity. Science 289:617-619.

Brinker, M., van Zyl, L., Liu, W., Craig, D., Sederoff, R.R., Clapham, D.H. and von Arnold S. 2004. Microarray analysis of gene expression during adventitious root development in *Pinus contorta.* Plant Physiology 135:1526-1539.

Buchanan, B.B., Gruissem, W., Jones, R.L. 2000. Biochemistry & Molecular Biology of Plants. American Society of Plant Physiologists, Rockville, Md.

C. elegans Sequencing Consortium. 1998. Genome sequence of the nematode *C. elegans*: a platform for investigating biology. Science 282:2012-2018.

Cantón, F.R., Suárez, M-F., José-Estanyol, M. and Cánovas, F.M. 1999. Expression analysis of a cytosolic glutamine synthetase gene in cotyledons of Scots pine seedlings: Developmental, light–dark regulation and spatial distribution of specific transcripts. Plant Mol. Biol. 40:623–634.

Carles, C.C. and Fletcher, J.C. 2003. Shoot apical meristem maintenance: the art of a dynamic balance. Trends Plant Sci. 8:394-401.

Carmell, M.A., Xuan, Z., Zhang, M.Q. and Hannon, G. 2002. The Argonaute family: tentacles that reach into RNAi, developmental control, stem cell maintenance and tumorigenesis. Gene Dev 16:2733-2742.

Castellano, M.M. and Sablowski, R. 2005. Intercellular signaling in the transition from stem cells to organogenesis in meristems. Curr. Opin. Plant Biol. 8:26-31.

Catalanotto, C., Azzalin, G., Macino, G., Cogoni, C. 2000. Gene silencing in worms and fungi. Nature 404:245.

Cerutti, L., Mian, N. and Bateman, A. 2000. Domains in gene silencing and cell differentiation proteins: the novel PAZ domain and redefinition of the Piwi domain. Trends Biochem. Sci. 25:481-482.

Chalupa, W. 1985. Somatic embryogenesis and plantlet regeneration from cultured immature and mature embryos of *Picea abies* (L.) Karst. Commun. Inst. For. Cech. 14:57-63.

Chan, R.L., Gago, G.M., Palena, C.M. and Gonzalez, D.H. 1998. Homeoboxes in plant development. Biochim. Biophys. Acta 1442:1-19.

Clark, S.E., Running, M.P. and Meyerowitz, E.M. 1995. *CLAVATA3* is a specific regulator of shoot and floral meristem development affecting the same processes as *CLAVATA1*. Development 121:2057-2067.

Ciavatta, V.T., Egertsdotter, U., Clapham, D., von Arnold, S. and Cairney, J. 2002. A promoter from the loblolly pine *PtNIP1;1* gene directs expression in an early-embryogenesis and suspensor-specific fashion. Planta 215: 694-698.

Clapham, D., Demel, P., Elfstrand, M., Koop, H-U., Sabala, I., von Arnold, S. 2000. Gene transfer by particle bombardment to embryogenic cultures of *Picea abies* and the production of transgenic plantlets. Scand. J. Forest. Res. 15:151-160.

Cox, D.N., Chao, A., Baker, J., Chang, L., Qiao, D. and Lin, H. 1998. A novel class of evolutionarily conserved genes defined by *piwi* are essential for stem cell renewal. Gene. Dev. 12:3715-3727.

Cronauermitra, S.S. and Krikorian, A.D. 1988. Plant-regeneration via somatic embryogenesis in the seeded diploid banana *Musa-ornata* roxb. Plant Cell Rep. 7:23-25.

De Vries, S.C., Booij, H., Meyerink, P., Huisman, G., Wilde, H.D., Thomas, T.L. and van Kammen, A. 1988. Acquisition of embryogenic potential in carrot cell suspension cultures. Plant 176:196-204.

Deng, W. and Lin, H. 2002. *miwi*, a murine homolog of *piwi* encodes a cytoplasmic protein essential for spermatogenesis. Dev. Cell 2:819-830.

Dewitt, J.C., Esendam, H.F., Honkanen, J.J. and Tuominen, U. 1990. Somatic embryogenesis and regeneration of flowering plants in rose. Plant Cell Rep. 9:456-458.

Dockx, J., Quaedvlieg, N., Keultjes, G., Kock, P., Weisbeek, P. and Smeekens, S. 1995. The homeobox gene *ATK1* of *Arabidopsis thaliana* is expressed in the shoot apex of the seedling and in flowers and inflorescence stems of mature plants. Plant Mol. Biol. 28:723-737.

Dong, J-Z. and Dunstan, D.I. 1996. Characterization of three heat-shock-protein genes and their developmental regulation during somatic embryogenesis in white spruce [*Picea glauca* (Moench) Voss]. Planta 200:85-91.

Dong, J-Z. and Dunstan, D.I. 2000. Molecular biology of somatic embryogenesis in conifers. p. 51-87. In: Molecular Biology of Woody Plants Vol. 1. Jain S.M. and Minocha, S.C. eds. Kluwar Academic Publishers, Dordrecht, The Netherlands.

Dunstan, D.I., Bock, C.A., Abrams, G.D. and Abrams, S.R. 1992. Metabolism of (+) and (-) abscisic acid by somatic embryo suspension cultures of white spruce. Phytochemistry 31:1451-1454.

Egertsdotter, U., Mo, L.H., and von Arnold, S. 1993. Extracellular proteins in embryogenic suspension cultures of Norway spruce (*Picea abies*). Physiol. Plant. 88:315-321.

Egertsdotter, U. and von Arnold, S. 1995. Importance of arabinogalactan proteins for the development of somatic embryos of Norway spruce (*Picea abies*). Physiol. Plant. 93:334-345.

Fagard, M., Boutet, S., Morel, J.B., Bellini, C. and Vaucheret, H. 2000. AGO1, QDE-2 and RDE-1 are related proteins required for post-transcriptional gene silencing in plants, quelling in fungi, and RNA interference in animals. P Natl. Acad. Sci. USA 97:11650-11654.

Filonova, L.H., Bozhkov, P.V. and von Arnold, S. 2000a. Developmental pathway of somatic embryogenesis in *Picea abies* as revealed by time-lapse tracking. J. Exp. Bot. 51: 249-264.

Filonova, L.H., Bozhkov, P.V., Brukhin, V.B., Daniel, G., Zhivotovsky, B. and von Arnold, S. 2000b. Two waves of programmed cell death occur during formation and development of somatic embryos in the gymnosperm, Norway spruce. J. Cell Sci. 113:4399-4411.

Filonova, L.H., von Arnold, S., Daniel, G. and Bozhkov, P.V. 2002. Programmed cell death eliminates all but one embryo in a polyembryonic plant seed. Cell Death Differ. 9:1057-1062.

Findley, S.D., Tamanaha, M., Clegg, N.J. and Ruohola-Baker, H. 2003. *Maelstrom*, a *Drosophila spindle*-class gene, encodes a protein that colocalizes with Vasa and RDE1/AGO1 homolog, Aubergine, in nuage. Development 130:859-871.

Finer, J.J., Reilley, A.A. and Smith, R.H. 1983. Stimulation of somatic embryogenesis in cotton (*Gossypium-klotzschianum andress*). In Vitro Cell Dev. B. 19:250.

Fletcher, J.C. and Meyerowitz, E.M. 2000. Cell signaling within the shoot meristem. Curr. Opin. Plant Biol. 3:23-30.

Forlani, S., Bonnerot, C., Capgras, S. and Nicholas, J.F. 1998. Relief of a repressed gene expression state in the mouse 1-cell embryo requires DNA replication. Development 125:3153-3166.

Groβ-Hardt, R. and Laux, T. 2003. Stem cell regulation in the shoot meristem. J. Cell Sci. 116:1659-1666.

Groot, E.P., Sinha, N. and Gleissberg, S. 2005. Expression patterns of *STM*-like *KNOX* and *Histone H4* genes in shoot development of the dissected-leaved basal eudicot plants *Chelidonium majus* and *Eschscholzia californica* (Papaveraceae). Plant Mol. Biol. 58:317-331.

Grossnickle, S.C. Ecophysiology of northern spruce species: the performance of planted seedlings. Ottawa, Canada: NRC Research Press. 2000.

Guillet-Claude, C., Isabel, N., Pelgas, B. and Bousquet, J. 2004. The evolutionary implications of knox-I gene duplications in conifers: correlated evidence from phylogeny, gene mapping, and analysis of functional divergence. Mol. Biol. Evol. 21:2232-2245.

Gupta, P.K. and Durzan, D.J. 1987. Biotechnology of somatic polyembryogenesis and plantlet regeneration in loblolly pine. Nat. Biotechnol. 5:147-151.

Haas, B.J., Volfovsky, N., Town, C.D., Troukhan, M., Alexandrov, N., Feldmann, K.A., Flavell, R.B., White, O. and Salzberg, S.L. 2002. Full-length messenger RNA sequences greatly improve genome annotation. Genome Biol. 3:RESEARCH0029.

Harry, I.S. and Thorpe, T.A. 1991. Somatic embryogenesis and plantlet regeneration from mature zygotic embryos of red spruce. Bot. Gaz. 152:446-452.

Hay, E.I. and Charest, P.J. 1999. Somatic embryo germination and desiccation tolerance in conifers. p. 61-69. In: Somatic embryogenesis in woody plants, vol. 4. Mohan Jian, S., Gupta, P.K. and Newton, R.J. eds. Kluwer Academic Publishers, Dordrecht, The Netherlands.

Hay, A., Jackson, D., Ori, N., and Hake, S. 2003. Analysis of the competence to respond to *KNOTTED1* activity in *Arabidopsis* leaves using a steroid induction system. Plant Physiol. 131:1671-1680.

Hjortswang, H.I., Sundås-Larsson, A., Bharathan, G., Bozhkov, P.V., von Arnold, S. and Vahala, T. 2002. *KNOTTED1*-like homeobox genes of a gymnosperm, Norway Spruce, expressed during somatic embryogenesis. Plant Physiol. Bioch. 40:837-843.

Holland, P.W.H. and Garcia-Fernàndez, J. 1996. Hox genes and chordate evolution. Dev. Biol. 173:382-395.

Inada, D.C., Bashir, A., Lee, C., Thomas, B.C., Ko, C., Goff, S.A. and Freeling, M. 2003. Conserved noncoding sequences in the grasses. Genome Res. 13:2030-2041.

Ito, Y., Eiguchi, M. and Kurata, N. Expression of novel homeobox genes in early embryogenesis in rice. Biochim. Biophys. Acta 1444:445-450.

Joy IV, R.W., Yeung, E.C., Kong, L. and Thorpe, T.A. 1991. Development of white spruce somatic embryos: I. Storage product deposition. In Vitro Cell. Dev. Biol. Plant 27:32-41.

Joy IV, R.W., Vogel, H.J. and Thorpe, T.A. 1997. Inorganic nitrogen metabolism in embryogenic white spruce cultures. A nitrogen 14-15 NMR study. J. Plant Physiol. 151:306-315.

Kamath, R.S., Fraser, A.G., Dong, Y., Poulin, G., Durbin, R., Gotta, M., Kanapin, A., Le Bot, N., Moreno, S., Sohrmann, M., Welchman, D.P., Zipperlen, P. and Ahringer, J. 2003. Systematic functionl analysis of the *Caenorhabditis elegans* genome using RNAi. Nature 421:231-237.

Kartha, K.K., Fowke, L.C., Leung, N.L., Caswell, K.L. and Hakman, I. 1988. Induction of somatic embryos and plantlets from cryopreserved cell cultures of white spruce (*Picea glauca*). J. Plant Physiol. 132:529-539.

Kataoka, Y., Takeichi, M. and Uemura, T. 2001. Developmental role and molecular characterization of *Drosophila* homologue of *Arabidopsis Argonaute1,* the founder of a novel gene superfamily. Genes Cells 6:313-325.

Kayes, J.M. and Clark, S.E. 1998. *CLAVATA2*, a regulator of meristem organ development in *Arabidopsis*. Development 125:3843-3851.

Kerstetter, R., Vollbrecht, E., Lowe, B., Veit, B., Yamaguchi, J. and Hake, S. 1994. Sequence analysis and expression patterns divide the maize knotted1-like homeobox genes into two classes. Plant Cell 6:1877-1887.

Kiysoue, T., Yamaguchi-Shinozaki, K., Shinozaki, K., Higashi, K., Satoh, S., Kamada, H. and Harada, H. 1992. Isolation and characterization of a cDNA that encodes ECP31, an embryogenic-cell protein from carrot. Plant Mol. Biol. 19:239-249.

Kong, L. 1994. Factors affecting white spruce somatic embryogenesis and embryo conversion. PhD dissertation, University of Calgary, Calgary, Alberta, Canada.

Kong, L. and Yeung, E.C. 1995. Effects of silver nitrate and polyethylene glycol on white spruce (*Picea glauca*) somatic embryo development: enhancing cotyledonary embryo formation and endogenous ABA content. Physiol. Plant. 93:298-304.

Kong, L., Attree, S.M. and Fowke, L.C. 1997. Changes in endogenous hormone levels in developing seeds, zygotic embryos, and megagametophyte in *Picea glauca* (Moench) Voss. Physiol. Plant. 101:23-30.

Kong, L., Attree, S.M., Evans, D.E., Binarova, P., Yeung, E.C. and Fowke, L.C. 1999. Somatic embryogenesis in white spruce: studies of embryo development and cell biology. p. 1-28. In: Somatic embryogenesis in woody plants, vol. 4. Jian, S.M., Gupta, P.K. and Newton, R.J. eds. Kluwer Academic Publishers, Dordrecht, The Netherlands.

Kuramochi-Miyagawa S., Kimura T., Yomogida K., Kuroiwa A., Tadokoro Y., Fujita Y, Sato M, Matsuda Y, Nakano T. 2001. Two mouse *piwi*-related genes: *miwi* and *mili*. Mech. Develop. 108:121-133.

Kyte J. and Doolittle, R. F. 1982. A simple method for displaying the hydropathic character of a protein. J. Mol. Biol. 157:105-132.

Lam, E. 2004. Controlled cell death, plant survival and development. Mol. Cell Biol. 5:305-315.

Laux, T., Mayer, K.F.X., Berger, J. and Jürgens, G. 1996. The *WUSCHEL* gene is required for shoot and floral meristem integrity in *Arabidopsis*. Development 122:87-96.

Lelu, M.A., Boulay, M.P. and Bornman, C.H. 1990. Somatic embryogenesis in cotyledons of *Picea abies* is enhanced by an adventitious bud inducing treatment. New For. 4:125-135.

Lenhard, M., Laux, T. 1999. Shoot meristem formation and maintenance. Curr. Opin. Plant Biol. 2:44-50.

Lin, X., Kaul, S., Rounsley, S.D., Shea, T.P., Benito, M.I., Town, C.D., Fujii, C.Y., Mason, T.M., Bowman, C.L., Barnstead, M.E., Feldblyum, T.V., Buell, C.R., Ketchum, K.A., Lee, J.J., Ronning, C.M., Koo, H., Moffat, K.S., Cronin, L.A., Shen, M., VanAken, S., Umayam, L., Tallon, L.J., Gill, J.E., Adams, M.D., Carrera, A.J., Creasy, T.H., Goodman, H.M., Somerville, C.R., Copenhaver, G.P., Preuss, D., Nierman, W.C., White, O., Eisen, J.A., Salzberg, S.L., Fraser, C.M, Venter, J.C. 1999. Sequence and analysis of chromosome 2 of the plant *Arabidopsis thaliana*. Nature 402:761-768.

Litvay, J.D., Verma, D.C., Johnson, M.A. 1985. Influence of a loblolly pine (*Pinus taeda* L.) culture medium and its components on growth and somatic embryogenesis of the wild carrot (*Daucus carota* L.). Plant Cell Rep. 4:325-328.

Long, J.A., Moan, E.I., Medford, J.I. and Barton, M.K. 1996. A member of the KNOTTED class of homeodomain proteins encoded by the *STM* gene of *Arabidopsis*. Nature 379:66-69.

Lu, C-Y. and Thorpe, T.A. 1987. Somatic embryogenesis and plantlet regeneration in Cultured immature embryos of *Picea glauca*. J. Plant Physiol. 128:297-302.

Lynn, K., Fernandez, A., Aida, M., Sedbrook, J., Tasaka, M., Masson, P. and Barton, M.K. 1999. The *PINHEAD/ZWILLE* gene acts pleiotropically in *Arabidopsis* development and has overlapping functions with the *ARGONAUTE1* gene. Development 126:469-481.

Matsuoka, M., Ichikawa, H., Saito, A., Tada, Y., Fujimura, T. and Kano-Murakami, Y. 1993. Expression of a rice homeobox gene causes altered morphology of transgenic plants. Plant Cell 5:1039-1048.

Mayer, K.F.X, Schoof, H. Haecker, A., Lenhard, M., Jürgens, G. and Laux, T. 1998. Role of *WUSCHEL* in regulating stem cell fate in the Arabidopsis shoot meristem. Cell 95:805-815.

McCabe, P.F., Levine, A., Meijer, P-J., Tapon, N.A. and Pennell, R.I. 1997. A programmed cell death pathway activated in carrot cells cultured at low density. Plant J. 12: 267-280.

Misra, S., Attree, S.M., Leal, I. and Fowke, L.C. 1993. Effect of abscisic acid, osmoticum, and desiccation on synthesis of storage proteins during the development of white spruce somatic embryos. Ann. Bot. 71:11-22.

Mo, L.H., Egertsdotter, U. And von Arnold, S. 1996. Secretion of specific extracellular proteins by somatic embryos of *Picea abies* is dependent on embryo morphology. Ann. Bot. 77:143-152.

Morel, J.B., Godon, C., Mourrain, P., Beclin, C., Boutet, S., Feuerbach, F., Proux, F. and Vaucheret, H. 2002. Fertile hypomorphic *ARGONAUTE* (*ago1*) mutants impaired in post-transcriptional gene silencing and virus resistance. Plant Cell 14:629-639.

Moussian, B., Schoof, H., Haecker, A., Jürgens, G. and Laux, T. 1998. Role of the *ZWILLE* gene in the regulation of central shoot meristem cell fate during *Arabidopsis* embryogenesis. EMBO J 17:1799-1809.

Muehlbauer, G.J., Fowler, J.E., Girard, L., Tyers, R., Harper, L. and Freeling, M. 1999. Ectopic expression of the maize homeobox gene *liguleless3* alters cell fates in the leaf. Plant Physiol. 119:651-662.

Nagase T., Kikuno R., Nakayama M., Hirosawa M. and Ohara, O. 2000. Prediction of the coding sequences of unidentified human genes. XVIII. The complete sequences of

100 new cDNA clones from brain which code for large proteins in vitro. DNA Res. 7:273-281.

Nagmani, R., Diner, A.M., Garton, S. and Zipf, A.E. 1995. Anatomical comparison of somatic and zygotic embryogeny in conifers. p. 23-48. In: Somatic Embryogenesis in woody plants, Vol. 1. Jain, S., Gupta, P.K. and Newton, R.J. eds. Kluwer Academic Publishers ,Dordrecht, The Netherlands.

Natural Resources Canada. 2006 April 26. Statistics and Facts on Forestry. http://www.nrcan.gc.ca/statistics/forestry/default.html. Accessed 2006 May 10.

Nishimura A, Ito M, Kamiya N, Sato Y, Matsuoka M. 2002. *OsPNH1* regulates leaf development and maintenance of the shoot apical meristem in rice. Plant J. 30:189-201.

Oliver, G., Wehr, R., Jenkins, N.A., Copeland, N.G., Cheyette, B.N., Hartenstein, V., Zipursky, S.L. and Gruss, P. 1995. Homeobox genes and connective tissue patterning. Development 121:693-705.

Oziasakins, P. and Vasil, I.K. 1982. Plant-regeneration from cultured immature embryos and inflorescences of *Triticum-aestivum* L. (Wheat) – Evidence for somatic embryogenesis. Protoplasma 110:95-105.

Parker, J.S., Roe, S.M. and Barford, D. 2004. Crystal structure of a PIWI protein suggests mechanisms for siRNA recognition and slicer activity. EMBO J. 23:4727–4737.

Pennell, R.I and Lamb, C. 1997. Programmed cell death in plants. Plant Cell 9:1157-1168.

Postma-Haarsma, A.D., Verwoert, I.I., Stronk, O.P., Koster, J., Lamers, G.E., Hoge, J.H. and Meijer, A.H. 1999. Characterization of the *KNOX* class homeobox genes *Oskn2* and *Oskn3* identified in a collection of cDNA libraries covering the early stages of rice embryogenesis. Plant Mol. Biol. 39:257-271.

Reiser, L., Sánchez-Baracaldo, P. and Hake, S. 2000. Knots in the family tree: evolutionary relationships and functions of *knox* homeobox genes. Plant Mol. Biol. 42:151-166.

Regan, S., Bourquin, V., Tuominen, H. and Sundberg, B. 1999. Accurate and high resolution in situ hybridization analysis of gene expression in secondary stem tissue. Plant J. 19:363-369.

Rieckhof, G.E., Casares, F., Ryoo, H.D., Abu-Shaar, M. and Mann, R.S. 1997. Nuclear translocation of extradenticle requires homothorax, which encodes an extradenticle-related homeodomain protein. Cell 91:171-183.

Roberts, D.R., Sutton, B.C.S. and Flinn, B.S. 1990. Synchronous and high frequency germination of interior spruce somatic embryos following partial drying at high relative humidity. Canadian J. Botany 68:1086-1090.

Ruddle, F.H., Bartels, J.L., Bently, K.L., Kappen, C., Murtha, M.T. and Pendelton, J.W. 1994. Evolution of Hox genes. Annu. Rev. Genet. 28:423-433.

Sambrook, J. and Russell, D.W. 2001. Molecular Cloning: A Laboratory Manual 3rd Edition. Cold Spring Harbor Laboratory Press, Cold Spring Harbor, New York pp. 7.21-7.45 and 14.4-14.13.

Sarot, E., Payen-Groschene, G., Bucheton, A. and Pelisson, A. 2004. Evidence for a piwi-dependent RNA silencing of the gypsy endogenous retrovirus by the *Drosophila* melanogaster flamenco gene. Genetics 166:1313-1321.

Sasaki, T., Matsumoto, T., Yamamoto, K., Sakata, K., Baba, T., Katayose, Y., Wu, J., Niimura, Y., Cheng, Z., Nagamura, Y., Antonio, B.A., Kanamori, H., Hosokawa, S., Masukawa, M., Arikawa, K., Chiden, Y., Hayashi, M., Okamoto, M., Ando, T., Aoki, H., Arita, K., Hamada, M., Harada, C., Hijishita, S., Honda, M., Ichikawa, Y., Idonuma, A., Iijima, M., Ikeda, M., Ikeno, M., Ito, S., Ito, T., Ito, Y., Ito, Y., Iwabuchi, A., Kamiya, K., Karasawa, W., Katagiri, S., Kikuta, A., Kobayashi, N., Kono, I., Machita, K., Maehara, T., Mizuno, H., Mizubayashi, T., Mukai, Y., Nagasaki, H., Nakashima, M., Nakama, Y., Nakamichi, Y., Nakamura, M., Namiki, N., Negishi, M., Ohta, I., Ono, N., Saji, S., Sakai, K., Shibata, M., Shimokawa, T., Shomura, A., Song, J., Takazaki, Y., Terasawa, K., Tsuji, K., Waki, K., Yamagata, H., Yamane, H., Yoshiki, S., Yoshihara, R., Yukawa, K., Zhong, H., Iwama, H., Endo, T., Ito, H., Hahn, J.H., Kim, H.I., Eun, M.Y., Yano, M., Jiang, J. and Gojobori, T. 2002. The genome sequence and structure of rice chromosome 1. Nature 420:312-316.

Schoof, H., Lenhard, M., Haecker, A., Mayer, K.F.X., Jürgens, G. and Laux, T. 2000. The stem cell population of *Arabidopsis* shoot meristems is maintained by a regulatory loop between *CLAVATA* and *WUSCHEL* genes. Cell 100:635-644.

Sentoku, N., Sato, Y., Kurata, N., Ito, Y., Kitano, H. and Matsuoka, M. 1999. Regional expression of the rice KN1-type homeobox gene family during embryo, shoot, and flower development. Plant Cell 11:1651-1664.

Serikawa, K.A., Martinez-Laborda, A. and Zambryski, P. 1996. Three *knotted1*-like homeobox genes in *Arabidopsis*. Plant Mol. Biol. 32:673-683.

Sharma, A.K., Nelson, M.C., Brandt, J.E., Wessman, M., Mahmud, N., Weller, K.P. and Hoffman, R. 2001. Human CD34(+) stem cells express the *hiwi* gene, a human homologue of the *Drosophila* gene *piwi*. Blood 97:426-434.

Singh H. 1978. Embryology of gymnosperms. Berlin: Borntrager

Smertenko, A.P., Bozhkov, P.V., Filonova, L.H., von Arnold, S. and Hussey, P.J. 2003. Re-organization of the cytoskeleton during developmental programmed cell death in *Picea abies* embryos. Plant J. 33: 813-824

Song, J.J., Smith, S.K., Hannon, G.J. and Joshua-Tor, L. 2004. Crystal structure of Argonaute and its implications for RISC slicer activity. Science 305:1434-1437.

Sorin, C., Bussell, J.D., Camus, I., Ljung, K., Kowalczyk, M., Geiss, G., McKhann, H., Garcion, C., Vaucheret, H., Sanderberg, G. and Bellini, C. 2005. Auxin and light control of adventitious rooting in *Arabidopsis* require ARGONAUTE 1. Plant Cell 17:1343-1359.

Stasolla, C. and Yeung, E.C. 1999. Ascorbic acid improves conversion of white spruce somatic embryos. In Vitro Cell. Dev.-Pl. 35:316-319.

Stasolla, C., Loukanina, N., Ashihara, H., Yeung, E.C., Thorpe, T.A. 2001. Ascorbic acid changes the pattern of purine metabolism during germination of white spruce somatic embryos. Tree Physiol. 21: 359-367.

Stasolla, C. and Yeung, E.C. 2001. Ascorbic Acid metabolism during white spruce somatic embryo maturation and germination. Physiol. Plant. 111:196-205.

Stasolla, C., Kong, L., Yeung, E.C. and Thorpe, T.A. 2002. Maturation of somatic embryos in conifers: morphogenesis, physiology, biochemistry, and molecular biology. In Vitro Cell. Dev.-Pl. 38:93-105.

Stasolla, C., van Zyl, L., Egertsdotter, U., Craig, D., Liu, W. and Sederoff, R.R. 2003. The effects of polyethylene glycol on gene expression of developing white spruce somatic embryos. Plant Physiol. 131:49-60.

Stasolla, C. and Yeung, E.C. 2003. Recent advances in conifer somatic embryogenesis: improving somatic embryo quality. Plant Cell Tiss. Org. 74:15-35.

Stasolla, C., Bozhkov, P.V., Chu, T.M., Van Zyl, L., Egertsdotter, U., Suarez, M.F., Craig, D., Wolfinger, R.D., Von Arnold, S. and Sederoff, R.R. 2004. Variation in transcript abundance during somatic embryogenesis in gymnosperms. Tree Physiol. 24:1073-1085.

Steelman, S., Moskow, J.J., Muzynski, K., North, C., Druck, T., Montgomery, J.C., Huebner, K., Daar, I.O. and Buchberg, A.M. 1997. Identification of a conserved family of Meis1-related homeobox genes. Genome Res. 7:142-156.

Steeves, T.A. and M. Sussex. 1989. Patterns in Plant Development. 2nd Edition. Cambridge: Cambridge University Press.

Steward, F., Mapes, M., Mears, K. 1958. Growth and organized development of cultured cells. II. Organization in cultures grown from freely suspended cells. Am. J. Bot. 45:705-708.

Strausberg, R.L., Feingold, E.A., Grouse, L.H., Derge, J.G., Klausner, R.D., Collins, F.S., Wagner, L., Shenmen, C.M., Schuler, G.D., Altschul, S.F., Zeeberg, B., Buetow, K.H., Schaefer, C.F., Bhat, N.K., Hopkins, R.F., Jordan, H., Moore, T., Max, S.I., Wang, J., Hsieh, F., Diatchenko, L., Marusina, K., Farmer, A.A., Rubin, G.M., Hong, L., Stapleton, M., Soares, M.B., Bonaldo, M.F., Casavant, T.L., Scheetz, T.E., Brownstein, M.J., Usdin, T.B., Toshiyuki, S., Carninci, P., Prange, C., Raha, S.S., Loquellano, N.A., Peters, G.J., Abramson, R.D., Mullahy, S.J., Bosak, S.A., McEwan, P.J., McKernan, K.J., Malek, J.A., Gunaratne, P.H., Richards, S., Worley, K.C., Hale, S., Garcia, A.M., Gay, L.J., Hulyk, S.W., Villalon, D.K., Muzny, D.M., Sodergren, E.J., Lu, X., Gibbs, R.A., Fahey, J., Helton, E., Ketteman, M., Madan, A., Rodrigues, S., Sanchez, A., Whiting, M., Madan, A., Young, A.C., Shevchenko, Y., Bouffard, G.G., Blakesley, R.W., Touchman, J.W., Green, E.D., Dickson, M.C., Rodriguez, A.C., Grimwood, J., Schmutz, J., Myers, R.M., Butterfield, Y.S., Krzywinski, M.I., Skalska, U., Smailus, D.E., Schnerch, A., Schein, J.E., Jones, S.J. and Marra, M.A. 2002. Generation and initial analysis of more than 15,000 full-length human and mouse cDNA sequences. P. Natl. A. Sci. USA 99:16899-16903.

Stuurman, J., Jaggi, F. and Kuhlemeier, C. 2002. Shoot meristem maintenance is controlled by a GRAS-gene mediated signal from differentiating cells. Genes Dev. 16:2213-2218.

Sundås-Larsson, A., Svenson, M., Liao, H. and Engström, P. 1998. A Homeobox gene with potential developmental control function in the meristem of the conifer *Picea abies*. P. Natl. A. Sci. USA 95:15118-15122

Tabara, H., Sarkissian, M., Kelly, W.G., Fleenor, J., Grishok, A., Timmons, L., Fire, A. and Mello, C.C. 1999. The *rde-1* gene, RNA interference and transposon silencing in *C. elegans*. Cell 99:123-132.

Tamaoki, M., Tsugawa, H., Minami, E., Kayano, T., Yamamoto, N., Kano-Murakami, Y. and Matsuoka, M. 1995. Alternative RNA products from a rice homeobox gene. Plant J. 7:927-938.

Tanaka Hall, T.M. 2005. Structure and function of Argonaute proteins. Structure 13:1403-1408.

Tautorus, T.E., Fowke, L.C. and Dunstan, D.I. 1991. Somatic embryogenesis in conifers. Can. J. Bot. 69:1873-1899.

Tioni, M.F., Gonzalez, D.H. and Chan, R.L. 2003. *Knotted1*-like genes are strongly expressed in differentiated cell types in sunflower. J. Exp. Bot. 54:681-690.

van Doorn, W.G. and Woltering, E.J. 2005. Many ways to exit? Cell death categories in plants. Trends Plant Sci.10:117-122.

Veit, B. 2004. Determination of cell fate in apical meristems. Curr. Opin. Plant Biol. 7:57-64.

Venglat, S.P., Dumonceaux, T., Rozwadowski, K., Parnell, L., Babic, V., Keller, W., Martienssen, R., Selvaraj, G. and Datla, R. 2002. The homeobox gene *BREVIPEDICELLUS* is a key regulator of inflorescence architecture in *Arabidopsis*. Proc. Natl. Acad. Sci. USA 99:4730-4735.

Volbrecht, E., Veit, B., Sinha, N. and Hake, S. 1991. The developmental gene *Knotted-1* is a member of the maize homeobox gene family. Nature 350:241-243.

von Arnold, S. and Hakman, I. 1988. Plantlet regeneration in vitro via adventitious buds and somatic embryos in Norway spruce (*Picea abies*). p. 199-215. In: Genetic manipulation of woody plants. Hanover, J.W. and Keathley, D.E. eds. Plenum Press, New York.

von Arnold, S., Sabala, I., Bozhkov, P., Dyachok, J. and Filonova, L. 2002. Developmental pathways of somatic embryogenesis. Plant Cell Tiss. Org. 69:233-249.

Westcott, R.J. 1992. Embryogenesis from non-juvenile Norway spruce (*Picea abies*). Abstr. In Vitro II 28:101A.

Yan, K.S., Yan, S., Farooq, A., Han, A., Zeng, L. and Zhou, M.M. 2003. Structure and conserved RNA binding of the PAZ domain. Nature 426:469-474.

Yeung, E.C. 1984. Histological and histochemical staining procedures. p. 689-697. In Cell culture and somatic cell genetics of plants Vol. 1. Vasil I.K. ed. Academic Press, Orlando.

Yeung, E.C. 1995. Structural developmental patterns in somatic embryogenesis. p. 205-249. In: In vitro embryogenesis in plants. Thorpe, T.A. ed. Kluwer Academic Publishers, Dordrecht, The Netherlands.

Yeung, E.C., Stasolla, C., Kong, L. 1998. Apical meristem formation during zygotic embryo development of white spruce. Can. J. Bot. 76:751-761.

Yeung, E.C. 1999. The use of histology in the study of plant tissue culture systems - some practical comments. In Vitro Cell. Dev.-Pl. 35:137-143.

Yuan, Y.R., Pei, Y., Ma, J.B., Kuryavyi, V., Zhadina, M., Meister, G., Chen, H.Y., Dauter, Z., Tuschl, T., Patel, D.J. 2005. Crystal structure of *A. aeolicus* Argonaute, a site-specific DNA-guided endoribonuclease, provides insights into RISC-mediated mRNA cleavage. Mol. Cell 19:405–419.

Zou C., Zhang Z., Wu S. and Osterman J.C. 1998. Molecular cloning and characterization of a rabbit eIF2C protein. Gene 211:187-194.

APPENDIX 1:

Media Formulations

LV Medium (½ strength) for white spruce

Stock Solutions:

1. Macro Stock

$CaCl_2$ 2 H_2O	0.22 g	0.44 g
$MgSO_4$ 7 H_2O	18.5 g	37.0 g
KNO_3	19.0 g	38.0 g
KH_2PO_4	3.4 g	6.8 g
NH_4NO_3	16.5 g	33.0 g
Make up volume to:	1 L	2 L
Store at 4°C		

2. Micro Stock

$NaMoO_4$ $2H_2O$	0.25 g
H_3BO_3	6.2 g
$CoCl_2$ $6H_2O$	0.026 g
KI	0.83 g
$ZnSO_4$ $7H_2O$	8.6 g
$MnSO_4$ $4H_2O$	5.54 g
$CuSO_4$ $5H_2O$	0.1 g
Make up volume to:	1600 mL
Store at 4°C	

3. Vitamin Stock

Nicotinic acid	0.1 g
Pyridoxine HCl	0.02 g
Thiamine HCl	0.02 g
Make up volume to	500 mL
Aliquot 1.25ml into eppendorf tubes	
Store at -20°C	

4. Fe Stock

$FeSO_4$ $7H_2O$	2.73g
Na-EDTA	3.62g
Make volume up to	1 L
Warm up solution when preparing stock	

½ LV Medium:

Macro Stock	50 mL
Micro Stock	4 mL
Vitamin Stock	1.25 mL
Fe Stock	5 mL
L-Glutamine	0.4 g
Caseine Enzymatic Hydrolysate	0.5 g
Inositol	50 mg

Induction Medium for white spruce and Norway spruce

½ LV in addition to:

Sucrose	50 g
BA (2 μM final concentration)	0.9 mL
2,4-D (10 μM final concentration)	2.2 mL

For BA and 2,4-D stocks dissolve 1 mg of BA or 2,4-D in 1 mL NaOH (1M).

pH 5.8

Make volume to: 1 L

Agar 8 g

Autoclave

Maintenance Medium for white spruce

½ LV in addition to:

Sucrose (3%)	30 g
BA (1 μM final concentration)	0.45 mL
2,4-D (10 μM final concentration)	2.2 mL

pH 5.8

Make volume to: 1 L

Agar 8 g

Autoclave

Maturation Medium for white spruce

½ LV in addition to:
Sucrose (5%) 50 g

pH 5.8

Make volume to: 1 L

Phytagel 4 g

Autoclave

ABA (50 μM) 13 mg
ABA should be filter sterilized using a 0.22 μM Millipore filter. Add ABA after media is autoclaved. Dissolve ABA in NaOH. Adjust media to pH 5.8 before adding ABA.

Germination Medium for white spruce and Norway spruce

½ LV in addition to:
Sucrose (1%) 10 g

pH 5.8

Make volume to: 1 L

Agar 8 g

Autoclave

Proliferation (Maintenance, LP) Medium for Norway Spruce

Stock Solutions:

1. Micro LP Stock

Zn-EDTA	4.716 g
$MnSO_4$ x $7H_2O$	1.6901 g
H_3BO_3	0.630 g
NaMoO4 x 2 H_2O	0.025 g
$CuSO_4$ x 5 H_2O	0.0025 g
CoCl x 6 H_2O	0.0025 g
KI	0.750 g
Make volume up to:	1 L

2. Norstogs Amino Acids Stock

L-Glutamine	0.020 g
L-Alanine	0.0025 g
L-Cysteine-HCL	0.0010 g
L-Arginine	0.0005 g
L-Leucine	0.0005 g
L-Phenylalanine	0.0005 g
L-Tyrosine	0.0005 g
Make volume up to:	1 L

3. LPx2 Stock

KNO_3	(95g/L)	80 mL
$MgSO_4x7H_2O$	(37g/L)	40 mL
KH_2PO_4	(34g/L)	40 mL
$CaCl_2x2H_2O$	(44g/L)	40 mL
Micro LP Stock		4 mL
Norstogs Stock		80 mL
Fe Stock		10 mL
Pyridoxine	(0.1g/100ml)	4 mL
Nicotinic Acid	(0.2g/100ml)	4 mL
Glycine	(0.2g/100ml)	4 mL
Thiamine-HCl		20 mg
Myo-Inositol		400 mg
Glucose		720 mg
Xylose		600 mg
Arabinose		600 mg
Make volume up to:		2 L

4. Glutamine Stock

Glutamine	9 g
Make volume up to:	200 mL

Warm to dissolve
Filter sterilize into 5 mL aliquots

Medium:

LP X 2	250 mL
NH_4NO_3	0.3 g
2,4-D (0.2g/200mL)	2 mL
BA (0.05g/500mL)	10 mL
Sugar	10 g
phytagel	2.4 g

pH to 5.8

Make up volume to	1 L

Autoclave

Glutamine Stock (225 mg/ 5mL)	10 mL (450 mg/L of media)

DKM Prematuration Medium for Norway spruce

Stock Solutions:

1. Macro Stock

NH_4NO_3	2.760 g
KNO_3	23.370 g
$CaCl_2$ x $2H_2O$	2.200 g
$MgSO_4$ x $7H_2O$	3.785 g
KH_2PO_4	0.850 g
Make volume to:	1 L

2. Micro Stock

H3BO3	0.620 g
$MnSO_4$ x $7H_2O$	3.001 g
$ZnSO_4$ x $7H_2O$	0.860 g
KI	0.083 g
Na_2MoO_4 x $2H_2O$	0.025 g
$CuSO_4$ x $5H_2O$	0.0025 g
$CoCl_2$ x $6H_2O$	0.0025 g
Make volume to:	100 mL

3. Vitamin Stock

Thiamine-HCl	0.050 g
Pyridoxine-HCl	0.025 g
Nicotinic acid	0.025 g
Glycine	0.100 g
Make volume to:	50 mL

Medium:

H_2O	200 mL	400 mL
DKM Macro stock	100 mL	200 mL
DKM Micro stock	0.5 mL	1 mL
Vitamins	0.5 mL	1 mL
Fe stock	5 mL	10 mL
Casein Hydrolysate, acid	0.5 g	1 g
Inositol	0.1 g	0.2 g
Sucrose	50 g	100 g

PH to 5.8 with HCl

Make up volume to	1 L	2 L
phytagel	3.5 g/L	
Autoclave		
Glutamine filter sterilized	using stock aliquots add 225 mg to each 500 mL volume ie. add one stock aliquot to each volume	

DKM Maturation Medium for Norway spruce

Prepare as above but add abscisic acid (ABA) filter sterilized to give 60 μM.
Dissolve 16 mg in 0.8 mL NaOH for 1 L
Dissolve 32 mg in 1.6 mL NaOH for 2 L

Recovery media

LP X 2	250 mL
NH_4NO_3	0.3 g
2,4-D (0.2g/200mL)	2 mL
BA (0.05g/500mL)	10 mL
Sugar	10 g
Inositol	45.04 g
pH 5.8 with HCl	
Make up volume to	1 L
phytagel	2.4 g
Autoclave	
Asparagine (filter sterilized – 0.75 g/50 mL)	10 mL

BASTA Transformation media

LP X 2	250 mL
NH4NO3	0.3 g
2,4-D (0.2g/200mL)	2 mL
BA (0.05g/500mL)	10 mL
Sugar	10 g
Inositol	45.04 g
pH 5.8	

Make up volume to	1 L
phytagel	2.4 g
Autoclave	
Asparagine (filter sterilized - 0.75g/50mL)	10 mL
BASTA (filter sterilized - 1mg/mL)	1 mL